TURUN
YLIOPISTO
UNIVERSITY
OF TURKU

ULTRASENSITIVE HETEROGENEOUS BIOAFFINITY ASSAYS

by Eliminating Nonspecific Binding of Upconverting Nanoparticles

Saara Kuusinen

TURUN YLIOPISTON JULKAISUJA – ANNALES UNIVERSITATIS TURKUENSIS
SARJA – SER. F OSA – TOM. 55 | TECHNICA – INFORMATICA | TURKU 2025

TURUN
YLIOPISTO
UNIVERSITY
OF TURKU

ULTRASENSITIVE HETEROGENEOUS BIOAFFINITY ASSAYS

by Eliminating Nonspecific Binding of Upconverting Nanoparticles

Saara Kuusinen

TURUN YLIOPISTON JULKAISUJA – ANNALES UNIVERSITATIS TURKUENSIS
SARJA – SER. F OSA – TOM. 55 | TECHNICA – INFORMATICA | TURKU 2025

University of Turku

Faculty of Technology
Department of Life Technologies
Biotechnology (Tech. field)
Doctoral programme in Technology

Supervised by

Professor Tero Soukka, PhD
Department of Life Technologies
Biotechnology
University of Turku
Turku, Finland

Satu Lahtinen, DSc (Tech)
Department of Life Technologies
Biotechnology
University of Turku
Turku, Finland

Terhi Riuttamäki, PhD
Uniogen Oy
Turku, Finland

Reviewed by

Docent Harri Hakala, PhD
Revvity Finland Oy
Turku, Finland

Assoc. Professor Paul Corstjens, PhD
Department of Cell and Chemical Biology
Leiden University Medical Centre
Leiden, Neatherlands

Opponent

Professor Ann-Christine Syvänen, PhD
Department of Medical Sciences
Molecular Precision Medicine
Uppsala University
Uppsala, Sweden

ISBN 978-952-02-0122-7 (PRINT)
ISBN 978-952-02-0123-4 (PDF)
ISSN 2736-9390 (Painettu/Print)
ISSN 2736-9684 (Sähköinen/Online)
Painosalama, Turku, Finland 2025

“If you only do what you can do,
you will never be more than you are now.”

-Master Shifu in Kung Fu Panda 3

UNIVERSITY OF TURKU
Faculty of Technology
Department of Life Technologies
Biotechnology (Tech. field)
SAARA KUUSINEN: Ultrasensitive Heterogeneous Bioaffinity Assays by Eliminating Nonspecific Binding of Upconverting Nanoparticles
Doctoral Dissertation, 143 pp.
Doctoral Programme in Technology (DPT)
May 2025

ABSTRACT

Bioaffinity assays are commonly used for specific detection of biomarkers in biological samples. Reducing the lowest detectable concentration, i.e. the analytical sensitivity of such assays, is beneficial for several reasons: it allows for earlier diagnostics of various diseases, enables introduction of new biomarkers and decreases the sample volume required for the analysis. Upconverting nanoparticles (UCNPs) have attracted wide interest as labels in sensitive bioaffinity assays due to their unique optical properties that enable the detection of trace amounts of UCNPs with relatively simple instrumentation. However, the background signal originating from the nonspecific binding of UCNP conjugates has hindered reaching ultrasensitivity that is required for detecting extremely low-abundance biomarkers.

The aim of this research was to improve the analytical sensitivity that can be achieved by upconversion-based bioaffinity assays, particularly by reducing the nonspecific binding of UCNP conjugates. The study included both, immunoassays and oligonucleotide hybridization assays. The plasma matrix related nonspecific binding of UCNP conjugates in immunoassays was studied by isolating the fractions of human plasma associated with elevated nonspecific binding and identifying the contents of the fractions by mass spectrometry. In hybridization assays, the probe hybridization stability with a short target sequence was enhanced by exploiting base stacking interactions using hairpin-structured DNA probes. Additionally, a novel hybridization complex transfer technique was developed to eliminate the nonspecific binding of UCNP conjugates on the detection surface.

A major part of plasma-related nonspecific binding in immunoassays was associated with complement component C1q. The background signal was strongly reduced by increasing the salt concentration in the assay buffer or by adding heparin as a polyanionic blocker. In hybridization assays, the hairpin-structured probes improved the analytical sensitivity by a factor of 18 compared to the corresponding linear probes. Moreover, the complex transfer procedure eliminated the backgroud signal from the nonspecifically bound UCNP conjugates, making the detection instrument the main sensitivity-limiting factor. The hybridization assays reached femto-attomolar detection limits for DNA analogue of miR-20a, making them promising tools for micro-RNA based diagnostics.

KEYWORDS: bioaffinity assays, nonspecific binding, upconverting nanoparticles

TURUN YLIOPISTO
Teknillinen tiedekunta
Bioteknologian laitos
Biotekniikka (tekn. ala)
SAARA KUUSINEN: Ultraherkkiä heterogeenisiä bioaffiniteettimäärityksiä käänteisviritteisten nanopartikkelien epäspesifisen sitoutumisen poistolla
Väitöskirja, 143 s.
Teknologian tohtoriohjelma
Toukokuu 2025

TIIVISTELMÄ

Bioaffiniteettimäärityksiä käytetään yleisesti biomerkkiaineiden spesifiseen havaitsemiseen biologisista näytteistä. Matalimman määrityksillä mitattavissa olevan pitoisuuden eli analyyttisen herkkyyden alentaminen on hyödyllistä monesta syystä: se mahdollistaa sairauksien diagnosoinnin varhaisemmassa vaiheessa, uusien biomerkkiaineiden käyttöönoton ja pienempien näytetilavuuksien käytön. Käänteisviritteiset nanopartikkelit (engl. upconverting nanoparticles, UCNP) ovat herättäneet kiinnostusta tällaisten määritysten leimoina, koska niiden optiset ominaisuudet mahdollistavat äärimmäisen alhaisten leimamäärien havaitsemisen verrattain yksinkertaisella laitteistolla. UCNP:iden epäspesifisestä sitoutumisesta johtuva taustasignaali on kuitenkin estänyt ultraherkkien määritysten kehittämisen.

Tutkimuksen tavoitteena oli parantaa UCNP:itä hyödyntävillä bioaffiniteettimäärityksillä saavutettavaa analyyttistä herkkyyttä erityisesti poistamalla UCNP:iden epäspesifisestä sitoutumisesta johtuvaa taustasignaalia. Tutkimukseen sisältyi sekä immuno- että hybridisaatiomäärityksiä. Plasmanäytteisiin liittyvää epäspesifistä sitoutumista immunomäärityksissä tutkittiin eristämällä ihmisen plasmasta fraktiot, jotka tuottivat korkeaa taustasignaalia ja tunnistamalla niiden sisältö massaspektrometrillä. Hybridisaatiomäärityksissä koettimien sitoutumista lyhyen kohdesekvenssin kanssa vahvistettiin emäspinoutumisesta johtuvalla vuorovaikutuksella, joka saatiin aikaan hiuspinnirakenteisilla DNA-koettimilla. Lisäksi kehitettiin hybridisaatiokompleksin siirtoon perustuva tekniikka epäspesifisestä sitoutumisesta johtuvan taustasignaalin poistamiseksi.

Valtaosa plasmaan liittyvästä taustasignaalista yhdistettiin komplementtiproteiini C1q:hun. Taustasignaali väheni selvästi, kun määrityspuskuriin lisättiin suolaa tai hepariinia. Hybridisaatiomäärityksissä hiuspinnirakenteiset koettimet paransivat analyyttistä herkkyyttä 18-kertaiseksi verrattuna lineaarisiin koettimiin. Lisäksi kompleksinsiirtomenetelmällä onnistuttiin poistamaan epäspesifisestä sitoutumisesta johtuva taustasignaali, jolloin mittalaitteesta tuli pääasiallinen analyyttistä herkkyyttä rajoittava tekijä. Määrityksillä saavutettiin femto-attomolaarisia herkkyyksillä miR-20a:ta vastaavalle DNA-sekvenssille, mikä tekee niistä lupaavia työkaluja mikro-RNA-pohjaiseen diagnostiikkaan.

ASIASANAT: bioaffiniteettimääritykset, epäspesifinen sitoutuminen, käänteisviritteiset nanopartikkelit

Table of Contents

Abbreviations

Ab	antibody
bDNA	branched DNA
BSA	bovine serum albumin
CHA	catalytic hairpin assembly
CLSI	Clinical and Laboratory Standards Institute
cTnI	cardiac troponin I
DELFIA	dissociation-enhanced lanthanide fluoroimmunoassay
DMF	dimethylformamide
DNA	deoxyribonucleic acid
EDC	N-(3-dimethylaminopropyl)-N′-ethylcarbodiimide
EDTA	ethylenediaminetetraacetic acid
ELISA	enzyme-linked immunosorbent assay
Fab	fragment antigen-binding
Fc	constant domain of an antibody
FRET	Förster resonance energy transfer
HCR	hybridization chain reaction
Ig	immunoglobulin
IUPAC	International Union of Pure and Applied Chemistry
K_a	association constant
LNA	locked nucleic acid
LoD	limit of detection
LoQ	limit of quantification
mAb	monoclonal antibody
MES	2-(N-morpholino)ethanesulfonate
miRNA	micro-RNA
NULISA	nucleic acid linked immune-sandwich assay
PAA	poly(acrylic acid)
pAb	polyclonal antibody
PCR	polymerase chain reaction
PEG	polyethylene glycol
PLA	proximity ligation assay

PNA	peptide nucleic acid
PSA	prostate-specific antigen
RCA	rolling circle amplification
RNA	ribonucleic acid
ScFv	single chain variable fragment
SDS-PAGE	sodium dodecyl sulfate polyacrylamide gel electrophoresis
SELEX	systematic evolution of ligands by exponential enrichment
sulfo-NHS	N-hydroxysulfosuccinimide
T_m	melting temperature
TSH	thyroid-stimulating hormone
qPCR	quantitative PCR
UCL	upconversion luminescence
UCNP	photon upconverting nanoparticle

List of Original Publications

This dissertation is based on the following original publications, which are referred to in the text by their Roman numerals:

I Kuusinen, S., Ekman, M., Raiko, K., Hannula, H., Lyytikäinen, A., Lahtinen, S. & Soukka, T. Complement C1q in plasma induces nonspecific binding of poly(acrylic acid)-coated upconverting nanoparticle antibody conjugates. *Anal Bioanal Chem*, 2022; **414**: 3741–3749.

II Kuusinen, S., Lahtinen, S. & Soukka, T. Upconversion Luminescence Based Direct Hybridization Assay to Detect Subfemtomolar miR-20 a DNA Analogue in Plasma. *Anal Sens*, 2024; **4**: e202400005.

III Máčala, J., Kuusinen, S., Lahtinen, S., Gorris, H.-H., Skládal, P., Farka, Z. & Soukka, T. Amplification-free Attomolar Detection of Short Nucleic Acids with Upconversion Luminescence: Eliminating Nonspecific Binding by Hybridization Complex Transfer. *Anal Chem*, 2025; **97**: 1775–1782.

1 Introduction

Bioaffinity assays are widely used in a variety of applications, including clinical and food diagnostics, environmental applications and forensics testing, to indicate the presence or absence or to determine the concentration of the analyte of interest in a sample. They are based on specific recognition of the target analyte by biomolecular affinity binders and a signal generation element, such as optical label, that transforms the binding event into a measurable signal. The basic principles of bioaffinity assays are relatively simple, making them suitable to a wide range of applications, from centralized laboratories to point-of-care settings.

Among bioaffinity assays, immunoassays relying on specific binding between antibodies and antigens are most widely used especially for the detection of proteins, peptides, bacteria, viruses and small molecules, such as steroids. Specific nucleic acid strands, on the other hand, can be detected using hybridization assays based on base pairing of complementary nucleic acid sequences. Even though nucleic acid targets are commonly detected by methods that are based on enzymatic amplification of the target sequence, such as quantitative polymerase chain reaction (qPCR), direct amplification-free hybridization assays are favorable, especially outside central laboratories or if more precise quantification is required.

Since the introduction of first immunoassays in 1959,[1] the assay development has generally aimed to improve the analytical sensitivity of the methods, i.e. their ability to detect minute concentrations of the target analyte.[2] Over the years, significant improvements have been made especially due to the advances in label technologies and the introduction of digital assay technologies, which are based on counting of single label molecules.[3-7] Nevertheless, further improvement in the analytical sensitivity of bioaffinity assays is still needed, as the ability to detect trace concentrations of disease biomarkers often enables earlier diagnostics and thus more timely start of the treatment.[8] Furthermore, ultrasensitive detection technologies enable the introduction of completely new biomarkers as well as use of lower sample volumes and less invasive sample materials, such as urine, sweat and saliva, that typically contain circulating biomarkers at much lower concentrations than blood.[8-10] Other important features in assay development include simplicity, affordability

and fast turnaround time as well as suitability for multiplexing and point-of-care testing.[11-13]

Photon upconverting nanoparticles (UCNP) are excellent labels for bioaffinity assays because their anti-Stokes shifted luminescence can be detected without autofluorescence background.[14-15] Biological samples and other assay materials generate autofluorescence that occurs at longer wavelengths (i.e. lower energy) than the excitation light.[16] In upconversion process, the energy from multiple low-energy near-infrared excitation photons is stacked and subsequently released as a single photon at higher energy.[17] As a result, the emission occurs at shorter wavelengths than the excitation, and there is no autofluorescence background at the visible wavelengths, dramatically improving the contrast between the signal of the label and the background signal from other materials and thus enabling ultrasensitive detection of UCNPs.[17-19] By conjugating UCNPs to bioaffinity binders, the biological recognition of the analyte of interest can be connected to the luminescence signal.

Even though the autofluorescence background can be avoided by using UCNP labels, background signal still arises from nonspecifically bound UCNP labels. Due to the extremely high detectability of UCNPs, even minimal nonspecific binding results in detectable background signal, which has been the main factor limiting the sensitivity of upconversion-based bioaffinity assays.[18, 20-26] Nonspecific binding can be reduced by surface modifications and optimization of assay conditions,[20, 23, 27] but it has been impossible to fully eliminate.

2 Literature Review

2.1 Bioaffinity assay principles

Bioaffinity assay principles are commonly classified into homogeneous and heterogeneous, as well as competitive and noncompetitive assays (**Figure 1**). Each assay principle has its benefits and limitations.

In homogeneous assays, the binding of the target analyte results in a measurable change in signal of the label without physical separation of bound and unbound reagents.[28] Such technologies include, for example, Förster resonance energy transfer (FRET)[29], fluorescence cross-correlation[30] and fluorescence polarization.[31] These assays are simple to perform, as only mixing of the assay components is needed, followed by the signal readout after a typically short incubation time. However, homogeneous assays suffer from limited sensitivity and they are more prone to interferences caused by the sample matrix than heterogeneous assays.[28]

The first immunoassays were carried out in solution, and the separation of bound and unbound reagents was based on immunoprecipitation or paper chromato-electrophoresis.[1] The introduction of heterogeneous immunoassays in 1967[32] enabled easier separation by using a solid phase. In heterogeneous assays, analyte-specific binders are immobilized on the surface of a solid phase, extracting target molecules from the sample during an incubation.[28] The separation of surface-bound and unbound reagents is usually done by aspirating the reaction solution from the surface and subsequent washing of the solid phase surface.[28] In one-step assays, the sample and the labeling reagent are added in a single step and incubated together, whereas in two-step assays, they are incubated in separate steps with a washing step in between, which diminishes the possible interferences caused by the sample material and may improve the separation of specifically and nonspecifically bound molecules.[33-34] Immobilizing the binders onto the solid-phase surface can limit the binding kinetics due to diffusion constraints, potentially leading to longer incubation times compared to homogeneous assays.[35-36] The binding kinetics of heterogeneous assays is therefore highly dependent on the choice of solid phase. The most commonly used solid phases are discussed in detail in section 2.4.

Both, homogeneous and heterogeneous assays can be implemented either in competitive or non-competitive format. Competitive assays utilize labeled analyte analogs for detection. The analyte in the sample and the labeled analog compete for a limited number of binding sites: the higher the analyte concentration in the sample, the lower fraction of binding sites is available for the binding of the labeled analyte analogs. Competitive assays essentially measure the fraction of binding sites unoccupied by the analyte. This results in decreasing signal with increasing analyte concentration.[37] The recognition by only one binder is required, and therefore, the competitive assay principle is mainly used for measuring concentrations of molecules that are too small for simultaneous recognition by two binders.[28, 37]

Non-competitive assays, first introduced by Addison and Hales in 1971,[38] employ two binders that recognize different binding sites of the analyte. The technology development was strongly linked to the development of hybridoma technology for monoclonal antibody production, enabling production of unlimited quantities of antibodies directed against a specific epitope in the analyte.[37, 39] In heterogeneous format, one of the binders is used for capturing the analyte to the solid-phase surface, and the other one is coupled with signal generation element and used for detection. In the presence of the analyte, a sandwich-like complex is formed, and hence, these assays are often referred to as sandwich-type or two-site assays. The signal is generated as a result of the analyte bridging the two binders together, resulting in increasing signal intensity with the increasing analyte concentration. This is the fundamental reason for why non-competitive assays can potentially detect much lower concentrations than competitive assays: it is generally easier to measure small differences in low signals than small differences in high signals.[40-41] Another benefit of the non-competitive assay format arises from the use of two target-specific binders for analyte recognition, improving the specificity of the assays. On the other hand, finding two binders that can simultaneously bind to the analyte may not be possible in case of small analyte molecules.[28]

Due to their superior analytical performance, this thesis mostly focuses on heterogeneous non-competitive bioaffinity assay technologies. Even though the literature mostly covers immunoassays, the same principles apply to hybridization assays and other bioaffinity assays, as well.

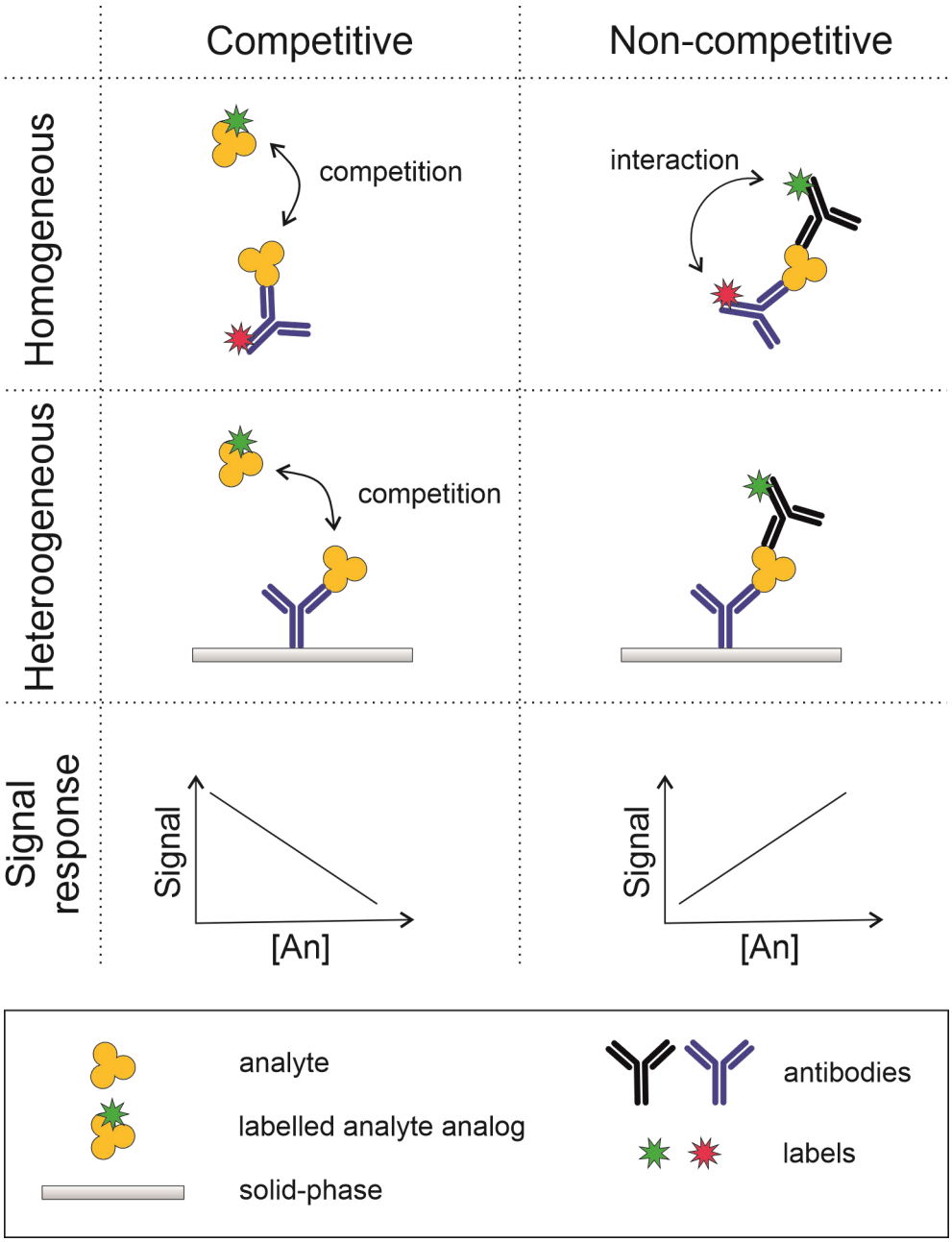

Figure 1. Schemes of bioaffinity assay principles and their characteristic dose response curves. The principles are illustrated as immunoassays utilizing antibodies as binders, but similar principles can be exploited using other types of binders.

2.2 Analytical sensitivity

Analytical sensitivity is an important characteristic of analytical methods and refers to the lowest analyte concentration that can be measured reliably.[2] It is generally evaluated by measuring the limit of detection (LoD), which is the lowest analyte concentration that can be reliably distinguished from blank samples. LoD is dependent on the signal response generated by the analyte binding as well as the variation of the background signal produced in the absence of the analyte.[2] The variation consists of the experimental error, variation in nonspecific binding of the label, and counting error of the detector.[42-44] There are several ways to determine the LoD. One common way is by determining the analyte concentration generating a signal response that corresponds to 3 × standard deviation of the zero calibrator, which assures a confidence level of >95%. Clinical and Laboratory Standards Institute (CLSI) guideline EP17 takes into account the variation in both, blank and low concentration samples, by determining the LoD as a concentration corresponding to signal response equivalent to 1.645 × standard deviation of blank samples + 1.645 × standard deviation of low concentration sample.[45] The International Union of Pure and Applied Chemistry (IUPAC) defines the sensitivity as the "slope of the calibration curve",[46] which does not take into account the variation in the measurement of blank samples, but rather describes the ability of the assay to discriminate small concentration differences.

It is important to understand that analyte concentration above the LoD does not guarantee precise quantification, as the definitions only ensure confidence that the sample contains analyte. Measurements of concentrations close to LoD may have very high uncertainty, making the quantification imprecise.[43] Another measure of analytical sensitivity is limit of quantification (LoQ), which is defined as the lowest analyte concentration that can be reliably detected with a certain precision, often with a coefficient of variation of 10% or 20%.[47] This is also called functional sensitivity.[28]

The analytical sensitivity of an assay is highly dependent on the assay components, including affinity binders, reporter technology, and in case of heterogeneous assays, the separation efficiency of the bound and unbound reagents. The role of each component in determining the assay sensitivity as well as other performance characteristics is described in sections 2.3-2.5. Additionally, numerous methods have been developed aiming to further improve the analytical sensitivity from what can be achieved with conventional assay principles, and those are discussed in section 2.6.

An assay employing binders with infinite affinity, labels with infinite specific activity and complete elimination of nonspecific binding could in theory detect a single analyte molecule. However, precise quantification is limited by the number of analyte molecules in the sample and Poisson statistics.[48] Woolley et al.

demonstrated that the theoretical minimum for LoQ with 10% precision is 131 molecules,[43] corresponding to approximately 2.2 aM concentration in 100 µL sample volume.

2.3 Affinity binders

This chapter describes the concepts of affinity and specificity as well as introduces the most commonly used bioaffinity binders: antibodies, nucleic acid probes and aptamers, focusing on their properties affecting the analytical performance of bioaffinity assays. Less frequently used binders, such as lectins, darpins and molecularly imprinted polymers are not discussed.

2.3.1 Affinity and specificity

Ligand binding reaction is expressed by the Law of Mass Action:

$$B + L \leftrightarrow BL \tag{1}$$

where B is the binder, L is the ligand and BL is the ligand-binder complex. Association constant K_a is an equilibrium constant of a ligand binding reaction:

$$K_a = \frac{k_a}{k_d} = \frac{[BL]}{[B_{free}][L_{free}]} \tag{2}$$

where k_a and k_d represent the rate constants of association and dissociation reactions, respectively, [BL] is the concentration of the complexes of ligands and binders and $[L_{free}]$ and $[B_{free}]$ are the concentrations of unbound ligands and binders at the equilibrium, respectively. Affinity can be also expressed as dissociation equilibrium constant K_d, which is equivalent to $1/K_a$.[49] High-affinity binders are necessary to efficiently capture extremely low concentrations of analyte, as required in ultrasensitive bioaffinity assays. The effect of the affinity is a particularly dominant determining factor the maximal sensitivity that can be achieved by competitive assays,[41] but it is also significant for non-competitive assays.

By substituting $[B_{free}]$ by $[B_{tot}]-[BL]$ and $[L_{free}]$ by $[L_{tot}]-[BL]$, where $[B_{tot}]$ and $[L_{tot}]$ are the total concentrations of binder and ligand, respectively, the equation 2 can be rearranged to:

$$K_a = \frac{[BL]}{([B_{tot}]-[BL])([L_{tot}]-[BL])} \tag{3}$$

At low ligand concentrations, when $[L_{tot}] << [B_{tot}]$, $[B_{free}] \approx [B_{tot}]$, the equation 3 can be simplified to:

$$K_a = \frac{[BL]}{[B_{tot}]([L_{tot}]-[BL])} = \frac{[BL]}{[BL]\left(\frac{[B_{tot}][L_{tot}]}{[BL]}-[B_{tot}]\right)} = \frac{1}{[B_{tot}]\left(\frac{[L_{tot}]}{[BL]}-1\right)} \tag{4}$$

By solving [BL] from the equation 4, it can be expressed as:

$$[BL] = \frac{[L_{tot}]}{\frac{1}{K_a[B_{tot}]} + 1} \quad (5)$$

indicating that increasing the binder concentration [B_{tot}] results in increased concentration of binder-ligand complexes at the equilibrium, and the effect of [B_{tot}] is the same as the effect of K_a. Thus, lower affinity can be compensated to some extent by increasing the binder concentration. However, it may also elevate the background signal from nonspecific binding.[50-53]

K_a reflects the concentrations of bound and free components at the equilibrium, but the rate constants may also play a significant role in the analytical sensitivity in non-equilibrium assays. For example, in lateral flow assays, the binding needs to occur during the short time during which the analyte flows past the test line, highlighting the importance of high k_a.[54] Additionally, prolonged incubation times required to compensate low k_a make heterogeneous assays more prone to nonspecific binding, thus resulting in higher LoDs.[55]

Another important characteristic of affinity binders is specificity. Bioaffinity assays are mostly used for detection of low-abundance target analyte in complex sample matrices containing much higher concentrations of non-target molecules. Therefore, even low cross-reactivity with high-abundance biomolecules may significantly interfere with the quantification of the analyte.

2.3.2 Antibodies

Immunoassays are based on antibodies (Ab) and their ability to specifically bind to their target. Antibodies can be generated against a wide range of target molecules, such as proteins, haptens and pathogens. Typical antibodies used in immunoassays have affinities between 10^8 M^{-1} and 10^{10} M^{-1}, which is considered as an affinity ceiling of *in vivo* generated antibodies.[28, 43, 56]

Antibodies, or immunoglobulins (Ig), are divided into five classes: IgG, IgM, IgA, IgD and IgE,[57] of which IgGs are almost exclusively used in immunoassays due to their high affinity. IgG is a bivalent, Y-shaped molecule with a molecular weight of approximately 150 kDa.[57] It consists of a constant domain (Fc) and two antigen binding fragments (Fab). The specificity and affinity of the antibody are determined by highly variable complementarity-determining regions at the ends of the Fab fragments.[58] (**Figure 2 A**)

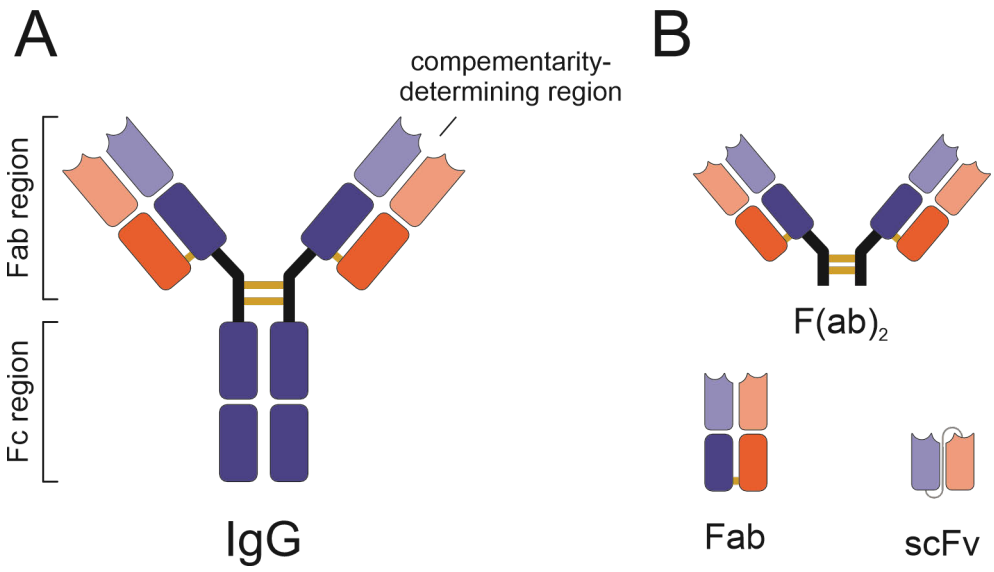

Figure 2. The structures of A) IgG and B) antibody fragments. IgG molecules consist of a conctant Fc region and two Fab fragments. The antigen binding sites are located at the ends of Fab regions. The two heavy chains (blue) are covalently connected via two disulfide bonds and each light chain (orange) is connected to the heavy chain with one disulfide bond.

Antibody reagents can also be classified into polyclonal and monoclonal antibodies. Polyclonal antibodies (pAbs) are produced in immunized laboratory animals and they contain heterogeneous mixtures of immunoglobulins with varying affinities and specificities against different epitopes in their target molecule.[59] On the other hand, monoclonal antibodies (mAbs) are homogeneous antibody reagents recognizing a specific epitope of the antigen with a certain affinity and selectivity. MAbs are produced in hybridoma cell lines, that are generated by fusing B lymphocytes of an immunized animal with immortal myeloma cells.[39] PAbs have relatively high batch to batch variation because they are dependent on the immune response of the individual immunized animals, whereas mAbs can be produced in virtually unlimited quantities without significant variation between batches.[39, 59-60] Modern biotechnology has also enabled the development of new antibodies completely without animal immunization by using *in vitro* technologies, such as phage display,[61] making the antibody development process faster and less expensive and avoiding the need for laboratory animals.[62]

Instead of intact IgGs, also antibody fragments can be used as binders in immunoassays. Bivalent $F(ab)_2$-fragments and monovalent Fab-fragments (**Figure 2 B**) can be produced by enzymatic cleavage of IgG molecules to remove the Fc part. Alternatively, they can be directly produced as recombinant proteins. Single chain variable fragments (scFv) contain only the variable fragments connected with a

flexible linker, and they are only produced as recombinant proteins.[57] The removal of constant regions may reduce unwanted interactions, such as complement activation,[63] and antibody fractions have been shown to decrease nonspecific interactions and consecutively improve the assay sensitivity.[64-65] However, they may be less stable than intact IgGs[66] and may require more sophisticated, site-specific conjugation techniques to retain their binding activity.[64-68]

2.3.3 Nucleic acid probes

Nucleic acid diagnostics is generally based on specific hybridization of complementary nucleic acid strands. As the nature of interactions in hybridization is relatively simple and based Watson-Crick base pairing,[69] the prediction of interactions between nucleic acid sequences is more straightforward than prediction of protein interactions. Furthermore, the development of automated synthesis methods has enabled inexpensive production of custom-made synthetic oligonucleotides.[70] Additionally, a wide range of modifications, such as reactive groups, fluorophores and haptens, can be included in the synthesis.[71] These features have made custom oligonucleotides an integral part of modern biotechnology.

The stability of nucleic acid probe hybridization is generally expressed as melting temperature (T_m). The strands of nucleic acid duplexes dissociate at elevated temperatures, and the stronger the hybridization, the higher temperature is required for denaturation. T_m is defined as the temperature at which 50% of the strands are in double stranded form and 50% in single stranded form.[72] T_m can be increased by increasing the number of nucleotides participating in the hybridization and by increasing the proportion of guanine and cytosine in the sequence.[73] It is also affected by the buffer composition, particularly the concentration of salts.[74] However, increasing the probe length or salt concentration also increases the probability of nonspecific hybridization with non-target sequences.

Due to their high stability and low cost, DNA oligonucleotide probes are most commonly used for DNA and RNA detection. Even though the hybridization of RNA-RNA and RNA-DNA duplexes can be thermodynamically more stable than DNA-DNA duplexes,[75] the poor stability of RNA molecules, due to enzymatic and chemical hydrolysis, has hindered the widespread use of RNA probes. Additionally, non-natural nucleic acid mimics with special hybridization properties have been developed, and they are advantageous as probes in certain applications.

Locked nucleic acids (LNA) are nucleic acid mimics that contain an additional 2'–C,4'–C-oxymethylene link (**Figure 3**).[76] The link conformationally restricts the LNA monomers, forcing the strand into A-type duplex geometry, which is especially favourable in hybridization with RNA.[76-77] LNA nucleotides can be included in the synthesis of DNA and RNA oligonucleotides, and compared to the corresponding

DNA sequence, 4–6 °C increases in T_m per LNA monomer have been reported.[76, 78] As a result of the improved hybridization stability with complementary sequences, LNA modified probes possess improved discrimination of mismatched nucleotides than DNA probes, making them well-suited tools for detection of mutations.[79-81]

Peptide nucleic acids (PNA) are DNA mimics in which the phosphodiester backbone of DNA is replaced by a peptide backbone mimic to which the nucleobases are attached (**Figure 3**).[82-83] This results in non-charged backbone, avoiding electrostatic repulsions that are present in hybridization of negatively charged natural nucleic acids.[84-85] The thermal stability of PNA-DNA and PNA-RNA duplexes is higher than that of the corresponding DNA-DNA or DNA-RNA duplexes, and the hybridization is not dependent on the ionic strength of the solution.[85-86] Moreover, PNA is highly resistant to enzymatic degradation.[84, 87] On the other hand, due to the non-charged backbone, PNA is less soluble in aqueous buffers and is therefore more prone to aggregation.[82] The neutral charge of PNA has made it an attractive alternative to DNA probes especially in electrochemical nucleic acid sensing[88-90], but PNA probes have also been used in optical[91-92] and quartz-crystal microbalance[93-94] based sensors.

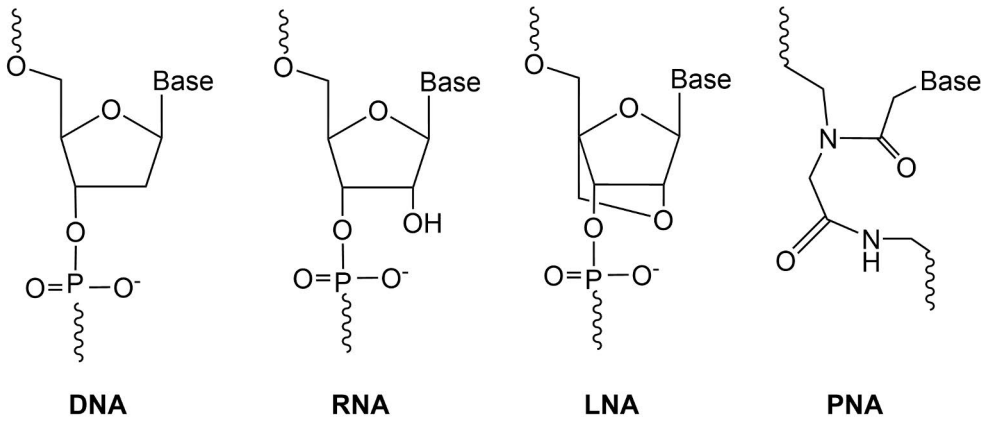

Figure 3. Structures of DNA, RNA, LNA and PNA backbones. Adapted from Kubota et al. (2006).[95]

Another way to improve the binding properties of nucleic acid probes is by using base stacking interactions, which refer to noncovalent forces between adjacent nucleobases.[96-97] Even though the thermodynamic basis of base stacking is not fully understood,[98] its contribution to the duplex stability is well documented.[96, 99-103] Due to the base stacking interactions, a double-stranded DNA duplex with a nick is almost as stable as a DNA duplex formed by two intact strands. Introducing a gap prevents the stacking, reducing the hybridization stability.[99] Base stacking has been

used in FRET-based biosensing of micro-RNAs (miRNA) by designing the probes in such way that the stacking interactions with the target miRNA allow for the formation stable duplex, bringing the donor and acceptor to close proximity to enable FRET.[104-105]

2.3.4 Aptamers

Aptamers are single stranded nucleic acid sequences with a specific three-dimensional structure making them capable of binding to specific non-nucleic acid targets.[106-107] Aptamers have been generated toward a wide range of targets, varying from ions[108-109] and small molecules[110-112] to proteins[113-114], sugar moieties[115-117] and even whole cells.[118-119] New aptamers can be developed by an artificial process called systematic evolution of ligands by exponential enrichment (SELEX), in which molecules with highest binding affinity to the target molecule are isolated from a pool of random RNA or DNA sequences.[106-107] Once the sequence has been identified, aptamers can be easily produced using automated oligonucleotide synthesis methods.[120]

Typically, the affinities of DNA and RNA aptamers obtained with the SELEX process vary between micromolar and nanomolar range,[121-123] but even picomolar affinities have been reported.[124-126] However, the three-dimensional structure and therefore, the target recognition of aptamers is considerably influenced by the environmental variables, such as pH and buffer composition, which may limit their applicability for target recognition in biological samples.[127] Moreover, biological samples contain nucleases, and modified nucleic acids may be needed to prevent the enzymatic degradation of aptamers.[128]

2.4 Solid phases

Heterogeneous assays utilize solid phases for separation of bound and unbound reagents. Immobilization of binders strongly affects the binding kinetics, because the binding rate is predominantly limited by the mass transport of the biomolecules to the capture surface and not by the binding reaction rate.[35-36, 129] Therefore, the choice of solid phase has a pivotal importance for the binding kinetics. Kinetics does not only affect the assay time, but also sensitivity, because nonspecific binding usually increases with the incubation time.[53, 55]

In conventional microtiter plate-based assays, the binding only occurs on the binder-coated surfaces of the microtiter wells. During the incubation with the sample, the binding quickly depletes the free analyte molecules close to the surface, creating a concentration gradient between the surface and the bulk solution (i.e. diffusion layer). The binding rate of bioaffinity assays is directly proportional to the concentrations of free analyte and binders:

$$r = k_a[L][B] \quad (6)$$

where r is the binding rate, k_a is the association rate constant of the binder, [L] is the concentration of the ligand and [B] is the concentration of the binder. Therefore, the reduction of local [L] reduces the binding rate. The mass transfer is typically enhanced by mixing the microtiter plates, reducing the thickness of the diffusion layer, but generally used orbital shaking does not completely eliminate this limitation.[35]

Microparticles provide an alternative solid support system that provides a large capture surface area and allows for more even distribution of the binders in the bulk solution. This decreases the diffusion distance between the analyte and binder molecules, improving the binding kinetics.[53, 130] Additionally, the concentration of the binders can be increased more freely than in microtiter plate-based systems by increasing the amount of particles in the reactions, whereas the surface area of a microtiter well is limited by the well dimensions. As seen from equation 6, this increases the binding rate. On the other hand, increasing the number of beads and thus the surface area typically results in lower signal to background ratios and elevated LoDs.[10, 131] Microparticles have also been used for preconcentrating the analyte from larger sample volumes to reach lower LoDs.[33, 132] The main drawback of particle-based assays is more complex handling of the particles compared to microtiter plates.

Membrane based solid-phase systems are commonly used in lateral flow assays, but they can also be used in other kinds of assay platforms, such as dot-blot assays and microarrays.[133-135] Nitrocellulose is the most widely used membrane material, but other materials, such as nylon and polyethersulfone can also be used.[36, 136] The porous 3D structure of the membranes enables immobilization of high amounts of binders to a small area.[36] In lateral flow assays, the reagents flow through the membrane driven by capillary forces. The analyte has to bind to the test line during the short time period during which it passes the test line, but the binding kinetics is enhanced by the high local binder concentration and short diffusion distance at the test line.[54, 137]

2.5 Detection technologies

Detection of bound biomolecules in bioaffinity assays generally relies on conjugation of detectable molecules, i.e. labels, to at least one of the assay components. Labels can be either directly detectable or require separate signal generation or amplification steps. Research aiming to improve immunoassay sensitivity has driven the development of detection technologies. Early immunoassays relied on radioisotope labels, but the sensitivity of such assays was strongly limited by the amount of radioactive decay events during the measurement time.[2, 41] Additionally, the safety issues related to handling and disposal of radioactive materials as well as limited stability of radioisotope tracers prompted the development of non-isotopic detection technologies.[40] Especially non-competitive bioaffinity assays greatly benefit from

detection technologies that are capable of producing more signal per binding event, i.e. have higher specific activity.[2, 41] Other important characteristics for ideal detection technology include high robustness, good label stability, low instrument requirements and suitability for multiplexing.[40, 138] This chapter introduces some of the commonly used optical detection technologies.

2.5.1 Enzymes

First enzyme-linked immunosorbent assays (ELISA) were introduced in 1971 by two groups independently: Engvall and Perlmann by using alkaline phosphatase[3] and van Weemen and Schuurs by using horseradish peroxidase.[4] To this day, these enzymes are most commonly used in ELISA.[28, 138-140] Detection of enzyme labels is based on enzymatic reaction converting suitable substrates into detectable products. The choice of substrate depends on the desired analytical sensitivity and the available instrumentation for the readout, and depending on the substrate, the product can enable colorimetric, chemiluminescent or fluorescent detection.[28, 140-141]

Typically used enzyme labels exhibit fast turnaround rates, producing large amounts of detectable molecules per binding event, thus providing efficient signal amplification.[138] Amplification of the signal greatly improves the analytical sensitivity of the assays, but especially with colorimetric substrates, the dynamic range is limited to 2–3 orders of magnitude.[142] Therefore, reliable quantification may require analyzing several dilutions of unknown samples. Fluorogenic substrates provide improved sensitivity and wider linear range compared to colorimetric substrates, but their detection is limited by autofluorescence background under continuous light excitation.[28, 143] Chemiluminescent substrates can reach lowest detection limits but the signal decays over time.[140, 144]

Enzymes and their substrates are also sensitive to storage and assay conditions and possible enzyme inhibitors in the sample may reduce enzyme activity, causing erroneous results.[138] Moreover, the diffusion of the reaction products limits the suitability of enzyme labels for spatial multiplexing, although multiplex ELISA arrays have also been developed.[145] These arrays rely on real-time imaging of chemiluminescence generated locally in the array spots by the enzyme reaction.[146-147]

2.5.2 Fluorescent labels

Conjugation of binders with fluorescent molecules enables direct detection of tracers, omitting the enzyme reaction. However, autofluorescence of the biomolecules and other assay materials upon photoexcitation increases the background signal, strongly limiting the sensitivity achieved by conventional fluorophores.[148-149]

Time-resolved fluorometry exploits the long excited-state lifetimes of lanthanide ions to temporally eliminate autofluorescence background, which has much shorter lifetime.[148] Lanthanide ions, such as Eu^{3+} or Tb^{3+}, are carried by organic chelates that permit their conjugation with affinity binders. Additionally, the chelates enhance the lanthanide fluorescence by harvesting excitation light and transferring the energy to the lanthanide ion.[150] Lanthanide chelates have narrow emission bands and large Stokes shift, making them excellent labels for sensitive bioaffinity assays.[150] In dissociation-enhanced lanthanide fluoroimmunoassay (DELFIA) technique, the lanthanides are coupled to the antibodies or other bioaffinity binders via non-fluorescent chelates. After carrying out the assay, a separate signal enhancement step is required, similarly to common enzyme labels. In the signal enhancement step of DELFIAs, the lanthanide ions are dissociated from the complexes upon addition of enhancement solution, to form fluorescent lanthanide chelates into the solution.[5] Intrinsically fluorescent lanthanide chelates,[151-154] on the other hand, allow for detection of lanthanide fluorescence directly from the surface, thus simplifying the workflow and enabling spatial multiplexing and microspot assays.[2, 40] To further enhance the sensitivity, lanthanide chelate doped nanoparticles have been used. A single nanoparticle can carry tens of thousands of lanthanide ions, strongly enhancing the signal response per binding event.[155-156]

Time-resolved fluorometry overcomes many of the disadvantages of radioisotope, enzyme and fluorophore labels and has improved the sensitivity of bioaffinity assays.[142, 153] However, the technology relies on relatively complex and expensive instrumentation, such as pulsed UV excitation source, retaining it mostly as a research and central laboratory technology. Additionally, the long excited-state lifetimes result in low photon flux, which may limit the detectability of trace amounts of lanthanide chelates.[157]

2.5.3 Oligonucleotide tags

Development of polymerase chain reaction (PCR) and other molecular biology techniques rendered specific nucleic acid sequences highly detectable via enzymatic or non-enzymatic amplification methods. Various methods have been used for detection of nucleic acid labels, including intercalating dyes, fluorescently labelled probes and sequencing.[10, 158-160] Due to the efficient amplification of the nucleic acid labels, the specific activity of the signal generating element used for their detection is less critical for analytical sensitivity. Depending on the amplification and detection methods, nucleic acid labels can be used for spatial, spectral and sequence-based multiplexing. Nucleic acid amplification techniques can be exploited also in protein detection by coupling nucleic acids to antibodies or other protein binders.[161]

2.5.4 Upconverting nanoparticles

UCNPs are inorganic nanocrystals consisting of a crystalline host matrix, such as $NaYF_4$, doped with lanthanide ions that give them their characteristic optical properties. Typical dopants are Yb^{3+} acting as a sensitizer and Er^{3+} or Tm^{3+} as an activator.[19, 162] In upconversion process, the sensitizers absorb excitation photons (Yb^{3+} at 980 nm) and transfers energy to activator ions. The activators have metastable, long-lived excited states, enabling stacking of the energy from two or more excitation photons before emitting it in a single photon. Due to this, the emission occurs at higher energy and shorter wavelength than the excitation, which is called anti-Stokes shift.[17, 19] The energy level diagram and emission spectrum of Er^{3+} doped UCNPs are presented in **Figure 4**.

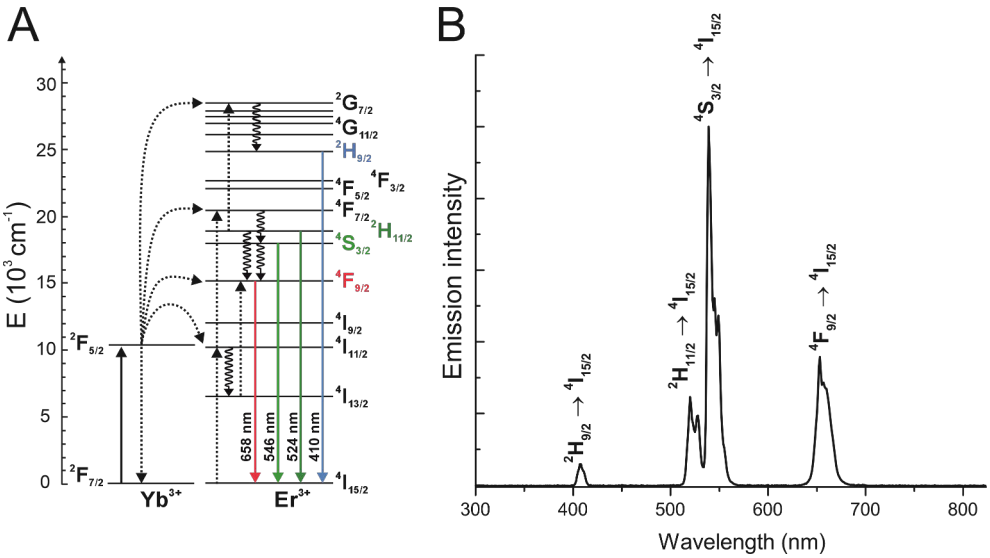

Figure 4. A) Energy level diagram of Yb^{3+}/Er^{3+} doped upconverting nanoparticles. Solid arrows represent photon absorption and emission, dotted lines represent energy transfer and wavy arrows represent relaxations. Alternative paths for red emission are excluded for simplicity. B) Emission spectrum of Yb^{3+}/Er^{3+} doped upconverting nanoparticles upon 980 nm excitation. Figure adapted from Lahtinen (2019)[163] and Würth et al. (2017).[164]

From the perspective of bioaffinity assays, UCNPs have numerous advantages. Most importantly, the large anti-Stokes shift allows for complete elimination of autofluorescence background, which always occurs at longer wavelengths than the excitation light.[14-15, 18, 165] Even though the quantum yield (i.e. the number of emitted photons per the number of absorbed photons) of UCNPs is low,[166] the anti-Stokes emission allows for increasing the excitation power density without increasing the autofluorescence background, dramatically improving the signal to background

ratio.[26, 167] Therefore, trace amounts of UCNPs can be detected with simple and inexpensive instruments, and with more sophisticated instrumentation, even single UCNPs can be detected.[15, 165, 168-169] Moreover, the luminescence can be read directly from the surface without additional enhancement steps, enabling spatial multiplexing.[170] By combining UCNPs doped with different activators, spectral multiplexing is also possible, but usually limited to 2 or 3 wavelengths.[171-172] Another benefit is that the luminescence remains stable over time and can be repeatedly measured without photobleaching.[173-174]

UCNPs are typically synthesized in organic solvents, and the as-synthesized UCNPs are capped with hydrophobic ligands, typically oleic acid.[19, 175-176] Various surface modification strategies have been developed to render UCNPs water dispersible and to introduce functional groups for conjugation with affinity binders.[27, 176] The oleic acid is usually removed, either by acid wash or ligand exchange reaction, followed by coating of the surface with hydrophilic ligands, such as polyethylene glycol (PEG), poly(acrylic acid) (PAA) or by silanization.[176-179] Alternatively, a second layer of amphiphilic ligands can be added on top of the oleic acid surface, forming a bilayer with hydrophilic outer surface.[27, 180] Another option is to chemically modify the hydrophobic ligands. i.e. via oxidation, to introduce hydrophilic functional moieties that can be used for the subsequent bioconjugation.[27]

The choice of surface modification has a remarkable role on the properties of the UCNP labels in bioaffinity assays. For example, PAA contains a large number of carboxylic groups for coordination with lanthanides as well as for conjugation with biomolecules. It forms a thin but dense layer on the nanoparticle surface. PAA coated UCNPs have been shown to have excellent colloidal stability and low tendency to aggregation.[181] On the other and, the strong negative charge of PAA makes them prone to nonspecific interactions with positively charged molecules. In contrast, PEG coating has a neutral charge[182] and PEG coated UCNPs are highly resistant to protein corona formation, reducing the nonspecific interactions.[183] PEG itself does not contain functional groups for bioconjugation, but PEG linkers with various functional groups are commercially available. The optimal surface modification always depends on the desired properties for the specific application. For example, lateral flow assays are particularly sensitive to particle aggregation,[184] *in vivo* applications require resistance to protein corona formation[185] and in FRET assays, the coating has to be thin as the FRET efficiency diminishes rapidly with increasing distance between the donor and acceptor.[186]

UCNPs have been used as labels in bioaffinity assays in various platforms, such as microtiter plate-based assays,[22, 24] lateral flow assays,[25, 165, 172, 184, 187-188] microarrays,[170] microfluidic assays[132] and FRET-based homogeneous assays,[105, 186] and they have proven their potential in ultrasensitive biosensing. For instance, Makhneva et al. (2022) compared HRP, carboxyfluorecein and UCNPs as labels for

prostate-specific antigen (PSA) detection, reaching 15 and 34 times lower LoDs with UCNPs compared to horseradish peroxidase and carboxyfluorecein, respectively. Francés-Soriano et al (2022) improved the LoD of FRET-based hybridization assay by more than 20-fold by replacing the quantum dot donors with UCNPs.[105] Juntunen et al. (2016) reached more than 50-fold improvement in LoD by using UCNP reporters compared to europium chelate doped nanoparticles in a lateral flow assay for detection of cTnI.[189]

Nonspecific binding is the main factor limiting the analytical sensitivity of upconversion-based heterogeneous bioaffinity assays.[18, 20-21, 24-26] This might be partly due to the larger surface area of nanoparticles compared to molecular labels and enzymes interacting with the capture surface,[21, 26, 185] but also due to the high detectability of UCNPs making even trace amounts of nonspecifically bound labels detectable.[22]

2.6 Methods to improve analytical sensitivity

To improve the analytical sensitivity of an assay, there are in principle two approaches: either enhancing the specific signal response from the analyte or reducing the background noise in the absence of the analyte. Optimizations of assay conditions, such as compositions of assay buffers, concentrations, pH, incubation times and temperatures, generally aim to do both and thus increase the signal-to-noise ratio. However, only a limited improvement can be achieved by simple optimizations, and therefore, more sophisticated methods have been developed to further push the limits of analytical performance.

2.6.1 Signal amplification

In addition to selecting a high specific activity reporter technology (discussed in section 2.5), the signal response per analyte binding event has been increased by various enzymatic and non-enzymatic cascade reactions. However, usually signal amplification eventually results in amplification of background signal as well, and the amplification translates into improvement of analytical sensitivity only if the specific signal is amplified more than the background signal. Especially with modern, highly detectable labels, only limited benefit can be achieved by signal amplification, unless it is combined with efficient background reduction.

2.6.1.1 Branched DNA assays

Branched DNA (bDNA) technology aims to improve the analytical sensitivity of hybridization assays by increasing the number of labels binding to a single target

molecule.[190-191] It employs a series of DNA probes that hybridize to each other and the target, forming a branched structure that connects several labels to one analyte binding event thus amplifying the signal.[191] bDNA technology has been mostly used for quantification of viruses,[190-195] but other applications include detection of bacteria[196] and studying mRNA expression levels.[197-199]

Three generations of bDNA assays have been developed. In the first-generation bDNA assays, several bDNA amplification probes hybridized with the target sequence, and each amplification probe contained several branches to which the enzyme labels were bound. The target was captured onto the solid phase by several immobilized capture probes.[190] The second-generation configuration developed by Kern et al. (1996) introduced preamplification probes to further increase the amount of labels, as each preamplification probe was able to hybridize with multiple amplification probes. This resulted in strong enhancement of the signal. Moreover, the background originating from nonspecific hybridization was reduced by decreasing the length of the capture probes and by using a pair of probes in a cruciform design instead of one longer probe to connect the preamplification probes with the target. The authors reported at least 20-fold improvement in sensitivity compared to the commercialized first-generation bDNA assay, Quantiplex HIV RNA 1.0.[191] The nonspecific hybridizations were further reduced in the third-generation bDNA assays by using non-natural isoG and isoC nucleobases in the synthesis of the probes.[200] These modified nucleobases hybridize with each other but not with the natural nucleobases.[201] As a result, LoDs of less than 100 copies/mL have been reached.[194-195, 200] However, including these modified nucleobases in the large number of probes required for the signal amplification increases the costs of the assays, which may limit the suitability of the technology in some applications.

In addition to enzymes, bDNA technology has also been applied to assays using nanoparticle reporters. Brandmeier et al. (2024) studied different bDNA assay configurations with UCNP labels and bacteriophage M13 as a model analyte.[202] A 13-fold improvement in analytical sensitivity was reached with bDNA signal amplification, compared to an assay without amplification. Even though the detection limits of assays employing highly detectable labels are usually limited by nonspecific binding rather than detectability of the label, the bDNA technology provides simple signal amplification, which can be particularly beneficial in point-of-care applications.[192]

Nucleic acid detection is routinely done using methods relying on target amplification, mostly by PCR.[203-205] The bDNA assays overcome some of the limitations of PCR technology: no expensive equipment, such as thermocyclers, are needed and cross-contamination between samples is less likely because the target is not amplified.[206-207] Furthermore, the sample pre-processing required for bDNA assays is minimal.[194, 197] As errors originating from nucleic acid extraction and

exponential target amplification are eliminated, relatively small differences in concentrations can be quantified.[193, 197-198, 206]

2.6.1.2 Immuno-PCR

The invention of PCR in 1985[208] revolutionized the sensitive detection of nucleic acid targets and prompted interest in developing something similar for protein biomarker detection. Proteins cannot be amplified as nucleic acids, but Sano et al. (1992) combined PCR with immunoassays by attaching a specific DNA sequence to an antibody and using its amplification by PCR to quantify the concentration of a protein analyte.[161] The early development of immuno-PCR was done by directly coating the purified analyte to microwells. Typically, LoDs between 580–5800 molecules (corresponding to 20–200 aM in 50 µL) were reached, demonstrating the potential of the detection system.[161, 209-210] However, these first versions of immuno-PCR were not yet suitable for analyzing real samples, in which the analyte of interest is present in a complex mixture of non-target proteins and other biomolecules. To enable the protein detection in biological samples, immuno-PCR was adapted to the sandwich assay format, typically resulting in femto–picomolar LoDs.[211-214]

The detection of the PCR products was first done by gel electrophoresis, which was time-consuming and had only narrow dynamic range due to the limited detectability of DNA bands with low analyte concentrations and saturation of PCR amplification with high analyte concentrations.[161, 212, 215] Niemeyer et al. (1996) compared different detection methods to improve the analytical sensitivity of immuno-PCR. In their study, the lowest LoD was reached when the amplification product of immuno-PCR was quantified by enzyme linked oligonucleotide assay.[216] However, after the development of real-time quantitative PCR,[217-218] real-time detection was also applied to immuno-PCR.[159] The real-time detection improved quantification precision and avoided the need for sample processing after amplification, reducing the manual workload and risk for cross-contaminating the samples. Moreover, it widened the dynamic range of immuno-PCR, because all of the samples with varying concentrations do not need to be at exponential phase at the end of the amplification.[159]

With real-time detection, the number of PCR cycles can be increased to improve the detection of PCR products without the saturation of the amplification limiting the quantification of the high concentrations. Thus, the analytical sensitivity of immuno-PCR is not anymore limited by the detectability of the PCR product. Instead, the sensitivity is generally limited by the nonspecific binding of the reporter antibody-DNA conjugate resulting in detectable amounts of reporter sequence during PCR amplification.[159, 211, 215, 219-220] Typical LoDs have remained at femto–picomolar range,[219-223] and the complexity of the method and difficulty to control

the background signal are limiting its usability in many applications. Moreover, due to the exponential amplification, even a small change in PCR efficiency results in huge difference in quantification, reducing the quantification precision.[224]

2.6.1.3 Other nucleic acid-based signal amplification systems

In contrast to PCR, isothermal amplification can be carried out using simpler instrumentation, because thermal cycling is not needed. Rolling circle amplification (RCA) is a commonly used isothermal amplification method that has also been used for detection of various targets.[225] In RCA, the hybridization of a circular primer initiates the extension of the DNA strand by strand displacement capable DNA polymerase, resulting in a long single-stranded DNA concatemer product (**Figure 5**, top).[226-227] Therefore, in binding assay detection systems, the RCA targets remain bound to the affinity binder thus preserving the spatial information, unlike PCR products.[10] RCA product can be detected by hybridizing with several fluorescently labelled short DNA probes, amplifying the signal per analyte binding event.[10, 227] RCA is a linear amplification process, thus overcoming the quantification imprecision related to exponential amplification.[224]

The main disadvantages of enzymatic amplification systems are limited stability of enzymes and their sensitivity to inhibitors. Non-enzymatic signal amplification systems of nucleic acid labels often utilize a series of toehold-mediated strand displacement reactions, which are highly programmable hybridization reactions where DNA or RNA strands displace other strands based on differences in the free energy of their hybridization. The reactions start by the hybridization of an initiator sequence to a single-stranded toehold domain. Subsequently, the initiator displaces the original strand via branch migration. By coupling multiple strand displacement reactions together, various signal amplification strategies have been engineered.[228-229]

In hybridization chain reaction (HCR), an initiator sequence propagates a series of strand displacement reactions between two sets of hairpin-structured oligonucleotides to form a nicked double stranded DNA helix (**Figure 5**, middle).[229-230] Opening of the original hairpins results in signal generation for example by using DNA intercalating dyes[228] or DNAzyme activity.[229, 231] Instead of a linear HCR product, also more complex, branched assemblies have been constructed.[232]

Another example of non-enzymatic amplification is catalytic hairpin assembly (CHA). Like HCR, a typical CHA also starts by hybridization of an initiator sequence with a hairpin-structured oligonucleotide, resulting in an opening of the hairpin. The single-stranded end of the opened hairpin hybridizes with another hairpin-structured oligonucleotide, which displaces the initiator. After the release, the initiator can initiate another cycle, and thus, a single binding event produces a

large amount of short double-stranded sequences that are released into the solution (**Figure 5**, bottom).[228]

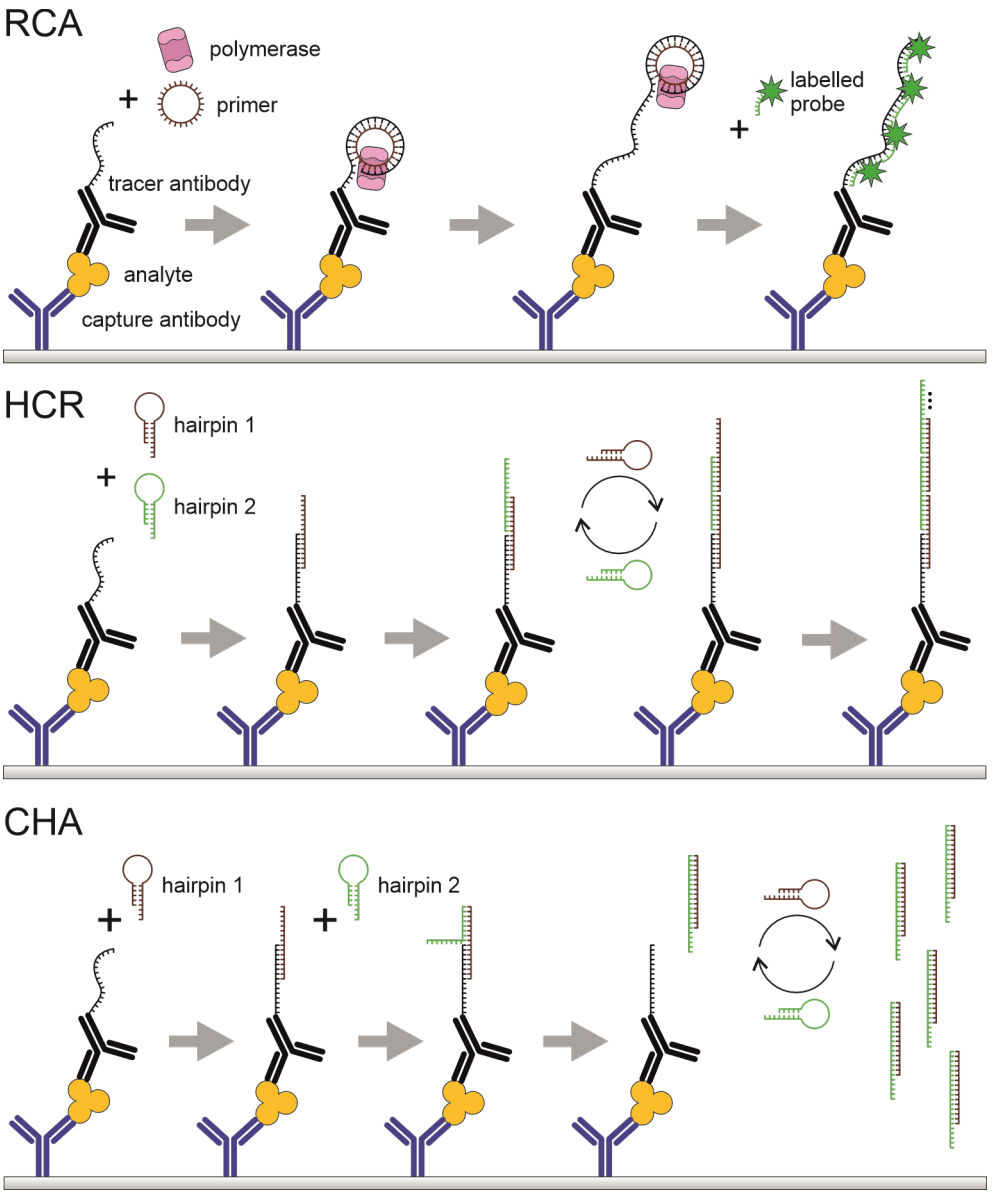

Figure 5. Schematic illustrations of signal amplification by rolling circle amplification (RCA), hybridization chain reaction (HCR) and catalytic hairpin assembly (CHA).

2.6.2 Background reduction

The background signal in bioaffinity assays using optical labels consists of background signal of the detector, the assay materials (autofluorescence), and nonspecific binding of reporter conjugates onto the detection surface.[42-43, 233] The higher the background signal and noise, the higher the specific signal has to be in order to be reliably distinguishable from the background. With high-affinity binders and highly detectable labels, nonspecific binding usually becomes the major limiting factor to reach ultrasensitivity.[2, 20, 22, 41, 233-235]

Some level of nonspecific interactions always occurs in bioaffinity assays, especially when analyzing biological samples, as they contain complex mixtures of non-target proteins and other biomolecules typically in much higher concentrations than the analyte of interest.[236] Proteins tend to stick to most surfaces and each other,[236-237] which can either increase[20, 55] or decrease[21, 50, 194, 238] the background signal and thus cause errors to the quantification of the analyte. Due to the biological variation, the amount of nonspecific binding varies between samples, thus hindering the elimination of background signal by simply subtracting the average background.[52] Therefore, various methods for reduction of background signal from nonspecific binding have been extensively studied.

2.6.2.1 Separation

Heterogeneous assay format decreases matrix related interferences compared to homogeneous assays, due to the addition of reagents in separate steps and removal of the unbound reagents before the next step.[28] However, a fraction of biomolecules can be adsorbed to the surface and immobilized binders nonspecifically, which may result in interactions with other assay components in later assay steps. As nonspecific interactions are much weaker than specific interactions, nonspecific binding can be decreased to some extent by stringent washing.[53] On the other hand, too harsh wash conditions eventually lead to losses in specific binding, too. In theory, rinsing of the surface dissociates molecules in respect to their dissociation rate constant, k_d. Most of the nonspecific interactions have higher k_d than specific interactions. However, a fraction of nonspecific binding has similar k_d as typical specific binding, and in that case, rinsing does not increase the ratio of specifically to nonspecifically bound molecules.[236]

Zhang et al. (2013) reduced nonspecific binding of DNA-labeled detection antibody in immuno-PCR by adding 0.1% sodium dodecyl sulfate to the washing buffer.[222] Even though the addition strongly decreased the background, the method is not selective and inevitably leads to some loss of specific signal, too. In order to strengthen the specific binding and thus to enable more stringent washing without detachment of specifically bound labels during washes, Mendez-Gonzalez et al.

(2018) developed a DNA sensor based on target-dependent photochemical ligation of the capture and tracer probes. Covalent coupling allowed for reduction of nonspecific binding by extreme wash conditions with significant improvement in the recovery of the specific signal. The assay reached an LoD of 20 fM for the detection of micro-RNA-195 DNA analogue.[239] Later, they used similar strategy combined with magnetic bead capture and showed 10-fold improvement in sensitivity with photochemical ligation compared to a reference assay without ligation.[240] Raiko et al. (2021) reduced nonspecific binding of PAA coated UCNP antibody conjugates in a heterogeneous immunoassay by using a wash buffer with pH 10.25 in the washing step after the UCNP incubation. The beneficial effect of high pH was most likely based on significantly reduced ionic interactions between negatively charged UCNP conjugates and plasma proteins adsorbed on the detection surface.[23] However, this approach is applicable only if the specific binding between the antibody and analyte of interest is not deteriorated at elevated pH.

2.6.2.2 Surface chemistry & blocking

In heterogeneous bioaffinity assays, the chemical properties of the capture surface have a crucial role on the nonspecific binding. Additionally, in assays that employ nanoparticle reporters, the surface modification of the reporters is of high importance, because of the large surface area interacting with biomolecules and other surfaces. Nanoparticles have been shown to adsorb proteins from biofluids, forming a protein corona, which affects their interactions with other surfaces and biomolecules.[183, 238, 241] Therefore, passivation of nanoparticle surface is of particular interest in *in vivo* applications and one-step assays, where the nanoparticles are in direct contact with biological fluids.

The most straightforward method to immobilize proteins and nucleic acids onto solid-phase surfaces is through passive adsorption. In case of proteins, passive adsorption is based on van der Waals and hydrophobic interactions between the solid-phase (e.g. polystyrene) and the proteins.[36, 242] Passive adsorption of nucleic acids is mainly achieved through van der Waals and electrostatic interactions.[243] Passive adsorption is a random process and thus does not allow for controlling the orientation of the binders.[36, 243] Additionally, proteins are partially denatured in the process, which may affect their binding affinity.[36]

Alternatively, various linker proteins can be used. Streptavidin is one of the most commonly used linker proteins due to its high affinity (K_a approximately 10^{14} M^{-1}) to biotin.[244] Streptavidin is a versatile linker, as it can be used for immobilization of any biotinylated molecules. Biotinylation and subsequent immobilization of antibodies to streptavidin coated polystyrene microtiter wells has been shown to improve the functionality of the capture surface compared to direct coating through

passive adsorption.[245] On the other hand, streptavidin coated surfaces may exhibit elevated nonspecific binding compared to directly coated surfaces.[55]

After coating the surface with affinity binders, the remaining protein binding surface is usually saturated with blockers to prevent nonspecific binding. Bovine serum albumin (BSA) and milk proteins are widely used for this purpose. In a study by Farajollahi et al. (2012), 1% BSA was shown to be more effective in blocking nonspecific binding in ELISA, compared to 1% milk powder and 2% casein[55], whereas in a study by Güven et al. (2014), skimmed milk was found to be most effective.[52] Their data also suggested that some serum samples contained antibodies against some blocking agents, thus inducing nonspecific binding. In contrast, Ahirwar et al. (2015) demonstrated that BSA blocking was insignificant in ELISA, as long as the washing buffer contained detergent.[246] Moreover, BSA preparations have been shown to vary in blocking effectiveness.[247] It can be concluded that blocking can never completely prevent nonspecific binding and if extreme sensitivity is required, the surface blocking may have to be individually optimized for each assay.

Another approach to prevent nonspecific binding is chemical modification of the surface prior to the immobilization of the affinity binders. Various anti-fouling surfaces have gained significant interest in the field of biosensing. They usually consist of highly hydrated molecules that are charge-neutral or have a low negative charge, reducing unwanted hydrophobic and electrostatic interactions with biomolecules.[248-249] PEG is widely used in anti-fouling surfaces, as it has proven to be highly resistant to protein adsorption in biological fluids.[183, 185, 250-252] PEG can be functionalized with various reactive groups, such as carboxyl, amine, azide, thiol or NHS ester, enabling easy conjugation with various biomolecules.[253] Other anti-fouling surface coatings include dextran[254] and zwitterionic polymers, such as poly(sulfobetaine) and poly(carboxybetaine).[248] Despite the effective inactivation of the surface itself, a dense layer of affinity binders on the capture surface may also induce nonspecific binding,[236] further complicating the elimination of nonspecific binding.

2.6.2.3 Sample pretreatment

Various sample pretreatment methods have been developed to reduce sample matrix related interferences. The most common pre-treatment is diluting the biological samples with artificial buffer, which may be supplemented with suitable additives to reduce nonspecific interactions and to favor specific binding.[236, 255-256] Dilution reduces the nonspecific binding by lowering the concentrations of interfering molecules, but it obviously reduces the analyte concentration accordingly.[236]

Especially in nucleic acid diagnostics, DNA or RNA isolation from the sample before analysis is common practice.[257-258] In case of protein biomarkers, isolation of the analyte from the sample is not as straightforward. McCutcheon et al. (2010) eliminated matrix interference in neutralizing antibody assay using protein A/G resin to separate immunoglobulins from serum samples before analysis. The pre-treatment resulted in improved sensitivity and elimination of interference caused by rheumatoid factor in rheumatoid arthritis patient samples.[259] However, most analytes cannot be easily isolated from high-abundance biomolecules. Moreover, purifications introduce an additional step to the workflow and may induce variation and sometimes bias to the quantification.[260]

Instead of isolating a specific analyte-containing fraction from the sample material, the depletion of nonspecifically binding molecules can also be used to reduce nonspecific binding of sample proteins to the detection surface. Güven et al. (2014) pretreated serum samples exhibiting elevated nonspecific binding by incubating them on uncoated ELISA wells before the assay. The nonspecific binding was reduced, but not completely eliminated.[52] Darmanis et al. (2010) incubated serum samples with microparticles coated with nonspecific goat IgG molecules to deplete potentially interfering substances prior to analysis.[261] The microparticles in the depletion step mimicked the actual capture microparticles but were lacking the analyte binding activity, and thus, only nonspecific binding could occur. They were able to reach similar LoDs in 100% serum or plasma as in 10% dilutions, which equals to 10-fold improvement in the analytical sensitivity calculated as concentrations in undiluted sample. Similarly, Näreoja et al. (2017) removed compounds interfering in an immunoassay for thyroid stimulating hormone (TSH) by incubating TSH spiked serum samples in anti-PSA antibody coated microtiter wells before analyzing them by the TSH immunoassay.[262] The pretreatment significantly increased the serum recovery of TSH at serum quantities over 5% compared to untreated samples.

By identifying the interfering molecules, targeted countermeasures can be designed. Bayoumu et al. (2021) reduced matrix-related background in lateral flow immunoassay by introducing an anti-IgM “scrub line” and dried ethylenediaminetetraacetic acid (EDTA) to the test strips.[188] As the treatment was incorporated into the test strip, additional steps were completely avoided, which is particularly desirable in point-of-care applications. Complement-related interference has also been inhibited by heating the samples prior to analysis, but this is feasible only for heat-resistant analytes.[63]

2.6.2.4 Complex transfer assays

Complex transfer assays overcome the sensitivity limitation set by the nonspecific binding by utilizing an elution step, which only detaches specifically bound immuno or hybridization complexes from the first capture surface. Nonspecifically bound molecules remain on the surface. Afterwards, the eluted complexes are transferred to a fresh secondary capture surface for re-capture and signal measurement.

The concept was originally developed by Kohno and Ishikawa (1987) for a serological enzyme immunoassay, where nonspecifically bound immunoglobulins result in high background signal. In the first capture step, they used antigen-dinitrophenyl-biotin conjugates immobilized onto an anti-dinitrophenyl IgG coated surface. After incubation with the serum sample and washing the surface, the specific immunocomplexes were eluted by adding excess of ϵN-2,4-dinitrophenyl-L-lysine, which displaced the antigen-dinitrophenyl conjugates from the anti-dinitrophenyl IgGs. The released complexes were re-captured onto an avidin coated surface. An excess of detection antibody-enzyme conjugate was added in a separate step after the complex transfer procedure, and thus, nonspecific binding of the reporter could still occur on the detection surface. Nevertheless, they achieved approximately 10 000-fold improvement in the detection sensitivity by eliminating the background originating from nonspecifically bound immunoglobulins and other sample components.[263] Later, the assay concept was further improved by incubating the sample simultaneously with the detection antibody-enzyme conjugate and antigen-dinitrophenyl conjugate, simplifying the assay protocol and eliminating the background signal originating from both, nonspecifically bound serum immunoglobulins and nonspecifically bound label conjugates (**Figure 6**).[264]

Watanabe and Hashida (2018) developed sandwich immunocomplex transfer enzyme immunoassays and conventional enzyme immunoassays for detection of three cytokines. Their detailed comparison revealed, that even though 44–82% of the nonspecifically bound reporters were released during the elution from the first capture surface, only 0.8–4.3% of those reporters bound nonspecifically to the second capture surface. The transfer of specifically bound immunocomplexes resulted in 34–66% losses in specific signals, but the elimination of 96–99.6% of the nonspecific binding by complex transfer procedure resulted in approximately 100-fold improvement in the limits of detection.[233]

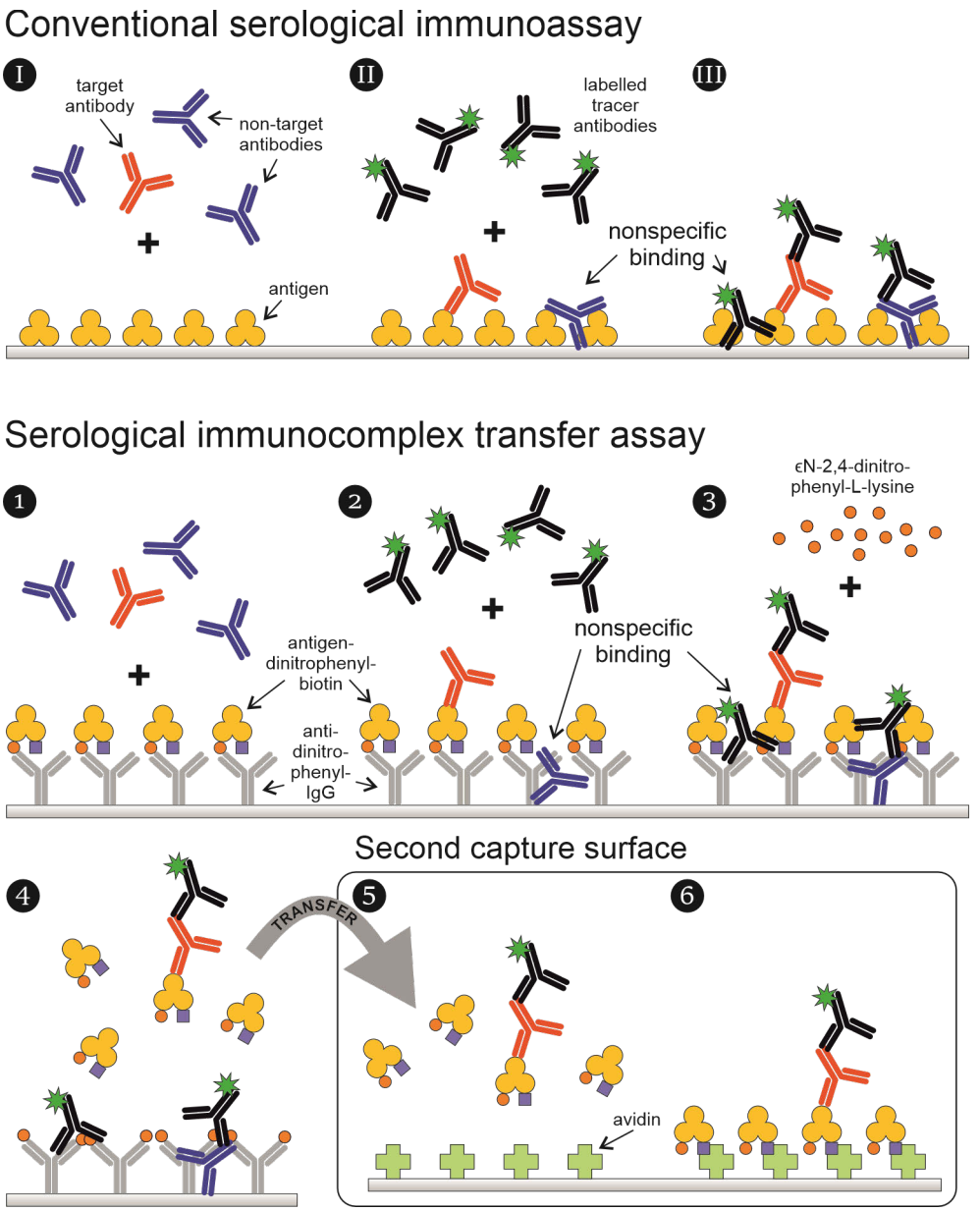

Figure 6. Schematic illustrations of conventional serological immunoassay (I-III) and serological immuno complex transfer assay (1-6). In conventional immunoassays, the background signal generated by nonspecifically bound tracer conjugates limits the sensitivity. In complex transfer assays, the specifically bound complexes are released by addition of εN-2,4-dinitrophenyl-L-lysine (orange) and recaptured onto a fresh capture surface, eliminating the sensitivity limitation set by the nonspecific binding.

Similar principle has been applied in reverse target capture hybridization assay for detection of *Listeria* cells. The target sequence in cell lysate was incubated with poly(dA)-tailed capture probes and labelled probes to form hybridization complexes, which were captured on oligo(dT) coated magnetic beads. After washing, the complexes were chemically eluted and recaptured on fresh oligo(dT) beads. The cycle was repeated and the final elution was done by increasing the temperature, followed by recapture on poly(dT) coated beads or nylon filter. The procedure efficiently eliminated background noise and enhanced the signal to noise ratio by 6.5–7.5 orders of magnitude, enabling detection of only six *Listeria* cells in the presence of 1.25×10^7 non-target cells in the sample.[265]

2.6.2.5 Co-localization assays

In co-localization assays, the background signal from nonspecific binding is reduced by requiring the binding of two labels at the same location to generate specific signal. Even though a certain proportion of labels bind nonspecifically, it is unlikely that nonspecific binding of multiple binders occurs at the exact same location.[33, 266]

Proximity ligation assays (PLA), first published by Fredriksson et al. (2002),[267] combine signal amplification of immuno-PCR assays and background reduction principle of co-localization assays. Two affinity binders are used for detection, each of which is labelled with different DNA oligonucleotides serving as proximity probes. Only simultaneous binding of both affinity binders to the same target brings the DNA probes to close proximity. In the next step, a complementary connector sequence hybridizes with both probes, enabling an enzymatic ligation followed by amplification and quantification of the ligation products by qPCR. Only ligated probes are amplified in PCR, while single proximity probes do not generate signal. The first PLA reached low femtomolar LoDs from only 5 µL sample volume, and the amount of PCR amplification from nonspecifically bound reporters was approximately three orders of magnitude lower than in immuno-PCR with the same reagents.[267]

Due to the extremely specific signal generation, washing steps are not necessary in PLA, unless the sample contains inhibitors of ligation or PCR amplification.[261, 267] On the other hand, washing off the unbound reagents allows for the use of higher concentrations of proximity probes and connector sequence, improving the ligation efficiency without increasing target-independent ligations and may therefore further improve the sensitivity and specificity of the assays.[33, 267] In homogeneous format, proximity probes have to be used at low concentrations to avoid nonspecific ligations in the absence of the target, which may limit the sensitivity of the assays especially with low affinity binders.[160, 267-269] Low probe concentrations may also result in depletion of the probes at high analyte concentrations, limiting the dynamic range of

the assay.[160, 268] Additionally, heterogeneous PLA format enables the use of larger sample volumes, and thus, detection of lower concentrations and improving the reproducibility.[33, 160, 261, 268] However, heterogeneous assay format is only possible, if three affinity binders can bind to the target analyte simultaneously, hindering its use for detection of small analytes.[33, 261]

PLA has been used in various applications, such as quantification of proteins,[267-268] pathogens[270] and cytokines[269] and detection and localization of interactions between various biomolecules *in vitro*[271] and *in situ*[272-273]. Low femtomolar LoDs are typically reached from less than 10 µL sample volumes.

Feng et al. (2023) overcame the requirement for three separate epitopes for heterogeneous proximity ligation assay in their nucleic acid linked immune-sandwich assay (NULISA), which combines the background elimination by proximity ligation and complex transfer assays.[158] In NULISA, both antibodies of a two-site immunocomplex are conjugated with unique DNA oligonucleotides, one of which contains an oligo-dA tail and the other one is biotinylated. The two-site immunocomplexes are first immobilized onto an oligo-dT coated surface. After washing, the immunocomplexes are released by adding low-salt buffer, as the hybridization of oligo-dA tail is highly sensitive to salt concentration. The released immunocomplexes are recaptured onto a streptavidin coated surface for detection. Each oligonucleotide is hybridized with a complementary reporter sequence, and upon analyte binding, the sequences are brought to proximity, enabling their ligation and subsequent detection of the ligated sequence by either PCR or sequencing. Due to an extremely specific signal generation and effective background elimination, the authors reported 10 aM LoDs from 20 µL sample volume, corresponding to only 120 analyte molecules. This is already below the theoretical minimum for quantification with less than 10% imprecision due to the limitations set by Poisson statistics.[43] The main limitation of the technology is the complexity of detection relying on PCR or sequencing.

Some co-localization assays have been developed by labeling both, capture and tracer binders, and by specifically counting only co-localized signals of both labels with high resolution microscopy. The principle has been employed in both, separation-based and separation-free formats, reaching sub-picomolar to picomolar LoDs for proteins and small molecules[50, 274-275] and attomolar LoDs for exosomes.[276] By only counting the colocalized signals of capture and tracer binders, the background from nonspecifically bound tracer binders can be almost completely eliminated.

In typical bioaffinity assays, the capture surface is saturated with binders to maximize the signal to background ratio,[40] making it impossible to image single labelled capture molecules. Colocalization assays that are based on labeling both, capture and tracer binders, require low enough surface density of capture binders to

enable discrimination of single molecules.[50, 274-275] As a result, only a fraction of the surface contains binders and contributes to the specific signal, while most of it is not reactive. According to Roger Ekins's theoretical calculations related to microspot assays (discussed in detail in section 2.6.3), reducing the amount of capture binders by decreasing the active surface area and the field of view in the readout results in increasing signal to background ratios.[40] In contrast, reducing the amount of capture binders by reducing the coating density results in decreasing signal to background ratios, because the nonspecific binding occurs also on the nonreactive surface and is proportional to the surface area.[40] The colocalization readout excludes the background signal originating from nonspecific binding on the nonreactive surface, but if the nonspecific binding occurs closer to a labeled binder than the resolution of the microscope, it cannot be discriminated from specific binding. With low capture binder density, most of the nonspecific binding occurs on the nonreactive surface, where it can be easily discriminated from the specific binding. However, it is possible that the improvement in the analytical sensitivity is mostly based on the decreased capture surface area, as per ambient analyte theory,[40] and that similar improvement could be achieved with microspot coating even without labeling the capture binders. Moreover, the low binder density may result in impaired analytical sensitivity, if the affinity of the binders is not high enough.[50] On the other hand, Hariri et al. (2022) reported that labeling of the capture binders allowed for normalization of the tracer signals to the signals of the capture antibody, thus eliminating the signal variation originating from heterogenicity in the binder density on the capture surface.[50] This corresponds to the ratiometric assay principle proposed by Ekins in 1980s.[277]

Even though co-localization assays have potential to strongly reduce background signal, most of these methods are either complex multi-step assays or require special instrumentation, such as high-resolution fluorescence microscopes.

2.6.3 Microspot assays

In microspot assays, the capture binders are immobilized to a small area, reducing the total capture binder concentration in the reaction. Intuitively, this could be expected to deteriorate assay sensitivity, as a smaller amount of analyte molecules is detected, but Roger Ekins showed in his pioneering work with immunoassays that if the readout is done directly from the surface and if the field of view in the readout is reduced accordingly with the spot size, the effect is actually opposite.[40]

The signal intensity in the direct surface readout detection is determined by the fractional occupancy of the binders in the readout area, assuming that the binder density on the surface is kept constant. Even though increasing the capture binder concentration increases the total amount of captured analyte molecules and labels,

the signal intensity is decreased (**Figure 7**). Consequently, the high capture binder concentration depletes the free analyte molecules from the bulk solution, reducing the fractional occupancy at the equilibrium. According to Ekins's ambient analyte theory, when the capture area is so small that the capture binder concentration is approximately $0.01/K_a$, less than 1% of the total analyte is bound from the bulk solution at equilibrium. As a result, the concentration of the unbound analyte remains almost unaffected, resulting in maximal fractional occupancy. At the same time, the amount of nonspecific binding per surface area remains constant, and thus, reducing the spot size decreases the number of nonspecific binding events in the spot area. Therefore, reducing the spot size increases the signal to background ratio.[37]

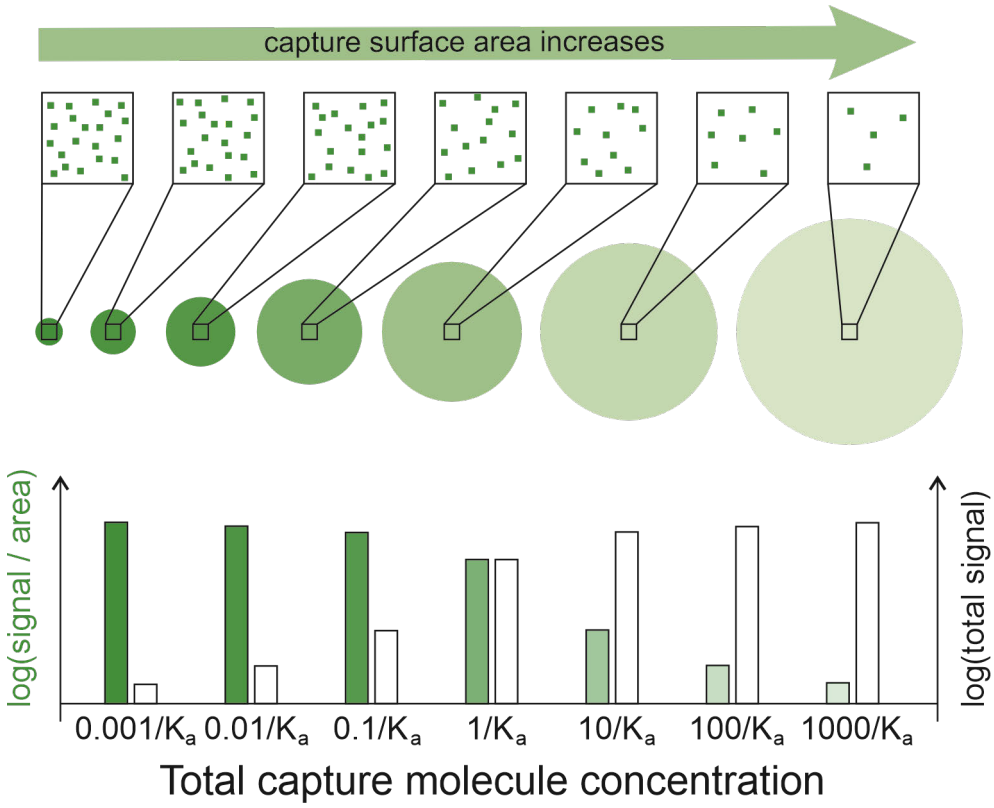

Figure 7. The effect of capture surface area on the specific signal intensity (specific signal per surface area) and total signal with the same analyte concentration and same surface density of capture molecules. Even though the increasing capture surface area increases the total signal, the signal intensity decreases. Reducing the surface area increases the signal intensity until it reaches a constant level at capture molecule concentration of $<0.1/K_a$. Reprinted from Drug Discovery Today, Vol 7, Issue 15, Templin, et al. Protein microarray technology, Copyright (2002), with permission from Elsevier.

The incubation times in bioaffinity assays are usually not long enough to reach equilibrium. Even though reducing the binder concentration decreases the absolute binding velocity (i.e. the number of analyte molecules bound per unit time), microspot assays have a kinetical benefit that the depletion of the analyte molecules from the reaction volume does not slow down the binding velocity over time, and the binding occurs at maximal velocity during the whole incubation.[42] Thus, the fractional occupancy and signal intensity of a microspot assay are higher at any time point compared to a corresponding assay with larger capture surface area, although reaching the maximal signal takes longer in case of microspot assays.[28, 40]

Microspot coating is particularly attractive for multiplexed assay designs, as it enables detection of large amounts of analytes from the same sample without compromising the analytical sensitivity.[40] Numerous different binders can be coated as an array of discrete spots, and spatial resolution avoids the need for separate labels for each analyte. The development of microarray technology was driven by the need for high throughput DNA and RNA analysis methods, but it was soon followed by the development of various protein microarrays. The main challenge limiting the wide adoption of protein microarrays is the reproducibility of the binder spots, and special instrumentation as well as the requirement of highly controlled and optimized printing conditions to produce high quality microarrays.[278-279] Tobos et al. (2020) developed a customizable antibody array by spotting anti-peptide antibodies onto a solid-phase surface.[279] By labelling the analyte specific capture antibodies with unique peptides, custom microspot arrays can be developed in a reproducible way without optimization of the spotting for each capture binder.

Even when ambient analyte conditions are not fulfilled, the signal to background ratio can be increased by reducing the capture surface area, especially by eliminating the binding sites that are outside the field of view in the readout, such as on the walls of microtiter plates.[280] For example, Ylikotila et al. (2005) used special microtiter wells with molded macrospot areas on the bottoms of the wells, avoiding the need for special spotting instrument. They reported 4–8-fold increases in signal intensities of TSH immunoassay with 4.9 mm^2 capture surface area compared to a conventional coating of the entire wells (200 µL coating volume, corresponding to approximately 1.5 cm^2 capture surface area).[281] Later, they did a similar study with cTnI immunoassay and reported 2-fold increase in signal intensity by replacing conventional coating (50 µL coating volume, corresponding to approximately 70 mm^2 capture surface area) by spot coating with 3.5 mm diameter (10 mm^2 capture surface area).[67] Furthermore, they demonstrated that also with spots too large to fulfil ambient analyte conditions, the signal intensities still increased more rapidly than with larger surface area. In both studies, using site-specifically biotinylated Fab fragments instead of mAbs further improved the signal intensities.[67, 281]

2.6.4 Readout modes

In conventional, analogue readout, the signal is measured by integrating the average signal generated by the labels on a relatively large surface area or volume. To generate signal that is detectable in such measurement, a large number of labels need to be measured. For example in typical ELISA, where the fluorescent products of the enzyme reaction diffuse into a few hundred microliter volume, hundreds of thousands of enzymes are needed to generate signal above the background.[7] In contrast, digital readout is based on counting of individual molecules by using high sensitivity microscopes for the readout, together with high specific activity labels that enable detection of single labels.[6, 42]

The most widely used digital bioaffinity assay technology is Simoa, which was developed by Rissin et al. (2010)[7] and commercialized by Quanterix company. It is a digital ELISA platform based on the capture of single analyte molecules on a high excess of magnetic capture beads, typically around 100 000–500 000 per reaction, resulting in either 1 or 0 immunocomplexes per bead.[7, 53] After forming the immunocomplexes and washing the unbound reagents, the beads are isolated into femtoliter array wells for the enzyme reaction and readout. Only one bead can fit in one well, and thus, each well contains either 1 or 0 enzyme labels. Due to the small volume, diffusion of the fluorescent reaction products does not limit the detectability of the enzyme labels, enabling the detection of single enzyme molecules. Thus, the beads can be classified into positive and negative outcomes.[7] (**Figure 8**) The quantification is done based on the proportion of positive beads and Poisson statistics.[7, 51] The technology provides 100-1000-fold improvements in analytical sensitivity over conventional ELISA, enabling detection of subfemtomolar protein concentrations in biological sample matrices.[7, 51]

The sensitivity of Simoa is limited by Poisson noise-associated coefficient of variation, $\sqrt{N}/N$, where N represents the number of detectable events. Poisson noise increases strongly with decreasing number of events, and therefore, high enough value for N is needed for reliable quantification. Even though hundreds of thousands of beads are used for capturing the immunocomplexes in Simoa, only 5–10% of those beads are loaded into the femtoliter array and subsequently analysed in the readout.[53, 282] The low sampling efficiency in bead loading limits the quantification of extremely low abundance analytes, and the full potential of the digital detection technology is not exploited.[53, 283] The sampling efficiency has been improved by isolating the beads into water-in-oil droplets instead of array wells, avoiding the limitation imposed by the limited number of wells in an array.[283] Alternatively, the need for isolating beads to small volumes can be completely avoided by using rolling circle amplification for nondiffusible on-bead signal generation.[10, 284] Both approaches have reached up to 25-fold improvement in analytical sensitivity compared to Simoa, due to the improved sampling efficiency as well as reduced

number of beads in the reaction resulting in higher signal-to-background ratios.[283-284]

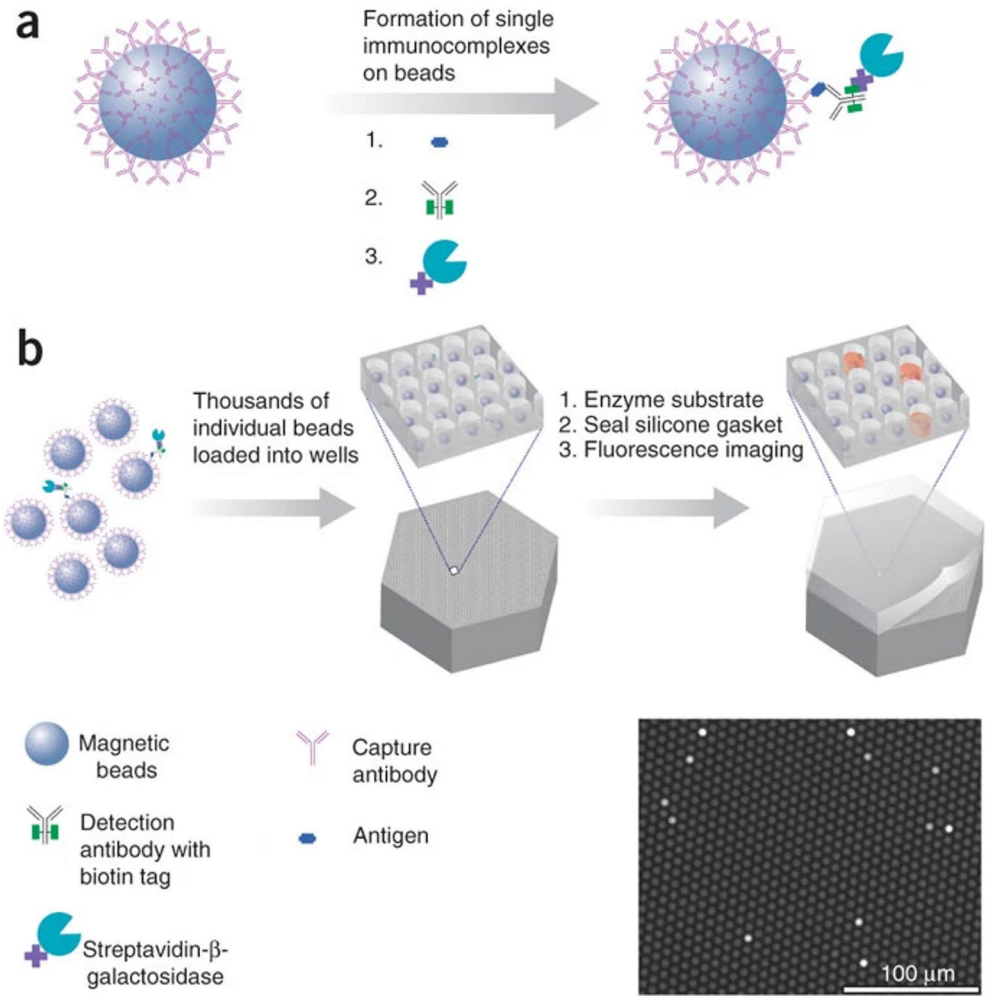

Figure 8. Schematic illustration of Simoa assay platform. a) a large number of capture antibody coated magnetic beads are incubated with the sample, biotinylated tracer antibodies and streptavidin-β-galactosidase conjugates to form single immunocomplexes on beads. b) The beads are loaded onto femtoliter-volume well arrays to isolate one bead per well. After the addition of enzyme substrate, the wells are sealed and fluorescence of the reaction product is imaged. Reproduced with permission from Rissin et al. (2010).[7] Copyright 2010 Springer Nature

Digital ELISA employs enzyme labels, which require separate signal amplification step. With intrinsically luminescent high specific activity labels, such as UCNPs,

digital readout can be done directly from the capture surface without signal amplification, enabling single molecule counting in conventional microtiter plate assay format. Digital readout has typically improved the LoD by approximately an order of magnitude compared to a similar assay with analogue readout.[132, 285-286]

The typical improvement factors achieved by switching from analogue to digital readout are much higher in ELISAs compared to UCNP-based assays, due to the higher detectability of UCNPs enabling more sensitive detection even with analogue readout. Digital readout can be considered an extremely sensitive method for detecting the label, but it does not automatically improve the analytical sensitivity of the assays, either, if the LoD is limited by other factors than the detectability of the label. For example, Schröder et al. (2017) achieved no improvement in the sensitivity of immuno-PCR by switching to digital readout mode, due to the nonspecific binding of tracer antibodies resulting in PCR amplification in the absence of the analyte.[235] Similarly, Brandmeier et al. (2021) reached approximately the same LoD for detection of cTnI with both, analogue and digital readout of UCNP labels, as the LoD was limited by the nonspecific binding, that is detectable with both readout modes.[21]

It is also important to understand that digital readout is not equal to directly counting the analyte molecules in the sample, and calibration is always required to convert the number of detectable events into analyte concentration.[53, 287] In Simoa optimized for lowest possible LoD, only a fraction of analyte molecules is labelled and subsequently detected.[53] However, the ability to detect the label with ultimate sensitivity allows for controlling the background signal by using minimal concentrations of labelling reagents and shorter incubation times, resulting in improved signal to background ratio and thus, better sensitivity.[53] Furthermore, the binary classification into negative and positive outcomes can be used to improve the quantification precision in assays based on exponential amplification[235, 288] and to eliminate variation originating from heterogenicity of the label, such as aggregation of nanoparticle labels.[21]

3 Aims of the Study

The aim of this study was to evaluate different methods to improve the analytical sensitivity of bioaffinity assays using UCNPs as reporters, focusing in particular on reducing the nonspecific binding of UCNP reporter conjugates.

The main objectives were:

I. To identify the main components in human plasma inducing matrix related nonspecific binding of PAA-coated UCNP antibody conjugates in immunoassays and to develop countermeasures to prevent the nonspecific interactions.

II. To develop a simple, direct hybridization assay for ultrasensitive amplification-free detection of short nucleic acid biomarkers from human plasma and to study the effect of base stacking interactions introduced by hairpin-structured probes on the assay performance.

III. To develop a hybridization complex transfer assay to eliminate background signal originating from nonspecifically bound label conjugates in hybridization assays.

4 Materials and Methods

A brief summary of the materials and methods is presented in this section. More detailed descriptions are provided in the original publications.

4.1 UCNP synthesis and surface modification

Oleic acid capped UCNPs ($NaYF_4$: 17% Yb^{3+}, 3% Er^{3+}) with an average diameter of approximately 25 nm were synthesized by high temperature co-precipitation synthesis in organic oils.[289] In the original publication **I**, the oleic acid was removed by HCl wash[22] and in the original publications **II** and **III**, by ligand exchange with BF_4.[290] Subsequently, the UCNPs were coated with poly(acrylic acid) (PAA, MW 2000, Sigma-Aldrich, USA) in order to obtain hydrophilic surface and to introduce carboxyl groups for conjugation with biomolecules. In the original publication **I**, PAA coating was done by incubating the UCNPs in 2.5% (w/v) aqueous PAA solution (pH 9) overnight under 1200 rpm shaking at room temperature. In the original publications **II** and **III**, PAA coating was done by incubating the UCNPs (16.7 mg/mL) overnight at 60 °C under 1400 rpm shaking in 3.8% (w/v) PAA in DMF containing 270 mM 1,8-diazabicyclo(5.4.0)undec-7-ene.

In order to conjugate the PAA coated UCNPs with antibodies or amino modified synthetic DNA probes, the free carboxyl groups of PAA were activated to react with primary amino groups by using standard carbodiimide chemistry:

In the original publication **I**, the carboxyl groups on the PAA coated UCNPs were activated with 20 mM N-(3-dimethylaminopropyl)-N′-ethylcarbodiimide (EDC) and 30 mM N-hydroxysulfosuccinimide (sulfo-NHS) in 20 mM sodium 2-(N-morpholino)ethanesulfonate (MES) buffer (pH 6.1) for 45 min. After washing, the UCNPs were incubated with anti-cTnI mAb 625 (HyTest, Finland, 0.083 mg mAb per 2 mg UCNPs) in MES buffer.[291] The reactions were stopped by adding 2 M 2-amino-N,N-dimethylacetamide (pH 11) to a final concentration of 50 mM.

In the original publications **II** and **III**, the PAA coated UCNPs were conjugated with amino modified DNA probes. As DNA does not contain carboxyl groups, the EDC/sulfo-NHS activation and DNA conjugation could be done in one step: 10 mg/mL of PAA coated UCNPs were incubated with 20 mM EDC, 30 mM sulfo-NHS and 80 µM amino modified DNA probes in 20 mM MES buffer (pH 6.5) for

2.5 h. The reaction was stopped by adding 50 mM 2-amino-N,N-dimethylacetamide from 2 M solution (pH 11).

The conjugates were washed four times by centrifugation and stored at +4 °C.

4.2 Bioaffinity assays

4.2.1 Immunoassays

Heterogeneous cTnI immunoassays in the original publication **I** were carried out as described previously.[20] In-house streptavidin coated microtiter plate[292] was prewashed before starting the assay and biotinylated capture antibodies (150 ng of mAb 19C7 and 50 ng of FAb 9707 per well) were added in 50 µL of assay buffer (Uniogen Oy, Finland) and incubated for 30 min under slow shaking. The wells were washed once and 10 µL of each sample was added with 40 µL of Tris buffer (50 mM Tris-HCl, pH 7.75, 9 g/L NaCl, 0.5 g/L NaN_3). After 30 min incubation, the wells were washed once and 200 ng of UCNP-mAb-625 conjugates were added in 50 µL of assay buffer supplemented with 0.2% (w/v) milk powder, 0.8 mg/mL native mouse IgG and 0.05 mg/mL denatured mouse IgG. The plates were incubated for 30 min under slow shaking, followed by four-fold washing. The plates were let dry at room temperature for at least 45 min before the readout.

4.2.2 Hybridization assays

In the original publications **II** and **III**, a synthetic DNA oligonucleotide corresponding to the miRNA sequence miR-20a was used as a model analyte in the assay development to avoid possible stability issues related to RNA. The oligonucleotide sequences and modifications are listed in **Table 1**.

Table 1. Oligonucleotide sequences and modifications used in this work.

Category	Name	Sequence (5'→3')[a]	Modifications	Original publication
Probes	Hairpin capture probe	TAT AAG CAC TTT AGG AGA CGT CCA TAT* GTA GGA CGT CTC C	T* = biotin dT	II & III
	Linear capture probe	TAT AAG CAC TTT AGG AGA CGT CCA TAT	3'-biotin-TEG	II
	Complex transfer first capture probe	TAT AAG CAC TTT AAG ACG TCC ATA TGC T	3'-biotin-TEG	III
	Hairpin tracer probe	CTC GTG ACC GTA GT*T ACC GGT CAC GAG CTA CCT GCA C	T* = amino C6 dT	II & III
	Linear tracer probe	TTA CCG GTC ACG AGC TAC CTG CAC	5'-aminolink-C6	II
	Releasing oligonucleotide	GGA CAT ATG GAC GTC TTA AAG TGC	none	III
Targets	DNA-miR-20a (complementary)	TAA AGT GCT TAT AGT GCA GGT AG	none	II & III
	DNA-miR-20b-5p (2 mismatches)	CAA AGT GCT CAT AGT GCA GGT AG	none	II & III
	1 mismatch	TAA AGT GCT TAT ATT GCA GGT AG	none	II & III
	3 mismatches	CAA AGT GCT CAT ATT GCA GGT AG	none	II & III

[a] Underlined nucleotides represent mismatches. * Internal modification (TEG = triethylene glycol).

In the original publication **II**, the direct hybridization assays were started by diluting the UCNP-DNA-probe conjugates to a concentration of 5 µg/mL into assay buffer (Uniogen Oy) supplemented with 2.25 M NaCl and 5 mM KF. The UCNP conjugate dilution was mixed with the samples or calibrators in 20:80 volume ratio. The hybridization reactions were incubated for 2 h 45 min under 1200 rpm shaking. Meanwhile, streptavidin coated microtiter plate (KaiSA Lockwell White) was prewashed with the wash buffer (Uniogen Oy) and capture probes with biotin modification were immobilized to the wells by adding 1.25 pmol of probes in 25 µL of assay buffer supplemented with 5% ethanol and incubating the plate for 30 min at room temperature without mixing to generate active capture surface only at the bottoms of the wells. The wells were washed once and 150 µL of pre-incubated hybridization reaction mixtures were added to the wells (corresponding to 30 µL of UCNP dilution and 120 µL of sample or calibrator). The reactions were incubated for 1 h under slow shaking, followed by four-fold wash with modified wash buffer

(wash buffer supplemented with 300 mM NaCl, 0.1% (w/v) Tween 20 and 1 mM KF). The plates were dried at room temperature for at least 45 min before the readout.

The hybridization complex transfer assay principle, developed in the original publication **III**, is illustrated in Figure 9. The assays were started by diluting the UCNP-DNA-probe conjugates to a concentration of 75 µg/mL into the assay buffer supplemented with 3.45 M NaCl and 5 mM KF and mixing with the samples or calibrators in 20:80 volume ratio. UCNP-target complexes were formed by incubating the reactions for 30 min at room temperature under slow rotation. (**Figure 9 I**)

In the first capture step, the complexes were captured either onto streptavidin coated microtiter plates or streptavidin coated magnetic beads, with the first capture probes immobilized on their surface via biotin modification. In case of microtiter plates, the probes were immobilized by adding 150 µL of 50 nM probe dilution in the assay buffer into each well and incubating the plate at room temperature under slow shaking for 30 min. The wells were washed once to remove unbound probes and 150 µL of hybridization reaction mixtures were added and incubated for 1 h under slow shaking to capture the UCNP-target complexes. The wells were washed four times with the modified wash buffer. In case of magnetic beads, the streptavidin coated beads were pre-washed twice and the capture probes were immobilized by incubating 1 mg/mL of beads with 100 nM capture probes in the assay buffer for 1 h under 1200 rpm shaking. The beads were washed three times and mixed with the hybridization reaction mixtures to a final concentration of 0.17 mg/mL. The UCNP-target complexes were captured by incubating the reactions for 1 h at room temperature under 1200 rpm shaking. (**Figure 9 II**) The beads were washed four times with the modified wash buffer.

The specifically bound UCNP-target complexes were released by adding releasing oligonucleotides (**Figure 9 III**) that hybridize with the capture probes displacing the target via toehold mediated strand displacement reaction (**Figure 9 IV**). In case of microtiter plates as the first capture surface, 5 pmol of the releasing oligonucleotides were added to the wells in 150 µL of elution buffer (assay buffer supplemented with 0.85 M NaCl and 1 mM KF) and incubated at room temperature under slow shaking for 45 min. In the magnetic bead-based assay, 0.1 nmol of releasing oligonucleotides per 1 mg of magnetic beads were added in 40 µL elution buffer per reaction and incubated at room temperature under 1200 rpm shaking for 30 min.

The second capture step was done on microtiter plate wells, coated with second capture probes as described for the direct hybridization assay in the original publication **II**, with the exception that in-house streptavidin coated microtiter plates[292] were used instead of commercial streptavidin coated microtiter plates.

When the first capture step was carried out in microtiter plate wells, 140 µL of eluted solutions were transferred to the second capture wells and incubated for 90 min at room temperature under slow shaking. When the first capture step was done on magnetic beads, 40 µL of the eluted solutions were transferred to the second capture wells (**Figure 9 V**) and incubated at room temperature under slow shaking for 30 min to recapture the complexes by the second capture probes. The wells were washed four times with the modified wash buffer and let dry for at least 45 min before the readout. (**Figure 9 VI**)

In the reference assay, the complexes formed in the first step were added directly to wells with the second capture probes immobilized on the bottom surface. The complexes were captured by incubating 150 µL of hybridization reaction mixtures per well under slow shaking for 1 h. (**Figure 9 R**) The wells were washed and dried as described for the complex transfer assay prior to the readout.

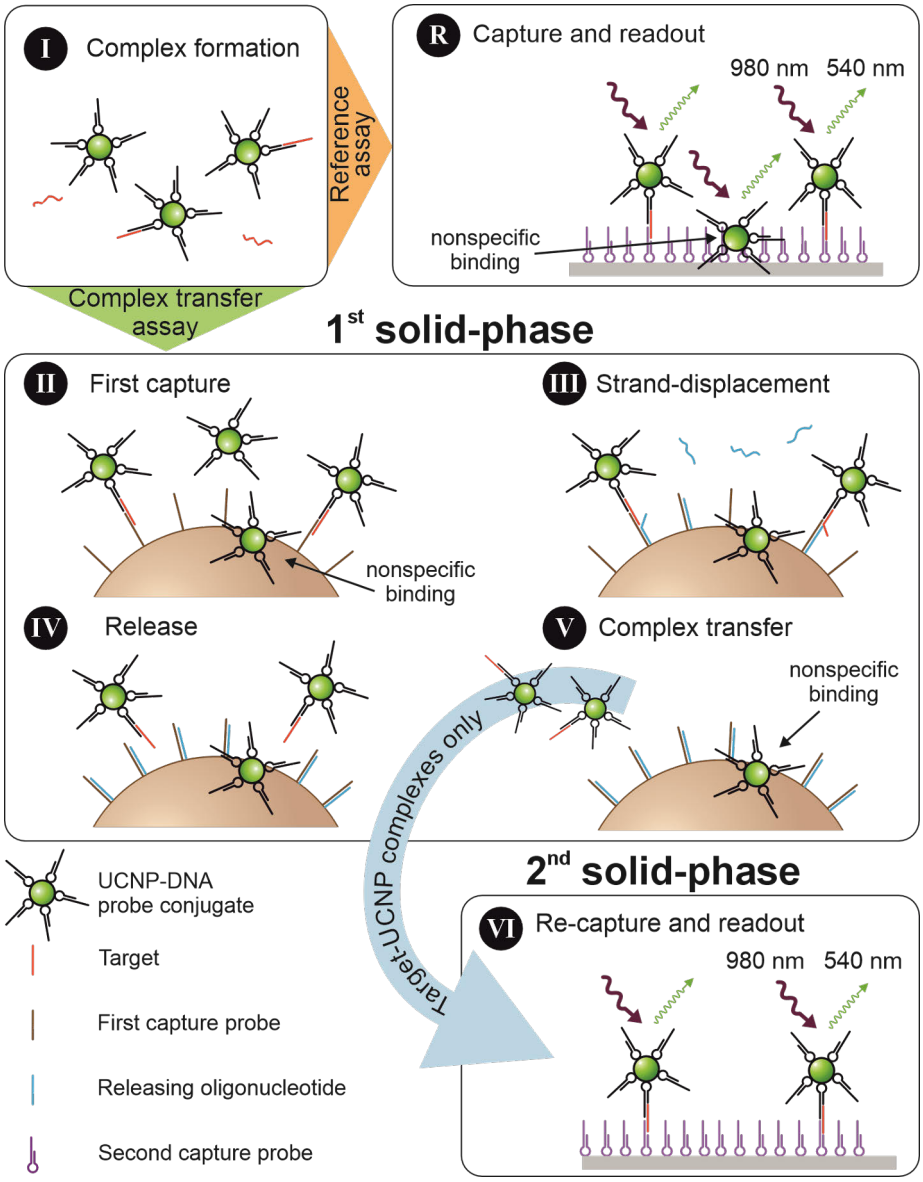

Figure 9. Principle of the hybridization complex transfer assay utilizing magnetic beads as the first capture surface. (I) The sample is mixed with the UCNP–DNA probe conjugates to form target–UCNP complexes. (II) The complexes are captured with DNA probes immobilized on the surface of magnetic beadss. (III) The beads are washed, and releasing oligonucleotides are added. Releasing oligonucleotides hybridize with the capture probes, displacing the target via toehold-mediated strand displacement. (IV) Target–UCNP complexes are released into the solution, and (V) the solution is transferred into microtiter plate wells coated with another capture probe. (VI) The target–UCNP complexes are collected with the capture probes, the wells are washed and dried, and UCL is measured. In the reference assay (R), the complexes formed in the step (I) are directly captured onto wells coated with the second capture probes. Figure reproduced from original publication **III**.

4.2.3 Upconversion luminescence readout

In all assays, the upconversion luminescence at 540 nm was measured from the bottoms of the wells upon 980 nm laser excitation using a modified[15] Chameleon plate reader (Hidex, Finland). A 3 × 3 -point raster with 2-second readouts and a point-to-point distance of 1.5 mm was measured from each well and an average of the 9 measurement points was calculated.

4.2.4 Assay evaluation

The standard curves were fitted with a logistic function using Origin 2016:

$$\mathrm{UCL} = \mathrm{UCL_{max}} + \frac{\mathrm{UCL_{min}} - \mathrm{UCL_{max}}}{1 + \left(\frac{c}{\mathrm{EC_{50}}}\right)^{s}} \quad (7)$$

where UCL represents upconversion luminescence, $\mathrm{UCL_{max}}$ and $\mathrm{UCL_{min}}$ represent the maximum and minimum UCL values of the sigmoidal curve, c is the analyte concentration, $\mathrm{EC_{50}}$ is the half maximal effective concentration and s is the slope at the inflection point of the curve. The LoDs were calculated from the standard curve equations as the analyte concentration corresponding to the signal response equivalent to three times the standard deviation of the zero calibrator:

$$\mathrm{UCL_{LoD}} = \mathrm{UCL_0} + 3 \times \mathrm{SD_0} \quad (8)$$

where $\mathrm{UCL_{LoD}}$ is the signal response at LoD and $\mathrm{UCL_0}$ and $\mathrm{SD_0}$ represent the signal response and standard deviation of the zero calibrator, respectively.

In order to calculate recovery percentages, known concentrations of the analyte were spiked into pooled plasma samples. The spiked and unspiked plasma samples were analysed with the assay, their concentrations were calculated from the calibration curve and the recovery percentage was calculated:

$$\mathrm{recovery} = \frac{\mathrm{c_{spiked\ plasma}} - \mathrm{c_{unspiked\ plasma}}}{\mathrm{c_{added}}} \quad (9)$$

where $\mathrm{c_{spiked\ plasma}}$ and $\mathrm{c_{unspiked\ plasma}}$ represent the concentrations of spiked and unspiked plasma, calculated from the calibration curve based on their respective signal responses, and $\mathrm{c_{added}}$ is the concentration of the analyte that was spiked to the plasma.

4.3 Identification of plasma components related to nonspecific binding of UCNP conjugates

In the original publication **I**, lithium heparin plasma was collected from 10 apparently healthy individuals in compliance with the declaration of Helsinki and pooled. In order to isolate the components associated with the nonspecific binding

of PAA-coated UCNP antibody conjugates in heterogeneous immunoassays, the plasma pool was consecutively fractionated by ammonium sulphate precipitation, gel filtration chromatography and anion exchange chromatography. After each separation step, the fractions were analysed with cTnI immunoassay to identify the fractions exhibiting highest nonspecific binding of UCNP conjugates. The protein concentrations of the fractions were determined based on the absorbance at 280 nm. The fractions associated with highest level of nonspecific binding were pooled and further fractionated in the next purification step.

After the anion exchange chromatography, the proteins of the fractions associated with elevated nonspecific binding were separated by sodium dodecyl sulfate polyacrylamide gel electrophoresis (SDS-PAGE). The samples were mixed with either Laemmli sample buffer or Laemmli sample buffer containing 5% β-mercaptoethanol (Bio-Rad, USA), denatured at 95 °C for 5 min and added to the wells of Mini-PROTEAN® TGX Precast gel (Bio-Rad) in 30 µL volume. The electrophoresis was run in TGS buffer (25 mM Tris-HCl, pH 8.3, 192 mM glycine, 0.1% SDS) under a constant voltage of 100 V for 90 min. The gel was stained for 1 h with Coomassie Blue staining solution (0.1% Coomassie Blue R250, 30% methanol, 5% acetic acid) and destained with 30% methanol and 5% acetic acid. The proteins in the lanes were identified using LC-ESI-MS/MS. Mass spectrometry analysis was purchased from the Turku Proteomics Facility, University of Turku and Åbo Akademi University.

5 Summary of Results and Discussion

5.1 C1q-associated nonspecific binding of UCNP conjugates

In the original publication **I**, the plasma components associated with the nonspecific binding of PAA-coated UCNP antibody conjugates were first isolated by fractionating the plasma pool by various sequential purification methods. After each step, the fractions exhibiting the highest nonspecific binding were identified in heterogeneous cTnI immunoassay and pooled for the next purification step. The last chromatography step, anion exchange chromatography, resulted in three peaks of elevated background signal in cTnI immunoassay (**Figure 10**, red). The fractions exhibiting the highest nonspecific binding were eluted at the beginning (fractions 10–16) and contained only a small proportion of the total protein concentration, suggesting that a small, positively charged fraction of the total protein induces a major part of the nonspecific binding and that the plasma fractions associated with the nonspecific binding were succesfully enriched. Fractions 11, 21 and 26 were chosen for mass spectrometry anaysis. The mass spectrometry revealed that the fractions contained various complement proteins and immunoglobulins and that subunits of complement component C1q were present in all of them.

In order to induce nonspecific binding in heterogeneous 2-step immunoassay, the interfering plasma components need to bind to the capture surface and remain bound during the washes. To study whether C1q actually binds to the solid phase surface, DELFIA method was used. Polyclonal anti-C1q antibodies labelled with Tb^{3+}-N1 chelates were added to the assay wells after incubation with the anion exchange fractions. A similar analysis was done with Tb^{3+}-N1-labelled polyclonal anti-IgM antibodies, because the fractions contained various immunoglobulin subunits and IgM has previously been associated with interferences in immunoassays.[188, 293] By using molecular labels, the false results related to the nonspecific binding of UCNPs could be avoided. The anti-C1q antibody generated high fluorescence signal especially in the fractions 10–13, which were also associated with highest nonspecific binding of UCNP conjugates (**Figure 10**, blue). The anti-C1q antibody generated lower but clearly distinguishable fluorescence

signals in the second and third peak of nonspecific binding. The binding of anti-IgM antibodies was mainly associated with the second peak of nonspecific binding (**Figure 10,** orange).

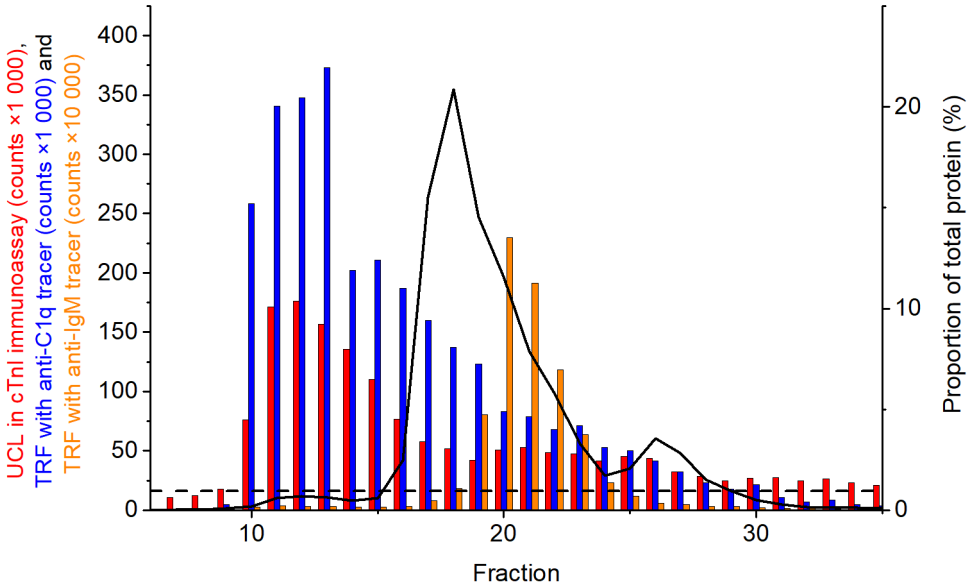

Figure 10. The nonspecific binding of UCNP-PAA antibody conjugates in (red), the binding of Tb-labelled anti-C1q antibodies (blue) and Tb-labelled anti-IgM antibodies (orange) onto anti-cTnI antibody coated microtiter wells after incubation with anion exchange fractions. The solid line shows theh proportion of total protein in each fraction, determined based on the absorbance at 280 nm. The dashed line represents the nonspecific binding of UCNP-antibody conjugates after incubation of buffer-based zero calibrator.

The binding of C1q to antibody coated surfaces has been previously reported to cause interference in immunoassays.[63] The six globular heads of C1q each have binding sites for IgG as well as several other targets,[294] and the high density of antibodies on the immunoassay capture surfaces may enhance the binding of C1q through high avidity. Furthermore, C1q is one of the most positively charged proteins in plasma,[295] which may induce electrostatic interactions with negatively charged PAA-coated UCNPs.

The addition of 100, 300 or 500 mM NaCl or 50 U/mL heparin to the assay buffer in the sample incubtion step almost completely hindered the nonspecific binding of UCNP conjugates, as well as the binding of labelled anti-C1q antibodies (**Figure 11**). Both, salt and heparin, can prevent electrostatic interactions by masking the opposite charges. The similar effect of the additions on both, the detection of C1q and the nonspecific binding of UCNPs, supports the hypothesis that the nonspecific binding is C1q mediated and occurs mainly via electrostatic interactions.

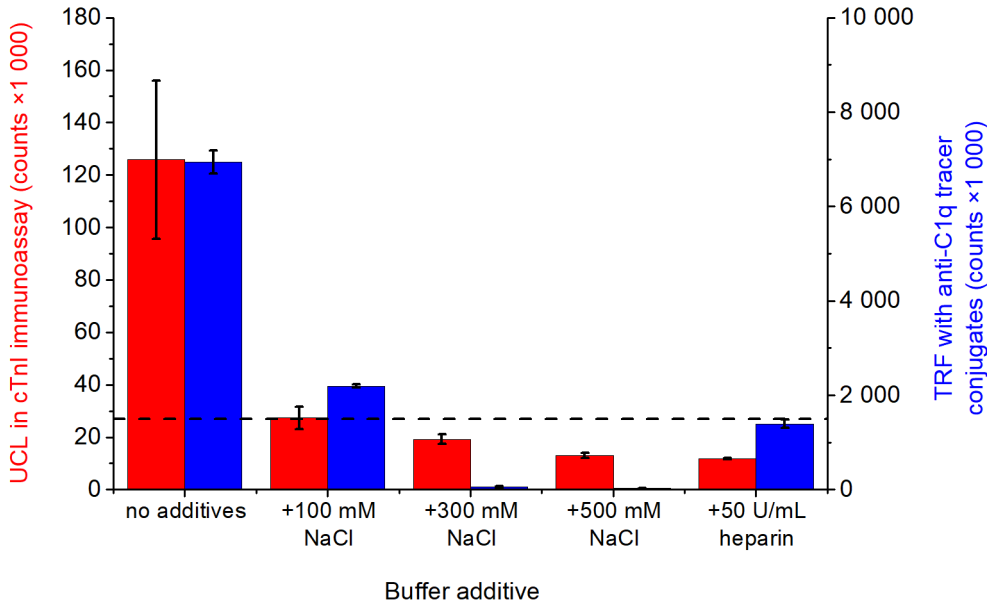

Figure 11. The effect of NaCl and heparin on the nonspecific binding of UCNP-PAA antibody conjugates (red) and on the binding of Tb-labelled anti-C1q antibodies (blue). The additions were made to the assay buffer (containing 150 mM NaCl) in the sample incubation step. The error bars represent standard deviations of three replicate measurements and the dashed line shows the nonspecific binding of UCNP-PAA antibody conjugates after incubation of buffer-based zero calibrator.

5.2 Hybridization assays

5.2.1 The effect of probe structure on hybridization efficiency and analytical sensitivity

In the original publication **II**, hairpin structured DNA probes employing base stacking to stabilize hybridization with the short target sequence were compared with corresponding linear probes in a direct hybridization assay. A synthetic DNA oligonucleotide corresponding to the sequence of miR-20a (DNA-miR-20a, 23 nucleotides) was used as a model analyte.

The effect of probe structure on hybridization efficiency was first studied by comparing the signal response in a salt concentration range from 150 mM to 840 mM. The assay was done with 40% calibrators and 60% UCNP dilutions in the total reaction volume. The specific signal response increased with the increasing salt concentration, the difference being largest between 150 mM and 300 mM NaCl (**Figure 12**). With hairpin structured capture and tracer probes, the specific signals were 1.8–5.2-fold higher than with linear probes in the tested salt concentration range. The results are in agreement with a study by Riccelli et al. (2001), which

showed that capturing the target by hairpin structured probes results in thermodynamically more stable duplexes than capture with linear probes.[296]

Interestingly, the background signals generated by nonspecifically bound UCNP conjugates were 1.9–16-fold higher with linear probes compared to the hairpin structured probes. Increasing the salt concentration from 150 mM to 300 mM reduced the nonspecific binding of both tracer probe conjugates, but at concentrations above 450 mM, the background signal remained approximately constant or increased.

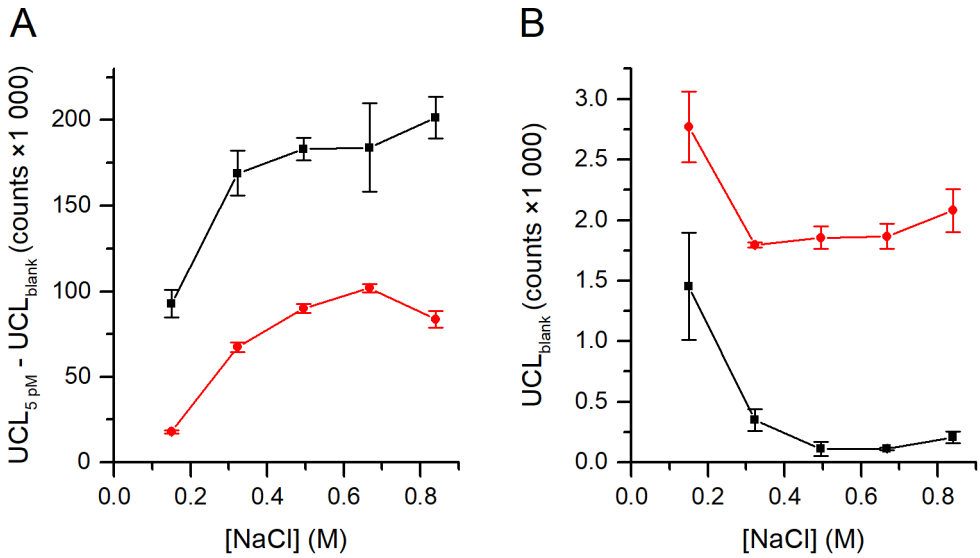

Figure 12. The effect of NaCl concentration on A) the specific signal response with 5 pM target analyte concentration and B) the nonspecific binding of UCNP-DNA probe conjugates with hairpin-structured (black) and linear (red) capture and tracer probes. The target dilutions and UCNPs in the assay buffer were mixed in 40:60 volume ratio and the NaCl concentrations refer to the concentration in the final reaction mixture. The error bars represent the standard deviations of three replicate measurements.

To evaluate the effect of probe structure on the assay performance, each calibrator was analysed with both probe pairs in three replicates, except for the zero calibrators, which were analysed in eight replicates. The assay was done with 80% calibrators and 20% UCNPs in the total reaction volume and with 600 mM NaCl in the final reaction mixture. A logistic regression was used for fitting the calibration curves. Analytical sensitivities were calculated from the calibration curves as the concentration corresponding to the signal equivalent to 3 × standard deviation of the zero calibrator. The assay with hairpin structured probes reached an LoD of 0.73 fM, which was approximately 18 times lower than the LoD of 13 fM reached with the linear probes (**Figure 13**). The difference was mainly caused by the 91% lower level

of nonspecific binding with the hairpin structured probes compared to the linear probes, but the hairpin structured probes also generated approximately 30% higher signal responses compared to the linear probes. The analytical sensitivities of enzyme-free miRNA assays are typically at picomolar level.[297] Reaching femtomolar detection limits without any target amplification demonstrates the significant potential of UCNPs as reporters in ultrasensitive biomarker detection.

To study the suitability of the assay for the measurement of the target analyte in real sample matrices, the plasma recovery percentages were determined. EDTA plasma pool aliquots were spiked with 0, 0.05, 0.5, 5 and 50 pM target analyte and analysed with the assay using hairpin-structured probes. The analysis resulted in 111 %, 93 %, 89 % and 76 % recoveries, respectively. The circulating miR-20a concentrations have been reported to be at picomolar level,[298] and therefore, the results indicate the suitability of the assay for measurement of miR-20a in blood. Moreover, by changing the probe sequences, the assay can be adapted for other target sequences and it is readily suitable for spatial multiplexing.

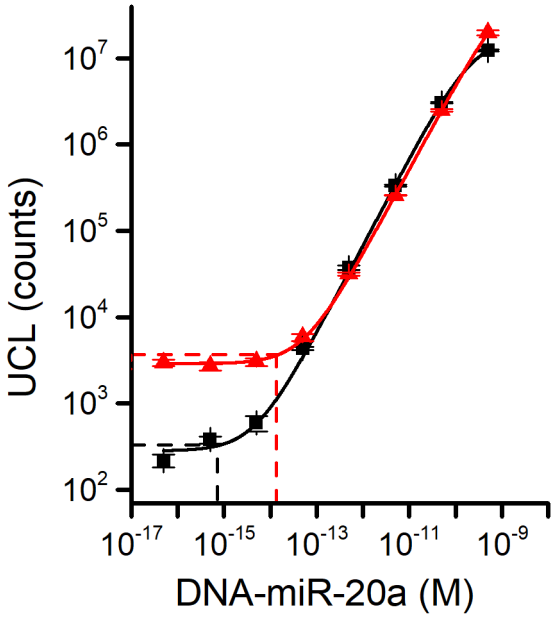

DNA-miR-20a plasma recoveries		
Spiked DNA-miR-20a (pM)	Measured DNA-miR-20a (pM)	Recovery %
0	0.009	--
0.05	0.064	111%
0.5	0.48	93%
5	4.4	89%
50	38	76%

Figure 13. The standard curves of the direct hybridization assays using linear (red) and hairpin-structured (black) capture and tracer probes and the plasma recoveries of the assay with hairpin-structured probes. The error bars represent standard deviations of replicate measurements and the dashed lines indicate the LoDs calculated as the concentrations corresponding to the signal equivalent to 3 × standard deviation of the zero calibrator.

5.2.2 The effect hybridization complex transfer on analytical sensitivity and cross-reactivity

In the original publication **III**, a novel hybridization complex transfer method was developed to eliminate the sensitivity limitation set by the nonspecific binding of UCNP reporters on the detection surface and thus, to improve the analytical sensitivity. As in the original publication **II**, DNA-miR-20a was used as a model analyte in the assay development to demonstrate the potential of the assay. The assay principle is based on the immune complex transfer assays, originally published by Kohno et al. (1987),[263] and it contains two target specific capture steps on two separate solid-phase surfaces. After the first capture step and washing, the specifically bound UCNP-target complexes are released by adding releasing oligonucleotides that hybridize with the capture probes and displace the target sequence via toehold mediated strand displacement. The nonspecifically bound UCNP reporters are not released. After the release, the solutions are transferred to microtiter plate wells coated with second capture probes to recapture the released target-UCNP complexes. Since the nonspecific binding occurred on the first capture surface and is not transferred to the second capture surface, the background signal originating from the nonspecific binding is completely excluded from the final readout. By using microtiter plates as solid phases in both capture steps, the complex transfer procedure improved the analytical sensitivity by a factor of 9 compared to a reference assay, where the complexes were directly captured onto the second capture surface without complex transfer. (**Figure 14 A**)

The performance of the complex transfer assay was further improved by using magnetic beads instead of microtiter plate wells as the first capture surface. Magnetic beads act as a more dynamic solid phase compared to microtiter plate wells, improving the binding kinetics by reducing the diffusion distances. Additionally, they enable increasing the capture probe concentration in the reaction, which can be used to further increase the reaction rate. Typically, increasing the capture surface area results in increased nonspecific binding.[40, 50-53] In the complex transfer assay, the nonspecific binding occurs on the first capture surface and is not transferred to the second capture surface, and therefore, the increased capture surface area does not increase the background signal in the readout.

The performance of the complex transfer with magnetic beads as the first capture surface was first demonstrated by using the same sample volumes as in the microtiter plate-based assay, 120 µL per well. The assay reached an LoD of 0.31 fM in assay buffer and 0.19 fM in EDTA plasma, which were 27- and 21-fold improvements compared to the reference assays without complex transfer. (**Figure 14 B-C**) The slightly lower LoD in plasma suggests that plasma components do not interfere with the complex transfer procedure and indicates that the assay principle is suitable for sensitive detection directly from biological matrices.

Another benefit of magnetic beads is that they can be used to preconcentrate analyte molecules by using larger sample volume in the first capture step and by doing the strand displacement reaction in significantly smaller volume, enabling detection of lower concentrations. By increasing the sample volume 5-fold, to 600 µL, the LoD was reduced by a factor of 6.7, resulting in an LoD of 46 aM. (**Figure 14 D**)

The analytical sensitivity values reached with the hybridization complex transfer assay correspond to 14 000–22 000 analyte molecules in the respective sample volumes, which is still 2 orders of magnitude above the theoretical limit set by the Poisson statistics.[43] The analytical sensitivity was limited by the detectability of the label together with the instrument background. Therefore, it can be expected that the LoDs could be further reduced by improving the detectability of the label, for example by using brighter or larger UCNPs, or by digital readout, which enables detection of lower number of UCNP reporters bound to the solid-phase surface. On the other hand, one of the advantages of the presented method is that there is no need for special instrumentation, such as sensitive, high-resolution imaging systems.

Even though the complex transfer procedure introduces additional steps to the assay protocol, the total assay time was approximately the same, while 16 times lower concentrations could be detected. The total elimination of nonspecific binding by the complex transfer enabled using 15-fold higher concentration of UCNP conjugates compared to the optimal UCNP concentration in the direct hybridization assay in the original publication **II**, which should, in theory, improve the kinetics in the complex formation step. Without the complex transfer steps, the higher label concentration would result in elevated nonspecific binding on the detection surface, limiting the analytical sensitivity. Additionally, using magnetic beads as the first capture step improves the capture kinetics, and increasing the bead concentration can be expected to further speed up the first capture step. Using a smaller volume in the strand displacement step and the subsequent recapture step (40 µL/well) reduced the diffusion distances in the second capture step, enabling shorter incubation times on the microtiter plate compared to the direct assay, where the reactions were carried out in a volume of 150 µL/well.

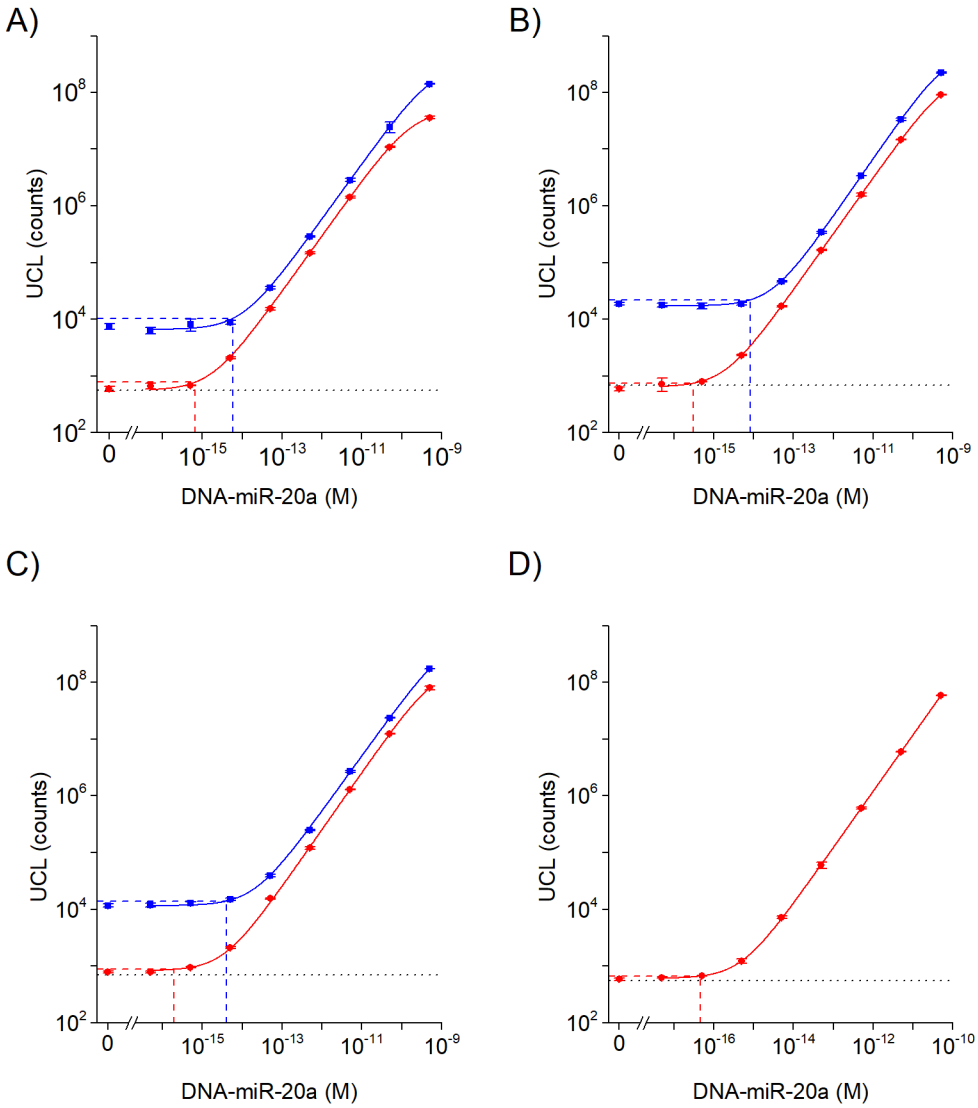

Figure 14. The calibration curves of hybridization complex transfer assays (red) and reference assays, where the UCNP-target complexes were directly captured onto the 2nd capure surfaces without the complex transfer (blue) with A) microtiter plate as the solid phase in both capture steps and target DNA in 120 µL of buffer per well B) magnetic beads as the solid phase in the first capture step and target DNA in 120 µL of buffer per reaction C) magnetic beads as the solid phase in the first capture step and target DNA in 120 µL of EDTA plasma pool per reaction D) magnetic beads as the solid phase in the first capture step and target DNA in 600 µL of buffer per reaction. The error bars represent the standard deviations of replicate measurements and the dotted lines show the instrument background. The dashed lines indicate the LoDs calculated as the concentrations corresponding to the signal equivalent to 3 × standard deviation of the zero calibrator.

The specificity of the complex transfer assay was studied by analysing 0.5 pM dilutions of synthetic DNA oligonucleotides containing minor variations to the complementary target sequence. The same dilutions were also analysed with the reference assay. In the complex transfer assay, the sequences containing one or two mismatches generated 1.8% and 0.4% of the signal response of the fully complementary target sequence, respectively. In the reference assay, the same sequences generated 19% and 2.6% of the signal response of the complementary target sequence (**Figure 15**). The improved sequence specificity can be explained by the additional target specific step in the complex transfer assay: in order to generate signal in the complex transfer assay, the sequence needs to hybridize with the tracer probe, as well as both, first and second capture probes. In the reference assay, cross-reactivity with the tracer probe and the capture probe is enough. The better discrimination between highly homologous sequences is essential for example in miRNA diagnostics, because some miRNAs differ only by single a nucleotide.

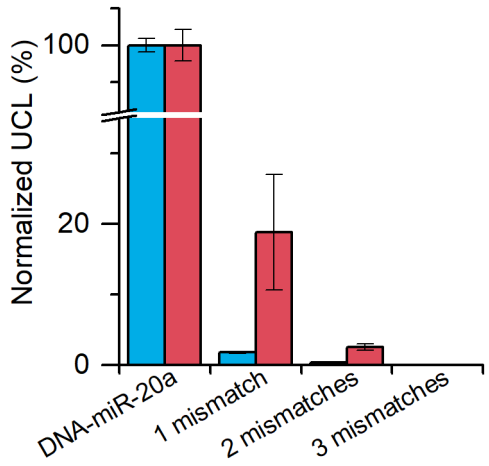

Figure 15. The cross-reactivity of the direct hybridization complex transfer assay with magnetic beads as the first capture surface (blue) and the reference assay without complex transfer (red). The luminescence signal responses of the non-target sequences were divided by the luminescence signals responses of the fully complementary target sequence. The target and non-target sequences were analysed at 0.5 pM concentration in both assays. The error bars represent the standard deviations of three replicate measurements.

6 Conclusions

The analytical sensitivity of bioaffinity assays is dependent on the specific signal response resulting from the recognition of the analyte as well as the variation in the background signal generated in the absence of the analyte. In heterogeneous bioaffinity assays using highly detectable labels, such as UCNPs, the background signal generated by nonspecific binding of label conjugates on the solid-phase surface is typically the major obstacle limiting the analytical sensitivity. Even though nonspecific binding can be reduced by optimizing reagents and assay conditions, it has proven difficult to control and separate optimizations may be required for each assay. Novel methods to further improve the discrimination of specific and nonspecific binding are needed to reach ultrasensitivity that is necessary for the detection of extremely low-abundance biomarkers.

This doctoral research focused on eliminating the nonspecific binding of UCNP label conjugates in heterogeneous bioaffinity assays to improve the analytical sensitivity. Ultrasensitive hybridization assays were developed for direct detection of short nucleic acid targets without nucleic acid extraction or amplification, both of which may increase the variation and bias in the quantification. The effect of enhanced specific interactions on the analytical sensitivity of a hybridization assay was studied by utilizing base stacking interactions introduced by hairpin-structured probes.

The main conclusions based on the original publications are:

I The nonspecific binding of PAA coated UCNP conjugates in heterogeneous bioaffinity assays with lithium heparin plasma as the sample matrix is mainly associated with the complement component C1q. C1q binds to the surface of the microtiter plate and subsequently binds UCNP conjugates. The interaction was shown to be mostly electrostatic and it could be prevented by increasing the ionic strength or by introducing a negatively charged blocker in the sample incubation step. Preventing the binding of C1q to the detection surface also prevented the nonspecific binding of UCNP conjugates.

II Hairpin-structured probes generated approximately 30% higher specific signal responses compared to the corresponding linear probes in a hybridization assay for short nucleic acid targets. The analytical sensitivity of the assay was improved by a factor of 18. The main reason for the improved sensitivity was the reduced background signal from nonspecific binding of UCNP reporters conjugated with the hairpin-structured probes compared to the corresponding linear probes.

III The analytical sensitivity of upconversion-based hybridization assay was significantly improved by eliminating the background signal originating from nonspecific binding of UCNP reporter conjugates. A novel hybridization complex transfer assay technique was developed to enable separation of specifically and nonspecifically bound UCNP reporters. The separation was based on a specific release of the target-UCNP complexes via toehold-mediated strand displacement reaction, followed by a recapture to a fresh second capture surface by another target-specific probe. Even though approximately 50% of the specific signal was lost in the complex transfer procedure, the complete elimination of nonspecific binding resulted in 27-fold improvement in analytical sensitivity. By using magnetic preconcentration from a larger sample volume of 600 µL, the analytical sensitivity could be further improved and a LoD of 46 aM was reached. Moreover, due to the two target-specific capture steps, the sequence specificity of the assay was improved compared to the reference assay.

In all of the original publications, the elimination of nonspecific binding of UCNP reporters proved to be the most important factor to increase the signal-to-background ratios and therefore to improve the analytical sensitivity. The background elimination was done **I**) by adjusting the buffer composition to prevent the unwanted nonspecific interactions identified in the study, **II**) by reagent optimization, in particular by using probes with hairpin structure, and **III**) by separation of specifically and nonspecifically bound fractions by complex transfer. The results highlight the importance of the background signal elimination in reaching ultralow LoDs in upconversion-based assays.

The results indicate that with UCNP reporters, short nucleic acid targets, such as miRNAs, could be detected directly from biological samples without nucleic acid extraction or amplification, in a standard microtiter plate assay format. This demonstrates the potential of upconversion-based hybridization assays as a powerful tool for diagnostics and screening of various diseases in the future.

Acknowledgements

This doctoral research was carried out during 2021–2025 at the Unit of Biotechnology, Department of Life Technologies, University of Turku. The financial support from Doctoral Programme in Technology, Instrumentarium Science Foundation, Turku University Foundation and Orion Research Foundation is gratefully acknowledged.

I wish to thank Professor Tero Soukka, Professor Urpo Lamminmäki and Assistant Professor Saara Wittfooth for the opportunity to conduct my research in the inspiring, high-quality environment at the Unit of Biotechnology.

I want to express my deepest gratitude to my principal supervisor, Professor Tero Soukka, for the valuable guidance and for the opportunity to work with various interesting research projects. Your enthusiasm for science, extensive expertise and endless stream of ideas have been truly inspiring and have helped me find joy in research, even when the journey has seemed challenging.

My heartfelt gratitude goes to my supervisor, Dr. Satu Lahtinen, for your everyday guidance and for sharing your expertise, especially in UCNPs and scientific writing. Following in your footsteps has made countless things so much easier, from writing my very first research proposal to navigating the graduation process. Your constant availability for discussions has helped me grow as a researcher and your encouragement has strengthened my belief in my own abilities.

I want to thank my supervisors and advisory committee members, Dr. Terhi Riuttamäki and Dr. Henna Päkkilä, for the encouraging atmosphere in the advisory committee meetings.

I wish express my appreciation to Docent Harri Hakala and Associate Professor Paul Corstjens for pre-examining this thesis and providing valuable feedback to improve the final version.

All the co-authors are gratefully acknowledged for their contributions. I want to especially thank Miikka Ekman for conducting a major part of the experimental work in the original publication I, and Dr. Jakub Máčala for the fruitful collaboration that led to the original publication III. Working with both of you has always been a pleasure and I truly appreciate your problem-solving skills and dedication to our projects.

In the summer of 2024, I had the privilege of visiting Associate Professor Hans-Heiner Gorris's group at Masaryk University, Brno, Czech Republic. I am sincerely thankful to Associate Professor Hans-Heiner Gorris, Professor Petr Skládal and Associate Professor Zdeněk Farka for the opportunity and guidance during my stay. I'm also very grateful to Dr. Julian Brandmeier, Dorota Sklenárová and Dr. Jakub Máčala for making me feel warmly welcomed and for keeping the shared braincell alive. With you, every day was fun, even when nothing made sense in the lab. I also want to thank Dr. Julian Brandmeier for being the best possible peer-support and for showing me the best slides in Brno.

I wish to thank the technical and administrative staff, especially Teija Luotohaara, Marianna Boundouvis and Jari Vehmas, for keeping everything running smoothly. I also wish to thank all my past and present co-workers at the Unit of Biotechnology, for creating a positive atmosphere. The fun and sometimes educational discussions during lunches and coffee breaks have provided the necessary counterbalance to the work days.

I wish to thank my mother, who has encouraged me to choose the path that feels right for me and who has always believed in my capabilities. I also want to thank my siblings, Iida, Olli and Aino for always staying united.

Finally, I want to thank Malte for your unconditional love, endless patience and for taking care of me over the years.

3.4.2025

Saara Kuusinen

List of References

[1] R. S. Yalow, S. A. Berson. Assay of plasma insulin in human subjects by immunological methods. *Nature* **1959**, *184*, 1648-1649.

[2] R. Ekins, C. F. Fau, J. Micallef. High specific activity chemiluminescent and fluorescent markers: their potential application to high sensitivity and 'multi-analyte' immunoassays. *J Biolumin Chemilumin* **1989**, *4*, 59-78.

[3] E. Engvall, P. Perlmann. Enzyme-linked immunosorbent assay (ELISA) quantitative assay of immunoglobulin G. *Immunochemistry* **1971**, *8*, 871-874.

[4] B. Van Weemen, A. Schuurs. Immunoassay using antigen—enzyme conjugates. *FEBS letters* **1971**, *15*, 232-236.

[5] I. Hemmilä, S. Dakubu, V.-M. Mukkala, H. Siitari, T. Lövgren. Europium as a label in time-resolved immunofluorometric assays. *Anal Biochem* **1984**, *137*, 335-343.

[6] Z. Farka, M. J. Mickert, M. Pastucha, Z. Mikušová, P. Skládal, H. H. Gorris. Advances in Optical Single-Molecule Detection: En Route to Supersensitive Bioaffinity Assays. *Angew Chem Int Ed* **2020**, *59*, 10746-10773.

[7] D. M. Rissin, C. W. Kan, T. G. Campbell, S. C. Howes, D. R. Fournier, L. Song, T. Piech, P. P. Patel, L. Chang, A. J. Rivnak. Single-molecule enzyme-linked immunosorbent assay detects serum proteins at subfemtomolar concentrations. *Nat Biotechnol* **2010**, *28*, 595-599.

[8] S. M. Hanash, S. J. Pitteri, V. M. Faca. Mining the plasma proteome for cancer biomarkers. *Nature* **2008**, *452*, 571-579.

[9] N. L. Anderson, N. G. Anderson. The human plasma proteome: history, character, and diagnostic prospects. *Mol Cell Proteomics* **2002**, *1*, 845-867.

[10] C. Wu, T. J. Dougan, D. R. Walt. High-throughput, high-multiplex digital protein detection with attomolar sensitivity. *ACS Nano* **2022**, *16*, 1025-1035.

[11] S. T. Chang, J. M. Zahn, J. Horecka, P. L. Kunz, J. M. Ford, G. A. Fisher, Q. T. Le, D. T. Chang, H. Ji, A. C. Koong. Identification of a biomarker panel using a multiplex proximity ligation assay improves accuracy of pancreatic cancer diagnosis. *J Transl Med* **2009**, *7*, 1-12.

[12] J. F. Rusling. Multiplexed electrochemical protein detection and translation to personalized cancer diagnostics. *Anal Chem* **2013**, *85*, 5304-5310.

[13] Z. Farka, J. C. Brandmeier, M. J. Mickert, M. Pastucha, K. Lacina, P. Skládal, T. Soukka, H. H. Gorris. Nanoparticle-based bioaffinity assays: from the research laboratory to the market. *Adv Mater* **2024**, *36*, 2307653.

[14] C. T. Xu, N. Svensson, J. Axelsson, P. Svenmarker, G. Somesfalean, G. Chen, H. Liang, H. Liu, Z. Zhang, S. Andersson-Engels. Autofluorescence insensitive imaging using upconverting nanocrystals in scattering media. *Appl Phys Lett* **2008**, *93*.

[15] T. Soukka, K. Kuningas, T. Rantanen, V. Haaslahti, T. Lövgren. Photochemical Characterization of Up-Converting Inorganic Lanthanide Phosphors as Potential Labels. *J Fluoresc* **2005**, *15*, 513-528.

[16] M. Monici. Cell and tissue autofluorescence research and diagnostic applications. *Biotechnol Annu Rev* **2005**, *11*, 227-256.

[17] F. Auzel. Upconversion and anti-stokes processes with f and d ions in solids. *Chem Rev* **2004**, *104*, 139-174.
[18] W. H. Wright, N. A. Mufti, N. T. Tagg, R. R. Webb, L. V. Schneider, in *Ultrasensitive Biochemical Diagnostics II, Vol. 2985*, SPIE, **1997**, pp. 248-255.
[19] M. Haase, H. Schäfer. Upconverting Nanoparticles. *Angew Chem Int Ed* **2011**, *50*, 5808-5829.
[20] S. Lahtinen, A. Lyytikäinen, N. Sirkka, H. Päkkilä, T. Soukka. Improving the sensitivity of immunoassays by reducing non-specific binding of poly(acrylic acid) coated upconverting nanoparticles by adding free poly(acrylic acid). *Microchim Acta* **2018**, *185*, 220-220.
[21] J. C. Brandmeier, K. Raiko, Z. Farka, R. Peltomaa, M. J. Mickert, A. Hlaváček, P. Skládal, T. Soukka, H. H. Gorris. Effect of Particle Size and Surface Chemistry of Photon-Upconversion Nanoparticles on Analog and Digital Immunoassays for Cardiac Troponin. *Adv Healthc Mater* **2021**, *10*, e2100506.
[22] N. Sirkka, A. Lyytikainen, T. Savukoski, T. Soukka. Upconverting nanophosphors as reporters in a highly sensitive heterogeneous immunoassay for cardiac troponin I. *Anal Chim Acta* **2016**, *925*, 82-87.
[23] K. Raiko, A. Lyytikäinen, M. Ekman, A. Nokelainen, S. Lahtinen, T. Soukka. Supersensitive photon upconversion based immunoassay for detection of cardiac troponin I in human plasma. *Clin Chim Acta* **2021**, *523*, 380-385.
[24] K. Kuningas, T. Rantanen, T. Lövgren, T. Soukka. Enhanced photoluminescence of up-converting phosphors in a solid phase bioaffinity assay. *Anal Chim Acta* **2005**, *543*, 130-136.
[25] P. Corstjens, M. Zuiderwijk, A. Brink, S. Li, H. Feindt, R. S. Niedbala, H. Tanke. Use of up-converting phosphor reporters in lateral-flow assays to detect specific nucleic acid sequences: a rapid, sensitive DNA test to identify human papillomavirus type 16 infection. *Clin Chem* **2001**, *47*, 1885-1893.
[26] T. Ukonaho, T. Rantanen, L. Jämsen, K. Kuningas, H. Päkkilä, T. Lövgren, T. Soukka. Comparison of infrared-excited up-converting phosphors and europium nanoparticles as labels in a two-site immunoassay. *Anal Chim Acta* **2007**, *596*, 106-115.
[27] A. Sedlmeier, H. H. Gorris. Surface modification and characterization of photon-upconverting nanoparticles for bioanalytical applications. *Chem Soc Rev* **2015**, *44*, 1526-1560.
[28] D. Wild, *The immunoassay handbook: theory and applications of ligand binding, ELISA and related techniques*, Newnes, **2013**.
[29] T. Förster. Zwischenmolekulare energiewanderung und fluoreszenz. *Ann Phys (Berl)* **1948**, *437*, 55-75.
[30] E. L. Elson, D. Magde. Fluorescence correlation spectroscopy. I. Conceptual basis and theory. *Biopolymers* **1974**, *13*, 1-27.
[31] W. Dandliker, G. Feigen. Quantification of the antigen-antibody reaction by the polarization of fluorescence. *Biochem Biophys Res Commun* **1961**, *5*, 299-304.
[32] L. Wide, R. Axén, J. Porath. Radioimmunosorbent assay for proteins. Chemical couplings of antibodies to insoluble dextran. *Immunochemistry* **1967**, *4*, 381-386.
[33] R. Y. Nong, D. Wu, J. Yan, M. Hammond, G. J. Gu, M. Kamali-Moghaddam, U. Landegren, S. Darmanis. Solid-phase proximity ligation assays for individual or parallel protein analyses with readout via real-time PCR or sequencing. *Nat Protoc* **2013**, *8*, 1234-1248.
[34] J. Favresse, M.-C. Burlacu, D. Maiter, D. Gruson. Interferences with thyroid function immunoassays: clinical implications and detection algorithm. *Endocr Rev* **2018**, *39*, 830-850.
[35] I. Pereiro, A. Fomitcheva-Khartchenko, G. V. Kaigala. Shake it or shrink it: Mass transport and kinetics in surface bioassays using agitation and microfluidics. *Anal Chem* **2020**, *92*, 10187-10195.
[36] J. E. Butler. Solid supports in enzyme-linked immunosorbent assay and other solid-phase immunoassays. *Methods* **2000**, *22*, 4-23.
[37] R. P. Ekins. Multi-analyte immunoassay. *J Pharm Biomed Anal* **1989**, *7*, 155-168.

[38] G. Addison, C. Hales. Two site assay of human growth hormone. *Horm Metab Res* **1971**, *3*, 59-60.
[39] G. Köhler, C. Milstein. Continuous cultures of fused cells secreting antibody of predefined specificity. *Nature* **1975**, *256*, 495-497.
[40] R. Ekins, F. Chu. Multianalyte microspot immunoassay--microanalytical" compact disk" of the future. *Clin Chem* **1991**, *37*, 1955-1967.
[41] T. Jackson, R. Ekins. Theoretical limitations on immunoassay sensitivity: current practice and potential advantages of fluorescent Eu3+ chelates as non-radioisotopic tracers. *J Immunol Methods* **1986**, *87*, 13-20.
[42] H. H. Gorris, T. Soukka. What digital immunoassays can learn from ambient analyte theory: A perspective. *Anal Chem* **2022**, *94*, 6073-6083.
[43] C. F. Woolley, M. A. Hayes, P. Mahanti, S. Douglass Gilman, T. Taylor. Theoretical limitations of quantification for noncompetitive sandwich immunoassays. *Anal Bioanal Chem* **2015**, *407*, 8605-8615.
[44] R. Ekins. Basic principles and theory. *Br Med Bull* **1974**, *30*, 3-11.
[45] D. W. Tholen, K. Linnet, M. Kondratovich, D. A. Armbruster, P. E. Garrett, R. L. Jones, M. H. Kroll, R. M. Lequin, T. J. Pankratz, G. Scassellati. Protocols for determination of limits of detection and limits of quantitation; approved guideline. *CLSI EP17-A* **2004**, *24*, 34.
[46] 'sensitivity' in *IUPAC Compendium of Chemical Terminology, 3rd ed.*, 3.0.1 ed., International Union of Pure and Applied Chemistry (IUPAC), **2019**.
[47] L. A. Currie. Limits for qualitative detection and quantitative determination. Application to radiochemistry. *Anal Chem* **1968**, *40*, 586-593.
[48] J. M. Hungerford, G. D. Christian. Statistical sampling errors as intrinsic limits on detection in dilute solutions. *Anal Chem* **1986**, *58*, 2567-2568.
[49] V. Paketurytė, V. Petrauskas, A. Zubrienė, O. Abian, M. Bastos, W.-Y. Chen, M. J. Moreno, G. Krainer, V. Linkuvienė, A. Sedivy. Uncertainty in protein–ligand binding constants: asymmetric confidence intervals versus standard errors. *Eur Biophys J* **2021**, *50*, 661-670.
[50] A. A. Hariri, S. S. Newman, S. Tan, D. Mamerow, A. M. Adams, N. Maganzini, B. L. Zhong, M. Eisenstein, A. R. Dunn, H. T. Soh. Improved immunoassay sensitivity and specificity using single-molecule colocalization. *Nat Commun* **2022**, *13*, 5359.
[51] D. M. Rissin, D. R. Fournier, T. Piech, C. W. Kan, T. G. Campbell, L. Song, L. Chang, A. J. Rivnak, P. P. Patel, G. K. Provuncher. Simultaneous detection of single molecules and singulated ensembles of molecules enables immunoassays with broad dynamic range. *Anal Chem* **2011**, *83*, 2279-2285.
[52] E. Güven, K. Duus, M. C. Lydolph, C. S. Jørgensen, I. Laursen, G. Houen. Non-specific binding in solid phase immunoassays for autoantibodies correlates with inflammation markers. *J Immunol Methods* **2014**, *403*, 26-36.
[53] L. Chang, D. M. Rissin, D. R. Fournier, T. Piech, P. P. Patel, D. H. Wilson, D. C. Duffy. Single molecule enzyme-linked immunosorbent assays: theoretical considerations. *J Immunol Methods* **2012**, *378*, 102-115.
[54] M. C. Brown, 'Antibodies: key to a robust lateral flow immunoassay' in *Lateral flow immunoassay*, Springer, **2008**, pp. 1-16.
[55] M. M. Farajollahi, D. B. Cook, S. Hamzehlou, C. H. Self. Reduction of non-specific binding in immunoassays requiring long incubations. *Scand J Clin Lab Invest* **2012**, *72*, 531-539.
[56] J. Foote, H. N. Eisen. Kinetic and affinity limits on antibodies produced during immune responses. *Proc Natl Acad Sci* **1995**, *92*, 1254-1256.
[57] W. Wang, S. Singh, D. L. Zeng, K. King, S. Nema. Antibody structure, instability, and formulation. *J Pharm Sci* **2007**, *96*, 1-26.
[58] D. R. Davies, S. Chacko. Antibody structure. *Acc Chem Res* **1993**, *26*, 421-427.

[59] N. S. Lipman, L. R. Jackson, L. J. Trudel, F. Weis-Garcia. Monoclonal versus polyclonal antibodies: distinguishing characteristics, applications, and information resources. *ILAR J* **2005**, *46*, 258-268.
[60] J. Voskuil. Commercial antibodies and their validation. *F1000Res* **2014**, *3*.
[61] G. P. Smith. Filamentous fusion phage: novel expression vectors that display cloned antigens on the virion surface. *Science* **1985**, *228*, 1315-1317.
[62] B. Valldorf, S. C. Hinz, G. Russo, L. Pekar, L. Mohr, J. Klemm, A. Doerner, S. Krah, M. Hust, S. Zielonka. Antibody display technologies: selecting the cream of the crop. *Biol Chem* **2022**, *403*, 455-477.
[63] O. P. Börmer. Interference of complement with the binding of carcinoembryonic antigen to solid-phase monoclonal antibodies. *J Immunol Methods* **1989**, *121*, 85-93.
[64] H. Hyytiä, M.-L. Järvenpää, N. Ristiniemi, T. Lövgren, K. Pettersson. A comparison of capture antibody fragments in cardiac troponin I immunoassay. *Clin Biochem* **2013**, *46*, 963-968.
[65] E.-C. Brockmann, M. Vehniäinen, K. Pettersson. Use of high-capacity surface with oriented recombinant antibody fragments in a 5-min immunoassay for thyroid-stimulating hormone. *Anal Biochem* **2010**, *396*, 242-249.
[66] S. J. Demarest, S. M. Glaser. Antibody therapeutics, antibody engineering, and the merits of protein stability. *Curr Opin Drug Discov Devel* **2008**, *11*, 675-687.
[67] J. Ylikotila, J. L. Hellström, S. Eriksson, M. Vehniäinen, L. Välimaa, H. Takalo, A. Bereznikova, K. Pettersson. Utilization of recombinant Fab fragments in a cTnI immunoassay conducted in spot wells. *Clinical biochemistry* **2006**, *39*, 843-850.
[68] A. Kushnarova-Vakal, R. Aalto, T. Huovinen, S. Wittfooth, U. Lamminmäki. Controlled labelling of tracer antibodies for time-resolved fluorescence-based immunoassays. *Sci Rep* **2024**, *14*, 18113.
[69] J. D. Watson, F. Crick. A structure for deoxyribose nucleic acid. *Nature* **1953**, *421*, 397–396.
[70] R. A. Hughes, A. D. Ellington. Synthetic DNA synthesis and assembly: putting the synthetic in synthetic biology. *Cold Spring Harb Perspect Biol* **2017**, *9*, a023812.
[71] J. Goodchild. Conjugates of oligonucleotides and modified oligonucleotides: a review of their synthesis and properties. *Bioconjug Chem* **1990**, *1*, 165-187.
[72] P. Doty, H. Boedtker, J. Fresco, R. Haselkorn, M. Litt. Secondary structure in ribonucleic acids. *Proc Natl Acad Sci* **1959**, *45*, 482-499.
[73] A. Panjkovich, F. Melo. Comparison of different melting temperature calculation methods for short DNA sequences. *Bioinformatics* **2005**, *21*, 711-722.
[74] C. Schildkraut, S. Lifson. Dependence of the melting temperature of DNA on salt concentration. *Biopolymers* **1965**, *3*, 195-208.
[75] B. I. Kankia, L. A. Marky. DNA, RNA, and DNA/RNA oligomer duplexes: A comparative study of their stability, heat, hydration, and Mg2+ binding properties. *J Phys Chem B* **1999**, *103*, 8759-8767.
[76] S. K. Singh, A. A. Koshkin, J. Wengel, P. Nielsen. LNA (locked nucleic acids): synthesis and high-affinity nucleic acid recognition. *Chem Commun* **1998**, 455-456.
[77] M. Petersen, K. Bondensgaard, J. Wengel, J. P. Jacobsen. Locked nucleic acid (LNA) recognition of RNA: NMR solution structures of LNA: RNA hybrids. *J Am Chem Soc* **2002**, *124*, 5974-5982.
[78] A. A. Koshkin, S. K. Singh, P. Nielsen, V. K. Rajwanshi, R. Kumar, M. Meldgaard, C. E. Olsen, J. Wengel. LNA (Locked Nucleic Acids): Synthesis of the adenine, cytosine, guanine, 5-methylcytosine, thymine and uracil bicyclonucleoside monomers, oligomerisation, and unprecedented nucleic acid recognition. *Tetrahedron* **1998**, *54*, 3607-3630.
[79] P. Mouritzen, A. T. Nielsen, H. M. Pfundheller, Y. Choleva, L. Kongsbak, S. Møller. Single nucleotide polymorphism genotyping using locked nucleic acid (LNA™). *Expert Rev Mol Diagn* **2003**, *3*, 27-38.

[80] S. Mishra, H. Lahiri, S. Banerjee, R. Mukhopadhyay. Molecularly resolved label-free sensing of single nucleobase mismatches by interfacial LNA probes. *Nucleic Acids Res* **2016**, *44*, 3739-3749.

[81] Y. You, B. G. Moreira, M. A. Behlke, R. Owczarzy. Design of LNA probes that improve mismatch discrimination. *Nucleic Acids Res* **2006**, *34*, e60-e60.

[82] P. E. Nielsen, M. Egholm, R. H. Berg, O. Buchardt. Sequence-selective recognition of DNA by strand displacement with a thymine-substituted polyamide. *Science* **1991**, *254*, 1497-1500.

[83] M. Egholm, O. Buchardt, P. E. Nielsen, R. H. Berg. Peptide nucleic acids (PNA). Oligonucleotide analogs with an achiral peptide backbone. *J Am Chem Soc* **1992**, *114*, 1895-1897.

[84] D. R. Corey. Peptide nucleic acids: expanding the scope of nucleic acid recognition. *Trends Biotechnol* **1997**, *15*, 224-229.

[85] S. Shakeel, S. Karim, A. Ali. Peptide nucleic acid (PNA)—a review. *J Chem Technol Biotechnol* **2006**, *81*, 892-899.

[86] P. E. Nielsen, M. Egholm, O. Buchardt. Peptide nucleic acid (PNA). A DNA mimic with a peptide backbone. *Bioconjug Chem* **1994**, *5*, 3-7.

[87] V. V. Demidov, V. N. Potaman, M. Frank-Kamenetskil, M. Egholm, O. Buchard, S. H. Sönnichsen, P. E. Nlelsen. Stability of peptide nucleic acids in human serum and cellular extracts. *Biochem Pharmacol* **1994**, *48*, 1310-1313.

[88] M. Kaisti, A. Kerko, E. Aarikka, P. Saviranta, Z. Boeva, T. Soukka, A. Lehmusvuori. Real-time wash-free detection of unlabeled PNA-DNA hybridization using discrete FET sensor. *Sci Rep* **2017**, *7*, 15734.

[89] B. Cai, S. Wang, L. Huang, Y. Ning, Z. Zhang, G.-J. Zhang. Ultrasensitive label-free detection of PNA–DNA hybridization by reduced graphene oxide field-effect transistor biosensor. *ACS Nano* **2014**, *8*, 2632-2638.

[90] M. Tian, M. Qiao, C. Shen, F. Meng, L. A. Frank, V. V. Krasitskaya, T. Wang, X. Zhang, R. Song, Y. Li. Highly-sensitive graphene field effect transistor biosensor using PNA and DNA probes for RNA detection. *Appl Surf Sci* **2020**, *527*, 146839.

[91] N. Svanvik, G. Westman, D. Wang, M. Kubista. Light-up probes: thiazole orange-conjugated peptide nucleic acid for detection of target nucleic acid in homogeneous solution. *Anal Biochem* **2000**, *281*, 26-35.

[92] A. Bertucci, A. Manicardi, A. Candiani, S. Giannetti, A. Cucinotta, G. Spoto, M. Konstantaki, S. Pissadakis, S. Selleri, R. Corradini. Detection of unamplified genomic DNA by a PNA-based microstructured optical fiber (MOF) Bragg-grating optofluidic system. *Biosens Bioelectron* **2015**, *63*, 248-254.

[93] J. Wang, P. E. Nielsen, M. Jiang, X. Cai, J. R. Fernandes, D. H. Grant, M. Ozsoz, A. Beglieter, M. Mowat. Mismatch-sensitive hybridization detection by peptide nucleic acids immobilized on a quartz crystal microbalance. *Anal Chem* **1997**, *69*, 5200-5202.

[94] A. Palaniappan, J. A. Cheema, D. Rajwar, G. Ammanath, L. Xiaohu, L. S. Koon, W. Yi, U. H. Yildiz, B. Liedberg. Polythiophene derivative on quartz resonators for miRNA capture and assay. *Analyst* **2015**, *140*, 7912-7917.

[95] K. Kubota, A. Ohashi, H. Imachi, H. Harada. Improved in situ hybridization efficiency with locked-nucleic-acid-incorporated DNA probes. *Appl Environ Microbiol* **2006**, *72*, 5311-5317.

[96] K. M. Guckian, B. A. Schweitzer, R. X.-F. Ren, C. J. Sheils, D. C. Tahmassebi, E. T. Kool. Factors contributing to aromatic stacking in water: evaluation in the context of DNA. *J Am Chem Soc* **2000**, *122*, 2213-2222.

[97] E. T. Kool. Hydrogen bonding, base stacking, and steric effects in DNA replication. *Annu Rev Biophys Biomol Struct* **2001**, *30*, 1-22.

[98] C. H. Mak. Unraveling base stacking driving forces in DNA. *J Phys Chem B* **2016**, *120*, 6010-6020.

[99] P. Yakovchuk, E. Protozanova, M. D. Frank-Kamenetskii. Base-stacking and base-pairing contributions into thermal stability of the DNA double helix. *Nucleic Acids Res* **2006**, *34*, 564-574.
[100] S. Bommarito, N. Peyret, J. S. Jr. Thermodynamic parameters for DNA sequences with dangling ends. *Nucleic Acids Res* **2000**, *28*, 1929-1934.
[101] M. Petersheim, D. H. Turner. Base-stacking and base-pairing contributions to helix stability: thermodynamics of double-helix formation with CCGG, CCGGp, CCGGAp, ACCGGp, CCGGUp, and ACCGGUp. *Biochemistry* **1983**, *22*, 256-263.
[102] N. Sugimoto, R. Kierzek, D. H. Turner. Sequence dependence for the energetics of dangling ends and terminal base pairs in ribonucleic acid. *Biochemistry* **1987**, *26*, 4554-4558.
[103] E. Protozanova, P. Yakovchuk, M. D. Frank-Kamenetskii. Stacked–unstacked equilibrium at the nick site of DNA. *J Mol Biol* **2004**, *342*, 775-785.
[104] X. Qiu, N. Hildebrandt. Rapid and multiplexed microRNA diagnostic assay using quantum dot-based forster resonance energy transfer. *ACS Nano* **2015**, *9*, 8449-8457.
[105] L. Francés-Soriano, N. Estebanez, J. Pérez-Prieto, N. Hildebrandt. DNA-coated upconversion nanoparticles for sensitive nucleic acid FRET biosensing. *Adv Funct Mater* **2022**, *32*, 2201541.
[106] C. Tuerk, L. Gold. Systematic evolution of ligands by exponential enrichment: RNA ligands to bacteriophage T4 DNA polymerase. *Science* **1990**, *249*, 505-510.
[107] A. D. Ellington, J. W. Szostak. Selection in vitro of single-stranded DNA molecules that fold into specific ligand-binding structures. *Nature* **1992**, *355*, 850-852.
[108] J. Ciesiolka, J. Gorski, M. Yarus. Selection of an RNA domain that binds Zn2+. *RNA* **1995**, *1*, 538-550.
[109] H.-P. Hofmann, S. Limmer, V. Hornung, M. Sprinzl. Ni2+-binding RNA motifs with an asymmetric purine-rich internal loop and a GA base pair. *RNA* **1997**, *3*, 1289-1300.
[110] N. de-los-Santos-Álvarez, M. J. Lobo-Castañón, A. J. Miranda-Ordieres, P. Tuñón-Blanco. Modified-RNA aptamer-based sensor for competitive impedimetric assay of neomycin B. *J Am Chem Soc* **2007**, *129*, 3808-3809.
[111] N. Rupcich, R. Nutiu, Y. Li, J. D. Brennan. Solid-phase enzyme activity assay utilizing an entrapped fluorescence-signaling DNA aptamer. *Angew Chem Int Ed* **2006**, *45*, 3295-3299.
[112] M. N. Stojanovic, D. W. Landry. Aptamer-based colorimetric probe for cocaine. *J Am Chem Soc* **2002**, *124*, 9678-9679.
[113] X. Fang, Z. Cao, T. Beck, W. Tan. Molecular aptamer for real-time oncoprotein platelet-derived growth factor monitoring by fluorescence anisotropy. *Anal Chem* **2001**, *73*, 5752-5757.
[114] M. Minunni, S. Tombelli, A. Gullotto, E. Luzi, M. Mascini. Development of biosensors with aptamers as bio-recognition element: the case of HIV-1 Tat protein. *Biosens Bioelectron* **2004**, *20*, 1149-1156.
[115] B. J. Boese, R. R. Breaker. In vitro selection and characterization of cellulose-binding DNA aptamers. *Nucleic Acids Res* **2007**, *35*, 6378-6388.
[116] S. Jeong, T.-Y. Eom, S.-J. Kim, S.-W. Lee, J. Yu. In vitro selection of the RNA aptamer against the Sialyl Lewis X and its inhibition of the cell adhesion. *Biochem Biophys Res Commun* **2001**, *281*, 237-243.
[117] W. Li, Y. Ma, Z. Guo, R. Xing, Z. Liu. Efficient screening of glycan-specific aptamers using a glycosylated peptide as a scaffold. *Anal Chem* **2020**, *93*, 956-963.
[118] D. Shangguan, Y. Li, Z. Tang, Z. C. Cao, H. W. Chen, P. Mallikaratchy, K. Sefah, C. J. Yang, W. Tan. Aptamers evolved from live cells as effective molecular probes for cancer study. *Proc Natl Acad Sci* **2006**, *103*, 11838-11843.
[119] C.-H. Wang, J.-J. Wu, G.-B. Lee. Screening of highly-specific aptamers and their applications in paper-based microfluidic chips for rapid diagnosis of multiple bacteria. *Sens Actuators B Chem* **2019**, *284*, 395-402.
[120] S. Song, L. Wang, J. Li, C. Fan, J. Zhao. Aptamer-based biosensors. *TrAC Trends Anal Chem* **2008**, *27*, 108-117.

[121] M. R. Gotrik, T. A. Feagin, A. T. Csordas, M. A. Nakamoto, H. T. Soh. Advancements in aptamer discovery technologies. *Acc Chem Res* **2016**, *49*, 1903-1910.
[122] T. Hermann, D. J. Patel. Adaptive recognition by nucleic acid aptamers. *Science* **2000**, *287*, 820-825.
[123] A. Valadés-Alcaraz, R. Reinosa, M. González-Hevilla, C. Medina-Sánchez, Á. Holguín. Development and Characterization of High-Affinity Aptamers for HIV Protease Detection. *Heliyon* **2024**, *10*, e38234.
[124] R. K. Mosing, S. D. Mendonsa, M. T. Bowser. Capillary electrophoresis-SELEX selection of aptamers with affinity for HIV-1 reverse transcriptase. *Anal Chem* **2005**, *77*, 6107-6112.
[125] X. Lu, L. F. Passalacqua, M. Nodwell, K. Y. Kong, G. Caballero-García, E. V. Dolgosheina, A. R. Ferré-D'Amaré, R. Britton, P. J. Unrau. Symmetry breaking of fluorophore binding to a G-quadruplex generates an RNA aptamer with picomolar KD. *Nucleic Acids Res* **2024**, *52*, 8039-8051.
[126] O. Kensch, B. A. Connolly, H.-J. Steinhoff, A. McGregor, R. S. Goody, T. Restle. HIV-1 reverse transcriptase-pseudoknot RNA aptamer interaction has a binding affinity in the low picomolar range coupled with high specificity. *J Biol Chem* **2000**, *275*, 18271-18278.
[127] L. Wan, A. Yoshikawa, M. Eisenstein, H. T. Soh. High-Throughput Strategy for Enhancing Aptamer Performance across Different Environmental Conditions. *ACS sensors* **2023**, *8*, 2519-2524.
[128] G. Mayer. The chemical biology of aptamers. *Angew Chem Int Ed* **2009**, *48*, 2672-2689.
[129] K. Ketomäki, H. Hakala, H. Lönnberg. Mixed-phase hybridization of short oligodeoxyribonucleotides on microscopic polymer particles: Effect of one-base mismatches on duplex stability. *Bioconjug Chem* **2002**, *13*, 542-547.
[130] L. F. Huergo, K. A. Selim, M. S. Conzentino, E. C. Gerhardt, A. R. Santos, B. Wagner, J. T. Alford, N. Deobald, F. O. Pedrosa, E. M. de Souza. Magnetic bead-based immunoassay allows rapid, inexpensive, and quantitative detection of human SARS-CoV-2 antibodies. *ACS sensors* **2021**, *6*, 703-708.
[131] C. W. Kan, C. I. Tobos, D. M. Rissin, A. D. Wiener, R. E. Meyer, D. M. Svancara, A. Comperchio, C. Warwick, R. Millington, N. Collier. Digital enzyme-linked immunosorbent assays with sub-attomolar detection limits based on low numbers of capture beads combined with high efficiency bead analysis. *Lab Chip* **2020**, *20*, 2122-2135.
[132] D. Sklenárová, A. Hlaváček, J. Křivánková, J. C. Brandmeier, J. Weisová, M. Řiháček, H. H. Gorris, P. Skládal, Z. Farka. Single-molecule microfluidic assay for prostate-specific antigen based on magnetic beads and upconversion nanoparticles. *Lab Chip* **2024**, *24*, 3536-3545.
[133] J. L. Tonkinson, B. A. Stillman. Nitrocellulose: a tried and true polymer finds utility as a post-genomic substrate. *Front Biosci* **2002**, *7*, c1-c12.
[134] R. Tang, M. Y. Xie, M. Li, L. Cao, S. Feng, Z. Li, F. Xu. Nitrocellulose membrane for paper-based biosensor. *Appl Mater Today* **2022**, *26*, 101305.
[135] J. Máčala, E. Makhneva, A. n. Hlaváček, M. Kopecký, H. H. Gorris, P. Skládal, Z. k. Farka. Upconversion Nanoparticle-Based Dot-Blot Immunoassay for Quantitative Biomarker Detection. *Anal Chem* **2024**.
[136] G. A. Posthuma-Trumpie, J. Korf, A. van Amerongen. Lateral flow (immuno) assay: its strengths, weaknesses, opportunities and threats. A literature survey. *Anal Bioanal Chem* **2009**, *393*, 569-582.
[137] M. A. Mansfield, 'Nitrocellulose membranes for lateral flow immunoassays: a technical treatise' in *Lateral flow immunoassay*, Springer, **2008**, pp. 1-19.
[138] L. J. Kricka. Selected strategies for improving sensitivity and reliability of immunoassays. *Clin Chem* **1994**, *40*, 347-357.
[139] P. Sengupta, C. W. Wang, Z. F. Ma, 'Enzyme-Linked Immunosorbent Assay (ELISA) technique for food analysis' in *Techniques to Measure Food Safety and Quality: Microbial,*

Chemical, and Sensory (Eds.: M. S. Khan, M. Shafiur Rahman), Springer, Cham, **2021**, pp. 91-115.

[140] S. Hosseini, P. Vázquez-Villegas, M. Rito-Palomares, S. O. Martinez-Chapa, *Enzyme-linked immunosorbent assay (ELISA): from A to Z*, Springer, **2018**.

[141] J. P. Gosling. A decade of development in immunoassay methodology. *Clin Chem* **1990**, *36*, 1408-1427.

[142] K. Pettersson, T. Katajamäki, K. Irjala, V. Leppanen, K. Majamaa-Voltti, P. Laitinen. Time-resolved fluorometry (TRF)-based immunoassay concept for rapid and quantitative determination of biochemical myocardial infarction markers from whole blood, serum and plasma. *Luminescence* **2000**, *15*, 399-407.

[143] Y. Wang, L. Yu, H. Zhang, R. Zhu, Z. Meng. Competitive ELISA based on pH-responsive persistent luminescence nanoparticles for autofluorescence-free biosensor determination of ochratoxin A in cereals. *Anal Bioanal Chem* **2023**, *415*, 1877-1887.

[144] G. Thorpe, L. Kricka. Enhanced chemiluminescent reactions catalyzed by horseradish peroxidase. *Methods in enzymology* **1986**, *133*, 331-353.

[145] S. X. Leng, J. E. McElhaney, J. D. Walston, D. Xie, N. S. Fedarko, G. A. Kuchel. ELISA and multiplex technologies for cytokine measurement in inflammation and aging research. *J Gerontol A Biol Sci Med Sci* **2008**, *63*, 879-884.

[146] C. I. Tobos, S. Kim, D. M. Rissin, J. M. Johnson, S. Douglas, S. Yan, S. Nie, B. Rice, K.-J. Sung, H. D. Sikes. Sensitivity and binding kinetics of an ultra-sensitive chemiluminescent enzyme-linked immunosorbent assay at arrays of antibodies. *J Immunol Methods* **2019**, *474*, 112643.

[147] Y. Zhong, X. Wu, J. Li, Q. Lan, Q. Jing, L. Min, C. Ren, X. Hu, A. Lambert, Q. Cheng. Multiplex immunoassay of chicken cytokines via highly-sensitive chemiluminescent imaging array. *Anal Chim Acta* **2019**, *1049*, 213-218.

[148] E. Soini, H. Kojola. Time-resolved fluorometer for lanthanide chelates--a new generation of nonisotopic immunoassays. *Clin Chem* **1983**, *29*, 65-68.

[149] E. Soini, I. Hemmilä. Fluoroimmunoassay: present status and key problems. *Clin Chem* **1979**, *25*, 353-361.

[150] H. Siitari, I. Hemmilä, E. Soini, T. Lövgren, V. Koistinen. Detection of hepatitis B surface antigen using time-resolved fluoroimmunoassay. *Nature* **1983**, *301*, 258-260.

[151] H. Takalo, V.-M. Mukkala, H. Mikola, P. Liitti, I. Hemmila. Synthesis of europium (III) chelates suitable for labeling of bioactive molecules. *Bioconjug Chem* **1994**, *5*, 278-282.

[152] P. Von Lode, J. Rosenberg, K. Pettersson, H. Takalo. A europium chelate for quantitative point-of-care immunoassays using direct surface measurement. *Anal Chem* **2003**, *75*, 3193-3201.

[153] J. Yuan, K. Matsumoto, H. Kimura. A new tetradentate β-diketonate− europium chelate that can be covalently bound to proteins for time-resolved fluoroimmunoassay. *Anal Chem* **1998**, *70*, 596-601.

[154] A. Scorilas, A. Bjartell, H. Lilja, C. Moller, E. P. Diamandis. Streptavidin-polyvinylamine conjugates labeled with a europium chelate: applications in immunoassay, immunohistochemistry, and microarrays. *Clin Chem* **2000**, *46*, 1450-1455.

[155] H. Harma, T. Soukka, T. Lovgren. Europium nanoparticles and time-resolved fluorescence for ultrasensitive detection of prostate-specific antigen. *Clin Chem* **2001**, *47*, 561-568.

[156] Y. Xu, Q. Li. Multiple fluorescent labeling of silica nanoparticles with lanthanide chelates for highly sensitive time-resolved immunofluorometric assays. *Clin Chem* **2007**, *53*, 1503-1510.

[157] U. Cho, D. P. Riordan, P. Ciepla, K. S. Kocherlakota, J. K. Chen, P. B. Harbury. Ultrasensitive optical imaging with lanthanide lumiphores. *Nat Chem Biol* **2018**, *14*, 15-21.

[158] W. Feng, J. C. Beer, Q. Hao, I. S. Ariyapala, A. Sahajan, A. Komarov, K. Cha, M. Moua, X. Qiu, X. Xu. NULISA: a proteomic liquid biopsy platform with attomolar sensitivity and high multiplexing. *Nat Commun* **2023**, *14*, 7238.

[159] P. W. Sims, M. Vasser, W. L. Wong, P. M. Williams, Y. G. Meng. Immunopolymerase chain reaction using real-time polymerase chain reaction for detection. *Anal Biochem* **2000**, *281*, 230-232.

[160] M. C. Hansen, L. Nederby, M. O.-B. Henriksen, M. Hansen, C. G. Nyvold. Sensitive ligand-based protein quantification using immuno-PCR: a critical review of single-probe and proximity ligation assays. *Biotechniques* **2014**, *56*, 217-228.

[161] T. Sano, C. L. Smith, C. R. Cantor. Immuno-PCR: very sensitive antigen detection by means of specific antibody-DNA conjugates. *Science* **1992**, *258*, 120-122.

[162] N. Menyuk, K. Dwight, J. Pierce. NaYF4: Yb, Er—an efficient upconversion phosphor. *Appl Phys Lett* **1972**, *21*, 159-161.

[163] S. Lahtinen, in *Upconverting Nanoparticles in Bioaffinity Assays: New Insights and Perspectives*, University of Turku, **2019**.

[164] C. Würth, M. Kaiser, S. Wilhelm, B. Grauel, T. Hirsch, U. Resch-Genger. Excitation power dependent population pathways and absolute quantum yields of upconversion nanoparticles in different solvents. *Nanoscale* **2017**, *9*, 4283-4294.

[165] J. Hampl, M. Hall, N. A. Mufti, M. Y. Yung-mae, D. B. MacQueen, W. H. Wright, D. E. Cooper. Upconverting phosphor reporters in immunochromatographic assays. *Anal Biochem* **2001**, *288*, 176-187.

[166] J.-C. Boyer, F. C. Van Veggel. Absolute quantum yield measurements of colloidal NaYF 4: Er3+, Yb3+ upconverting nanoparticles. *Nanoscale* **2010**, *2*, 1417-1419.

[167] S. Wilhelm. Perspectives for upconverting nanoparticles. *ACS Nano* **2017**, *11*, 10644-10653.

[168] A. L. Ouellette, J. J. Li, D. E. Cooper, A. J. Ricco, G. T. Kovacs. Evolving point-of-care diagnostics using up-converting phosphor bioanalytical systems. *Anal Chem* **2009**, *81*, 3216-3221.

[169] Z. Farka, M. J. Mickert, A. Hlavacek, P. Skladal, H. H. Gorris. Single molecule upconversion-linked immunosorbent assay with extended dynamic range for the sensitive detection of diagnostic biomarkers. *Anal Chem* **2017**, *89*, 11825-11830.

[170] F. Van De Rijke, H. Zijlmans, S. Li, T. Vail, A. K. Raap, R. S. Niedbala, H. J. Tanke. Up-converting phosphor reporters for nucleic acid microarrays. *Nat Biotechnol* **2001**, *19*, 273-276.

[171] V. Kale, H. Päkkilä, J. Vainio, A. Ahomaa, N. Sirkka, A. Lyytikäinen, S. M. Talha, A. Kutsaya, M. Waris, I. Julkunen. Spectrally and spatially multiplexed serological array-in-well assay utilizing two-color upconversion luminescence imaging. *Anal Chem* **2016**, *88*, 4470-4477.

[172] M. Ekman, T. Salminen, K. Raiko, T. Soukka, K. Gidwani, I. Martiskainen. Spectrally separated dual-label upconversion luminescence lateral flow assay for cancer-specific STn-glycosylation in CA125 and CA15-3. *Anal Bioanal Chem* **2024**, 1-10.

[173] S. Wu, G. Han, D. J. Milliron, S. Aloni, V. Altoe, D. V. Talapin, B. E. Cohen, P. J. Schuck. Non-blinking and photostable upconverted luminescence from single lanthanide-doped nanocrystals. *Proc Natl Acad Sci* **2009**, *106*, 10917-10921.

[174] J. Zhou, S. Xu, J. Zhang, J. Qiu. Upconversion luminescence behavior of single nanoparticles. *Nanoscale* **2015**, *7*, 15026-15036.

[175] J. Shen, L.-D. Sun, C.-H. Yan. Luminescent rare earth nanomaterials for bioprobe applications. *Dalton Trans* **2008**, 5687-5697.

[176] S. Wilhelm, M. Kaiser, C. Würth, J. Heiland, C. Carrillo-Carrion, V. Muhr, O. S. Wolfbeis, W. J. Parak, U. Resch-Genger, T. Hirsch. Water dispersible upconverting nanoparticles: effects of surface modification on their luminescence and colloidal stability. *Nanoscale* **2015**, *7*, 1403-1410.

[177] N. Bogdan, F. Vetrone, G. A. Ozin, J. A. Capobianco. Synthesis of ligand-free colloidally stable water dispersible brightly luminescent lanthanide-doped upconverting nanoparticles. *Nano Lett* **2011**, *11*, 835-840.

[178] A. Dong, X. Ye, J. Chen, Y. Kang, T. Gordon, J. M. Kikkawa, C. B. Murray. A generalized ligand-exchange strategy enabling sequential surface functionalization of colloidal nanocrystals. *J Am Chem Soc* **2011**, *133*, 998-1006.

[179] N. Estebanez, M. Gonzalez-Bejar, J. Perez-Prieto. Polysulfonate cappings on upconversion nanoparticles prevent their disintegration in water and provide superior stability in a highly acidic medium. *ACS omega* **2019**, *4*, 3012-3019.

[180] A. Schroter, C. Arnau del Valle, M. J. Marín, T. Hirsch. Bilayer-Coating Strategy for Hydrophobic Nanoparticles Providing Colloidal Stability, Functionality, and Surface Protection in Biological Media. *Angew Chem Int Ed* **2023**, *62*, e202305165.

[181] S. F. Himmelstoß, T. Hirsch. Long-term colloidal and chemical stability in aqueous media of NaYF4-type upconversion nanoparticles modified by ligand-exchange. *Part Part Syst Charact* **2019**, *36*, 1900235.

[182] R. Gref, A. Domb, P. Quellec, T. Blunk, R. Müller, J.-M. Verbavatz, R. Langer. The controlled intravenous delivery of drugs using PEG-coated sterically stabilized nanospheres. *Adv Drug Deliv Rev* **2012**, *64*, 316-326.

[183] A. Nsubuga, M. Sgarzi, K. Zarschler, M. Kubeil, R. Hübner, R. Steudtner, B. Graham, T. Joshi, H. Stephan. Facile preparation of multifunctionalisable 'stealth' upconverting nanoparticles for biomedical applications. *Dalton Trans* **2018**, *47*, 8595-8604.

[184] E. Juntunen, R. Arppe, L. Kalliomäki, T. Salminen, S. M. Talha, T. Myyryläinen, T. Soukka, K. Pettersson. Effects of blood sample anticoagulants on lateral flow assays using luminescent photon-upconverting and Eu(III) nanoparticle reporters. *Anal Biochem* **2016**, *492*, 13-20.

[185] C. D. Walkey, J. B. Olsen, H. Guo, A. Emili, W. C. Chan. Nanoparticle size and surface chemistry determine serum protein adsorption and macrophage uptake. *J Am Chem Soc* **2012**, *134*, 2139-2147.

[186] R. Deng, J. Wang, R. Chen, W. Huang, X. Liu. Enabling Förster resonance energy transfer from large nanocrystals through energy migration. *J Am Chem Soc* **2016**, *138*, 15972-15979.

[187] I. Martiskainen, S. M. Talha, K. Vuorenpää, T. Salminen, E. Juntunen, S. Chattopadhyay, D. Kumar, T. Vuorinen, K. Pettersson, N. Khanna. Upconverting nanoparticle reporter–based highly sensitive rapid lateral flow immunoassay for hepatitis B virus surface antigen. *Anal Bioanal Chem* **2021**, *413*, 967-978.

[188] S. Bayoumy, I. Martiskainen, T. Heikkilä, C. Rautanen, P. Hedberg, H. Hyytiä, S. Wittfooth, K. Pettersson. Sensitive and quantitative detection of cardiac troponin I with upconverting nanoparticle lateral flow test with minimized interference. *Sci Rep* **2021**, *11*, 18698.

[189] E. Juntunen, R. Arppe, L. Kalliomäki, T. Salminen, S. M. Talha, T. Myyryläinen, T. Soukka, K. Pettersson. Effects of blood sample anticoagulants on lateral flow assays using luminescent photon-upconverting and Eu (III) nanoparticle reporters. *Anal Biochem* **2016**, *492*, 13-20.

[190] M. Urdea, T. Horn, T. Fultz, M. Anderson, J. Running, S. Hamren, D. Ahle, C. Chang. Branched DNA amplification multimers for the sensitive, direct detection of human hepatitis viruses. *Nucleic Acids Symp Ser* **1991**, 197-200.

[191] D. Kern, M. Collins, T. Fultz, J. Detmer, S. Hamren, J. J. Peterkin, P. Sheridan, M. Urdea, R. White, T. Yeghiazarian. An enhanced-sensitivity branched-DNA assay for quantification of human immunodeficiency virus type 1 RNA in plasma. *J Clin Microbiol* **1996**, *34*, 3196-3202.

[192] K. Sun, X. Wang, Y. Qu, H. Wang, J. Cheng. Amplification-Free Nucleic Acid Testing with a Fluorescence One-Step-Branched DNA-Based Lateral Flow Assay (FOB-LFA). *Anal Chem* **2023**, *95*, 13605-13613.

[193] J. D. Yao, M. G. Beld, L. L. E. Oon, C. H. Sherlock, J. Germer, S. Menting, S. Y. Se Thoe, L. Merrick, R. Ziermann, J. Surtihadi. Multicenter evaluation of the VERSANT hepatitis B virus DNA 3.0 assay. *J Clin Microbiol* **2004**, *42*, 800-806.

[194] T. Elbeik, J. Surtihadi, M. Destree, J. Gorlin, M. Holodniy, S. A. Jortani, K. Kuramoto, V. Ng, R. Valdes Jr, A. Valsamakis. Multicenter evaluation of the performance characteristics of the Bayer VERSANT HCV RNA 3.0 assay (bDNA). *J Clin Microbiol* **2004**, *42*, 563-569.

[195] C. A. Gleaves, J. Welle, M. Campbell, T. Elbeik, V. Ng, P. E. Taylor, K. Kuramoto, S. Aceituno, E. Lewalski, B. Joppa. Multicenter evaluation of the Bayer VERSANT™ HIV-1 RNA 3.0 assay: analytical and clinical performance. *J Clin Virol* **2002**, *25*, 205-216.

[196] C. Kolbert, J. Arruda, P. Varga-Delmore, X. Zheng, M. Lewis, J. Kolberg, D. Persing. Branched-DNA assay for detection of the mecA gene in oxacillin-resistant and oxacillin-sensitive staphylococci. *J Clin Microbiol* **1998**, *36*, 2640-2644.

[197] M. Flagella, S. Bui, Z. Zheng, C. T. Nguyen, A. Zhang, L. Pastor, Y. Ma, W. Yang, K. L. Crawford, G. K. McMaster. A multiplex branched DNA assay for parallel quantitative gene expression profiling. *Anal Biochem* **2006**, *352*, 50-60.

[198] K. T. Soh, P. K. Wallace, 'RNA flow cytometry using the branched DNA technique' in *Flow Cytometry Protocols* (Eds.: T. S. Hawley, R. G. Hawley), Springer Nature, New York, **2018**, pp. 49-77.

[199] D. P. Hartley, C. D. Klaassen. Detection of chemical-induced differential expression of rat hepatic cytochrome P450 mRNA transcripts using branched DNA signal amplification technology. *Drug Metab Dispos* **2000**, *28*, 608-616.

[200] M. L. Collins, B. Irvine, D. Tyner, E. Fine, C. Zayati, C.-a. Chang, T. Horn, D. Ahle, J. Detmer, L.-P. Shen. A branched DNA signal amplification assay for quantification of nucleic acid targets below 100 molecules/ml. *Nucleic Acids Res* **1997**, *25*, 2979-2984.

[201] T. Horn, C.-A. Chang, M. L. Collins. Hybridization properties of the 5-methyl-isocytidine/isoguanosine base pair in synthetic oligodeoxynucleotides. *Tetrahedron Lett* **1995**, *36*, 2033-2036.

[202] J. C. Brandmeier, S. Kuusinen, Z. Farka, T. Soukka, H. H. Gorris. Upconversion-Linked Branched DNA Hybridization Assay for the Detection of Bacteriophage M13. *Adv Opt Mater* **2024**, 2402041.

[203] A. P. Sokolenko, E. N. Imyanitov. Molecular diagnostics in clinical oncology. *Front Mol Biosci* **2018**, *5*, 76.

[204] A. Afzal. Molecular diagnostic technologies for COVID-19: Limitations and challenges. *J Adv Res* **2020**, *26*, 149-159.

[205] S. Bustin. INVITED REVIEW Quantification of mRNA using real-time reverse transcription PCR (RT-PCR): trends and problems. *J Mol Endocrinol* **2002**, *29*, 23-39.

[206] G. J. Tsongalis. Branched DNA technology in molecular diagnostics. *Am J Clin Pathol* **2006**, *126*, 448-453.

[207] H. Alter, R. Sanchez-Pescador, M. Urdea, J. Wilber, R. Lagier, A. Di Bisceglie, J. Shih, P. Neuwald. Evaluation of branched DNA signal amplification for the detection of hepatitis C virus RNA. *J Viral Hepat* **1995**, *2*, 121-132.

[208] R. K. Saiki, S. Scharf, F. Faloona, K. B. Mullis, G. T. Horn, H. A. Erlich, N. Arnheim. Enzymatic amplification of β-globin genomic sequences and restriction site analysis for diagnosis of sickle cell anemia. *Science* **1985**, *230*, 1350-1354.

[209] V. Ruzicka, W. März, A. Russ, W. Gross. Immuno-PCR with a commercially available avidin system. *Science* **1993**, *260*, 698-699.

[210] H. Zhou, R. J. Fisher, T. S. Papas. Universal immuno-PCR for ultra-sensitive target protein detection. *Nucleic Acids Res* **1993**, *21*, 6038.

[211] R. D. Joerger, T. M. Truby, E. R. Hendrickson, R. M. Young, R. C. Ebersole. Analyte detection with DNA-labeled antibodies and polymerase chain reaction. *Clin Chem* **1995**, *41*, 1371-1377.

[212] Y. Numata, Y. Matsumoto. Rapid detection of α-human atrial natriuretic peptide in plasma by a sensitive immuno-PCR sandwich assay. *Clin Chim Acta* **1997**, *259*, 169-176.

[213] E. R. Hendrickson, T. M. H. Truby, R. D. Joerger, W. R. Majarian, R. C. Ebersole. High sensitivity multianalyte immunoassay using covalent DNA-labeled antibodies and polymerase chain reaction. *Nucleic Acids Res* **1995**, *23*, 522-529.

[214] P. P. Sanna, F. Weiss, M. E. Samson, F. E. Bloom, E. M. Pich. Rapid induction of tumor necrosis factor alpha in the cerebrospinal fluid after intracerebroventricular injection of

lipopolysaccharide revealed by a sensitive capture immuno-PCR assay. *Proc Natl Acad Sci* **1995**, *92*, 272-275.

[215] K. Saito, D. Kobayashi, M. Sasaki, H. Araake, T. Kida, A. Yagihashi, T. Yajima, H. Kameshima, N. Watanabe. Detection of human serum tumor necrosis factor-α in healthy donors, using a highly sensitive immuno-PCR assay. *Clin Chem* **1999**, *45*, 665-669.

[216] C. M. Niemeyer, M. Adler, D. Blohm. Fluorometric polymerase chain reaction (PCR) enzyme-linked immunosorbent assay for quantification of immuno-PCR products in microplates. *Anal Biochem* **1997**, *246*, 140-145.

[217] R. Higuchi, C. Fockler, G. Dollinger, R. Watson. Kinetic PCR analysis: real-time monitoring of DNA amplification reactions. *Bio/technology* **1993**, *11*, 1026-1030.

[218] C. A. Heid, J. Stevens, K. J. Livak, P. M. Williams. Real time quantitative PCR. *Genome Res* **1996**, *6*, 986-994.

[219] E. Dráberová, L. Stegurová, V. Sulimenko, Z. Hájková, P. Dráber, P. Dráber. Quantification of α-tubulin isotypes by sandwich ELISA with signal amplification through biotinyl-tyramide or immuno-PCR. *J Immunol Methods* **2013**, *395*, 63-70.

[220] M. Hashimoto, M. Aoki, B. Winblad, L. O. Tjernberg. A novel approach for Aβ1–40 quantification using immuno-PCR. *J Neurosci Methods* **2012**, *205*, 364-367.

[221] S. He, S. Yu, Y. Feng, L. He, L. Liu, C. Y. Effah, Y. Wu. A digital immuno-PCR assay for simultaneous determination of 5-methylcytosine and 5-hydroxymethylcytosine in human serum. *Anal Chim Acta* **2022**, *1192*, 339321.

[222] H. Zhang, Y. Xu, Q. Huang, C. Yi, T. Xiao, Q. Li. Natural phage nanoparticle-mediated real-time immuno-PCR for ultrasensitive detection of protein marker. *Chem Commun* **2013**, *49*, 3778-3780.

[223] N. Guan, Y. Li, H. Yang, P. Hu, S. Lu, H. Ren, Z. Liu, K. S. Park, Y. Zhou. Dual-functionalized gold nanoparticles probe based bio-barcode immuno-PCR for the detection of glyphosate. *Food Chem* **2021**, *338*, 128133.

[224] N. Boulter, F. G. Suarez, S. Schibeci, T. Sunderland, O. Tolhurst, T. Hunter, G. Hodge, D. Handelsman, U. Simanainen, E. Hendriks. A simple, accurate and universal method for quantification of PCR. *BMC Biotechnol* **2016**, *16*, 1-14.

[225] L. Xu, J. Duan, J. Chen, S. Ding, W. Cheng. Recent advances in rolling circle amplification-based biosensing strategies-A review. *Anal Chim Acta* **2021**, *1148*, 238187.

[226] M. You, P. Peng, Z. Xue, H. Tong, W. He, P. Mao, Q. Liu, C. Yao, F. Xu. A fast and ultrasensitive ELISA based on rolling circle amplification. *Analyst* **2021**, *146*, 2871-2877.

[227] M. Dekaliuk, Z. Farka, N. Hildebrandt. The pros and cons of nucleic acid-amplified immunoassays—a comparative study on the quantitation of prostate-specific antigen with and without rolling circle amplification. *Anal Bioanal Chem* **2024**, 1-10.

[228] J. Liu, Y. Zhang, H. Xie, L. Zhao, L. Zheng, H. Ye. Applications of catalytic hairpin assembly reaction in biosensing. *Small* **2019**, *15*, 1902989.

[229] J. Wu, J. Lv, X. Zheng, Z.-S. Wu. Hybridization chain reaction and its applications in biosensing. *Talanta* **2021**, *234*, 122637.

[230] R. M. Dirks, N. A. Pierce. Triggered amplification by hybridization chain reaction. *Proc Natl Acad Sci* **2004**, *101*, 15275-15278.

[231] J. Xu, J. Wu, C. Zong, H. Ju, F. Yan. Manganese porphyrin-dsDNA complex: a mimicking enzyme for highly efficient bioanalysis. *Anal Chem* **2013**, *85*, 3374-3379.

[232] P. Yin, H. M. Choi, C. R. Calvert, N. A. Pierce. Programming biomolecular self-assembly pathways. *Nature* **2008**, *451*, 318-322.

[233] T. Watanabe, S. Hashida. The immune complex transfer enzyme immunoassay: Mechanism of improved sensitivity compared with conventional sandwich enzyme immunoassay. *J Immunol Methods* **2018**, *459*, 76-80.

[234] R. Schmidt, J. Jacak, C. Schirwitz, V. Stadler, G. Michel, N. Marmé, G. J. Schütz, J. r. D. Hoheisel, J.-P. Knemeyer. Single-molecule detection on a protein-array assay platform for the exposure of a tuberculosis antigen. *J Proteome Res* **2011**, *10*, 1316-1322.
[235] H. Schröder, M. Grösche, M. Adler, M. Spengler, C. M. Niemeyer. Immuno-PCR with digital readout. *Biochem Biophys Res Commun* **2017**, *488*, 311-315.
[236] A. Frutiger, A. Tanno, S. Hwu, R. F. Tiefenauer, J. Voros, N. Nakatsuka. Nonspecific binding—fundamental concepts and consequences for biosensing applications. *Chem Rev* **2021**, *121*, 8095-8160.
[237] D. R. Walt. Ubiquitous sensors: when will they be here? *ACS Nano* **2009**, *3*, 2876-2880.
[238] H. de Puig, I. Bosch, M. Carré-Camps, K. Hamad-Schifferli. Effect of the protein corona on antibody–antigen binding in nanoparticle sandwich immunoassays. *Bioconjug Chem* **2017**, *28*, 230-238.
[239] D. Mendez-Gonzalez, S. Lahtinen, M. Laurenti, E. López-Cabarcos, J. Rubio-Retama, T. Soukka. Photochemical ligation to ultrasensitive DNA detection with upconverting nanoparticles. *Anal Chem* **2018**, *90*, 13385-13392.
[240] D. Mendez-Gonzalez, P. P. Silva-Ibáñez, F. Valiente-Dies, O. G. Calderón, J. L. Mendez-Gonzalez, M. Laurenti, A. Egatz-Gómez, E. Díaz, J. Rubio-Retama, S. Melle. Oligonucleotide sensor based on magnetic capture and photoligation of upconverting nanoparticles in solid surfaces. *J Colloid Interface Sci* **2021**, *596*, 64-74.
[241] M. P. Monopoli, C. Åberg, A. Salvati, K. A. Dawson. Biomolecular coronas provide the biological identity of nanosized materials. *Nat Nanotechnol* **2012**, *7*, 779-786.
[242] P. Esser. Principles in adsorption to polystyrene. *Thermo Scientific Nunc Bulletin* **1988**, *6*, 1-5.
[243] K. Thapa, W. Liu, R. Wang. Nucleic acid-based electrochemical biosensor: Recent advances in probe immobilization and signal amplification strategies. *Wiley Interdiscip Rev: Nanomed Nanobiotechnology* **2022**, *14*, e1765.
[244] N. M. Green, '[5] Avidin and streptavidin' in *Methods in enzymology, Vol. 184*, Elsevier, **1990**, pp. 51-67.
[245] J. Davies, A. Dawkes, A. Haymes, C. Roberts, R. Sunderland, M. Wilkins, M. Davies, S. Tendler, D. Jackson, J. Edwards. A scanning tunneling microscopy comparison of passive antibody adsorption and biotinylated antibody linkage to streptavidin on microtiter wells. *J Immunol Methods* **1994**, *167*, 263-269.
[246] R. Ahirwar, S. Bariar, A. Balakrishnan, P. Nahar. BSA blocking in enzyme-linked immunosorbent assays is a non-mandatory step: a perspective study on mechanism of BSA blocking in common ELISA protocols. *RSC advances* **2015**, *5*, 100077-100083.
[247] Y. Xiao, S. N. Isaacs. Enzyme-linked immunosorbent assay (ELISA) and blocking with bovine serum albumin (BSA)—not all BSAs are alike. *J Immunol Methods* **2012**, *384*, 148-151.
[248] J. B. Schlenoff. Zwitteration: coating surfaces with zwitterionic functionality to reduce nonspecific adsorption. *Langmuir* **2014**, *30*, 9625-9636.
[249] R. G. Chapman, E. Ostuni, M. N. Liang, G. Meluleni, E. Kim, L. Yan, G. Pier, H. S. Warren, G. M. Whitesides. Polymeric thin films that resist the adsorption of proteins and the adhesion of bacteria. *Langmuir* **2001**, *17*, 1225-1233.
[250] A. Jain, R. Liu, Y. K. Xiang, T. Ha. Single-molecule pull-down for studying protein interactions. *Nat Protoc* **2012**, *7*, 445-452.
[251] T. Pochechueva, A. Chinarev, N. Bovin, A. Fedier, F. Jacob, V. Heinzelmann-Schwarz. PEGylation of microbead surfaces reduces unspecific antibody binding in glycan-based suspension array. *J Immunol Methods* **2014**, *412*, 42-52.
[252] M. Zheng, F. Davidson, X. Huang. Ethylene glycol monolayer protected nanoparticles for eliminating nonspecific binding with biological molecules. *J Am Chem Soc* **2003**, *125*, 7790-7791.

[253] L. Shi, J. Zhang, M. Zhao, S. Tang, X. Cheng, W. Zhang, W. Li, X. Liu, H. Peng, Q. Wang. Effects of polyethylene glycol on the surface of nanoparticles for targeted drug delivery. *Nanoscale* **2021**, *13*, 10748-10764.

[254] A. Saftics, B. Türk, A. Sulyok, N. Nagy, E. Agócs, B. Kalas, P. Petrik, M. Fried, N. Q. Khánh, A. Prósz, 'Dextran-based hydrogel layers for biosensors' in *Nanobiomaterial Engineering: Concepts and Their Applications in Biomedicine and Diagnostics* (Eds.: P. Chandra, R. Prakash), Springer, **2020**, pp. 139-164.

[255] P. Brown-Augsburger, X. M. Yue, J. A. Lockridge, J. A. McSwiggen, D. Kamboj, K. M. Hillgren. Development and validation of a sensitive, specific, and rapid hybridization-ELISA assay for determination of concentrations of a ribozyme in biological matrices. *J Pharm Biomed Anal* **2004**, *34*, 129-139.

[256] L. Li, L. Zhou, Y. Yu, Z. Zhu, C. Lin, C. Lu, R. Yang. Development of up-converting phosphor technology-based lateral-flow assay for rapidly quantitative detection of hepatitis B surface antibody. *Diagn Microbiol Infect Dis* **2009**, *63*, 165-172.

[257] S. V. Mullegama, M. O. Alberti, C. Au, Y. Li, T. Toy, V. Tomasian, R. R. Xian, 'Nucleic acid extraction from human biological samples' in *Biobanking: Methods and protocols* (Ed.: W. H. Yong), Humana New York, **2019**, pp. 359-383.

[258] N. Ali, R. d. C. P. Rampazzo, A. D. T. Costa, M. A. Krieger. Current nucleic acid extraction methods and their implications to point-of-care diagnostics. *Biomed Res Int* **2017**, *2017*, 9306564.

[259] K. M. McCutcheon, V. Quarmby, A. Song. Development and optimization of a cell-based neutralizing antibody assay using a sample pre-treatment step to eliminate serum interference. *J Immunol Methods* **2010**, *358*, 35-45.

[260] V. Kloten, M. H. Neumann, F. Di Pasquale, M. Sprenger-Haussels, J. M. Shaffer, M. Schlumpberger, A. Herdean, F. Betsou, W. Ammerlaan, T. af Hällström. Multicenter evaluation of circulating plasma microRNA extraction technologies for the development of clinically feasible reverse transcription quantitative PCR and next-generation sequencing analytical work flows. *Clin Chem* **2019**, *65*, 1132-1140.

[261] S. Darmanis, R. Y. Nong, M. Hammond, J. Gu, A. Alderborn, J. Vänelid, A. Siegbahn, S. Gustafsdottir, O. Ericsson, U. Landegren. Sensitive plasma protein analysis by microparticle-based proximity ligation assays. *Mol Cell Proteomics* **2010**, *9*, 327-335.

[262] T. Näreoja, J. M. Rosenholm, U. Lamminmäki, P. E. Hänninen. Super-sensitive time-resolved fluoroimmunoassay for thyroid-stimulating hormone utilizing europium (III) nanoparticle labels achieved by protein corona stabilization, short binding time, and serum preprocessing. *Anal Bioanal Chem* **2017**, *409*, 3407-3416.

[263] T. Kohno, E. Ishikawa. A novel enzyme immunoassay of anti-insulin IgG in guinea pig serum. *Biochem Biophys Res Commun* **1987**, *147*, 644-649.

[264] T. Kohno, T. Mitsukawa, S. Matsukura, Y. Tsunetoshi, E. Ishikawa. More sensitive and simpler immune complex transfer enzyme immunoassay for antithyroglobulin IgG in serum. *J Clin Lab Anal* **1989**, *3*, 163-168.

[265] D. V. Morrissey, M. Lombardo, J. K. Eldredge, K. R. Kearney, E. P. Groody, M. L. Collins. Nucleic acid hybridization assays employing dA-tailed capture probes: I. Multiple capture methods. *Anal Biochem* **1989**, *181*, 345-359.

[266] E. Schallmeiner, E. Oksanen, O. Ericsson, L. Spångberg, S. Eriksson, U.-H. Stenman, K. Pettersson, U. Landegren. Sensitive protein detection via triple-binder proximity ligation assays. *Nat Methods* **2007**, *4*, 135-137.

[267] S. Fredriksson, M. Gullberg, J. Jarvius, C. Olsson, K. Pietras, S. M. Gústafsdóttir, A. Östman, U. Landegren. Protein detection using proximity-dependent DNA ligation assays. *Nat Biotechnol* **2002**, *20*, 473-477.

[268] L. Zhu, H. Koistinen, P. Wu, A. Närvänen, E. Schallmeiner, S. Fredriksson, U. Landegren, U.-H. Stenman. A sensitive proximity ligation assay for active PSA. *Biol Chem* **2006**, *387*, 769-772.

[269] M. Gullberg, S. M. Gústafsdóttir, E. Schallmeiner, J. Jarvius, M. Bjarnegård, C. Betsholtz, U. Landegren, S. Fredriksson. Cytokine detection by antibody-based proximity ligation. *Proc Natl Acad Sci* **2004**, *101*, 8420-8424.

[270] S. M. Gustafsdottir, A. Nordengrahn, S. Fredriksson, P. Wallgren, E. Rivera, E. Schallmeiner, M. Merza, U. Landegren. Detection of individual microbial pathogens by proximity ligation. *Clin Chem* **2006**, *52*, 1152-1160.

[271] S. M. Gustafsdottir, J. Schlingemann, A. Rada-Iglesias, E. Schallmeiner, M. Kamali-Moghaddam, C. Wadelius, U. Landegren. In vitro analysis of DNA–protein interactions by proximity ligation. *Proc Natl Acad Sci* **2007**, *104*, 3067-3072.

[272] O. Söderberg, M. Gullberg, M. Jarvius, K. Ridderstråle, K.-J. Leuchowius, J. Jarvius, K. Wester, P. Hydbring, F. Bahram, L.-G. Larsson. Direct observation of individual endogenous protein complexes in situ by proximity ligation. *Nat Methods* **2006**, *3*, 995-1000.

[273] O. Söderberg, K.-J. Leuchowius, M. Gullberg, M. Jarvius, I. Weibrecht, L.-G. Larsson, U. Landegren. Characterizing proteins and their interactions in cells and tissues using the in situ proximity ligation assay. *Methods* **2008**, *45*, 227-232.

[274] H. Zhang, Y. Liu, K. Zhang, J. Ji, J. Liu, B. Liu. Single molecule fluorescent colocalization of split aptamers for ultrasensitive detection of biomolecules. *Anal Chem* **2018**, *90*, 9315-9321.

[275] J. Liu, X. Yang, K. Wang, Q. Wang, W. Liu, D. Wang. Solid-phase single molecule biosensing using dual-color colocalization of fluorescent quantum dot nanoprobes. *Nanoscale* **2013**, *5*, 11257-11264.

[276] S. Zong, Y. Liu, K. Yang, Z. Yang, Z. Wang, Y. Cui. Eliminating nonspecific binding sites for highly reliable immunoassay via super-resolution multicolor fluorescence colocalization. *Nanoscale* **2021**, *13*, 6624-6634.

[277] R. Ekins, F. Chu, E. Biggart. Development of microspot multi-analyte ratiometric immunoassay using dual fluorescent-labelled antibodies. *Anal Chim Acta* **1989**, *227*, 73-96.

[278] V. Romanov, S. N. Davidoff, A. R. Miles, D. W. Grainger, B. K. Gale, B. D. Brooks. A critical comparison of protein microarray fabrication technologies. *Analyst* **2014**, *139*, 1303-1326.

[279] C. I. Tobos, A. J. Sheehan, D. C. Duffy, D. M. Rissin. Customizable multiplex antibody array immunoassays with attomolar sensitivities. *Anal Chem* **2020**, *92*, 5613-5619.

[280] T. K. Christopoulos, E. S. Lianidou, E. P. Diamandis. Ultrasensitive time-resolved fluorescence method for α-fetoprotein. *Clin Chem* **1990**, *36*, 1497-1502.

[281] J. Ylikotila, L. Välimaa, M. Vehniäinen, H. Takalo, T. Lövgren, K. Pettersson. A sensitive TSH assay in spot-coated microwells utilizing recombinant antibody fragments. *J Immunol Methods* **2005**, *306*, 104-114.

[282] D. H. Wilson, D. M. Rissin, C. W. Kan, D. R. Fournier, T. Piech, T. G. Campbell, R. E. Meyer, M. W. Fishburn, C. Cabrera, P. P. Patel. The Simoa HD-1 analyzer: a novel fully automated digital immunoassay analyzer with single-molecule sensitivity and multiplexing. *J Lab Autom* **2016**, *21*, 533-547.

[283] L. Cohen, N. Cui, Y. Cai, P. M. Garden, X. Li, D. A. Weitz, D. R. Walt. Single molecule protein detection with attomolar sensitivity using droplet digital enzyme-linked immunosorbent assay. *ACS Nano* **2020**, *14*, 9491-9501.

[284] C. Wu, P. M. Garden, D. R. Walt. Ultrasensitive detection of attomolar protein concentrations by dropcast single molecule assays. *J Am Chem Soc* **2020**, *142*, 12314-12323.

[285] M. J. Mickert, Z. Farka, U. Kostiv, A. Hlaváček, D. Horák, P. Skládal, H. H. Gorris. Measurement of Sub-femtomolar Concentrations of Prostate-Specific Antigen through Single-Molecule Counting with an Upconversion-Linked Immunosorbent Assay. *Anal Chem* **2019**, *91*, 9435-9441.

[286] J. C. Brandmeier, N. Jurga, T. Grzyb, A. Hlavacek, R. Oborilova, P. Skládal, Z. Farka, H. H. Gorris. Digital and analog detection of SARS-CoV-2 nucleocapsid protein via an upconversion-linked immunosorbent assay. *Anal Chem* **2023**, *95*, 4753-4759.

[287] P. J. Macdonald, Q. Ruan, S. Y. Tetin. Direct single-molecule counting for immunoassay applications. *Anal Biochem* **2019**, *566*, 139-145.

[288] M. F. Abasıyanık, K. Wolfe, H. Van Phan, J. Lin, B. Laxman, S. R. White, P. A. Verhoef, G. M. Mutlu, B. Patel, S. Tay. Ultrasensitive digital quantification of cytokines and bacteria predicts septic shock outcomes. *Nat Commun* **2020**, *11*, 2607.

[289] E. Palo, M. Tuomisto, I. Hyppänen, H. C. Swart, J. Hölsä, T. Soukka, M. Lastusaari. Highly uniform up-converting nanoparticles: Why you should control your synthesis even more. *J Lumin* **2017**, *185*, 125-131.

[290] S. Lahtinen, M. Baldtzer Liisberg, K. Raiko, S. Krause, T. Soukka, T. Vosch. Thulium- and Erbium-Doped Nanoparticles with Poly(acrylic acid) Coating for Upconversion Cross-Correlation Spectroscopy-based Sandwich Immunoassays in Plasma. *ACS Appl Nano Mater* **2021**, *4*, 432-440.

[291] K. Kuningas, T. Rantanen, T. Ukonaho, T. Lövgren, T. Soukka. Homogeneous assay technology based on upconverting phosphors. *Anal Chem* **2005**, *77*, 7348-7355.

[292] L. Välimaa, K. Pettersson, M. Vehniäinen, M. Karp, T. Lövgren. A High-Capacity Streptavidin-Coated Microtitration Plate. *Bioconjug Chem* **2003**, *14*, 103-111.

[293] N. Bolstad, D. J. Warren, K. Nustad. Heterophilic antibody interference in immunometric assays. *Best Pract Res Clin Endocrinol Metab* **2013**, *27*, 647-661.

[294] B. Ghebrehiwet, 'Chapter 3 - C1q' in *The Complement FactsBook (Second Edition)* (Eds.: S. Barnum, T. Schein), Academic Press, **2018**, pp. 23-32.

[295] H. P. Heinz. Biological functions of C1q expressed by conformational changes. *Behring Inst Mitt* **1989**, *84*, 20-31.

[296] P. Riccelli, F. Merante, K. Leung, S. Bortolin, R. Zastawny, R. Janeczko, A. S. Benight. Hybridization of single-stranded DNA targets to immobilized complementary DNA probes: comparison of hairpin versus linear capture probes. *Nucleic Acids Res* **2001**, *29*, 996-1004.

[297] J. Pu, M. Liu, H. Li, Z. Liao, W. Zhao, S. Wang, Y. Zhang, R. Yu. One-step enzyme-free detection of the miRNA let-7a via twin-stage signal amplification. *Talanta* **2021**, *230*, 122158.

[298] X. Zhou, W. Zhu, H. Li, W. Wen, W. Cheng, F. Wang, Y. Wu, L. Qi, Y. Fan, Y. Chen, Y. Ding, J. Xu, J. Qian, Z. Huang, T. Wang, D. Zhu, Y. Shu, P. Liu. Diagnostic value of a plasma microRNA signature in gastric cancer: a microRNA expression analysis. *Sci Rep* **2015**, *5*, 11251.

TURUN
YLIOPISTO
UNIVERSITY
OF TURKU

Painosalama, Turku, Finland 2025

ISBN 978-952-02-0122-7 (PRINT)
ISBN 978-952-02-0123-4 (PDF)
ISSN 2736-9390 (Painettu/Print)
ISSN 2736-9684 (Sähköinen/Online)